Functionalizing liposomes with aptamers for active targeting of tumor cells

Walhan Alshaer

NNT : 2016SACLS055

THESE DE DOCTORAT
DE
L'UNIVERSITE PARIS-SACLAY
PREPAREE A
L'UNIVERSITE PARIS-SUD

ECOLE DOCTORALE N° 569

Innovation thérapeutique: du fondamental à l'applique

Discipline: Pharmacotechnie et biopharmacie

Par

Mr. Walhan ALSHAER

Fonctionnalisation de liposomes par des aptamères pour le ciblage actif des cellules cancéreuses

Thèse présentée et soutenue à Chatenay-Malabry, le 21/3/2016

Composition du Jury :

Prof. Patrick COUVREUR	(Université Paris-Sud)	Président
Prof. Elias FATTAL	(Université Paris-Sud)	Directeur de thèse
Dr. Hervé HILLAIREAU	(Université Paris-Sud)	Co-directeur de thèse
Prof. Karine ANDRIEUX	(Université Paris Descartes)	Rapporteur
Dr. Khuloud AL-JAMAL	(King's College London)	Rapporteur
Prof. Said ISMAIL	(University of Jordan)	Examinateur
Dr. Frédéric DUCONGE	(CEA, Institut d'imagerie biomédicale)	Examinateur

To my family

To the memory of Mr. Samih Darwazah

Acknowledgements

I would like to express my sincere gratefulness to my advisor professor Elias FATTAL, for welcoming in his team, the continuous support of my Ph.D study and related research, for his patience, motivation, and immense knowledge. His guidance and advice helped me in all the time of research and writing of this thesis. I could not have imagined having a better advisor and mentor for my Ph.D study.

I am fortunate to have Dr. Hervé HILLAIREAU as my co-advisor. This thesis was made possible due to his masterly guidance, spirit of adventure in research and persistent help. I owe him lots of appreciation for having shown me this way of research.

I would like to word a real gratitude and thankfulness to professor Said ISMAIL, for his distinguished scientific knowledge, support, and collaboration during the years of my PhD study.

I also want to express my deep appreciation to Dr. Juliette VERGNAUD for her scientific advice, and help in performing experiments.

I warmly wish to thank Dr. Nicolas TSAPIS for his kindness, support and the scientific discussions during the years of my thesis.

I would like to thank Prof. Karine ANDRIEUX and Dr. Khuloud AL-JAMAL for being the reporters of my thesis. My thanks go to the rest of my thesis committee: Prof. Patrick COUVREUR and Dr. Frédéric DUCONGE for sharing the very precious time with me and I feel doubly honored.

I also wish to thanks Prof. Amélie BOCHOT, Dr. Anderay MAKSIMENTKO, and Dr. Simona MURA for the advice and the scientific discussions.

My sincere thanks also goes to Mme Lisbeth NGOUANET from the French embassy in Jordan for her supporting of my PhD study.

I am grateful to AL HIKMA pharmaceutical company and the Campus France for funding and supporting my PhD study.

I would like to thank the whole team and IT administrators: Sylvie Zemmour, Dominique MARTIN, Fatiha HAMZA, and Patricia LIVET.

My sincere thanks to the many people contributed to my studies. Hélène CHACUN and Stéphanie DENIS for their scientific expertise radioactivity and handling of hazardous products, and in cell culture, respectively. I sincerely wish to thank Valerie DOMERGUE and all the staff of the animal house for their help in the animal experiments, Valérie Nicolas for her help in performing the confocal lazer microscopy experiments, Claudine DELOMENIE for help with Q-PCR, Magali NOIRAY for help in binding affinity experiments.

I also would like to thank Nidaa ABABNEH for her distinguished work on aptamers selection.

I would like express my deep thanks to all friends. Félix SAUVAGE, Nadège GRABOWSKI, Chantal AL SABBAGH, Adam BOHR, Alain NGUESSAN, Christian RUGE, Dinh Duy Pham, Giovanna GIACALONE, Ludivine MOUSNIER, Mathilde LORSCHEIDER, Sophie HOUVENAGE, Naila EL KECHAI, Rosana SIMON, Tanguy BOISSENOT, Thais Leite Nascimento, Alice Gaudin, Davide BRAMBILLA, Dunja SOBOT, Gopan GOPALAKRISHNAN, Moritz BECK BROICHSITTER, Nadia ABED, Valentina AGOSTONI, Ilaria BERTOLINI, Melania RIVANO.

Table of contents

Abbreviations

ACTB	Actin, Beta
Ag	Silver
ALK	Anaplastic lymphoma kinase
AMD	Age macular degeneration
ATCC	American type culture collection
Au	Gold
AuNR-ASP-Ce6	Gold nanorods (AuNR)aptamer switch probe (ASP) linking chlorin e6 (Ce6)
CBA	Cytometric Beads Array
CD	Cluster of differentiation
CD44	Cluster of differentiation 44
CdSe/ZnS	Cadmium selenide/zink
CEA	Carcinoembryonic antigen
CSC	Cancer stem cell
CuInS2	Copper indium disulfide
DAG	Diacyl-glycerol
DAPI	6-diamidino-2-phenylindole dihydrochloride
DLS	Dynamic Light Scattering
DPPC	1, 2-dihexadecanoyl-sn-glycero-3-phosphocholine
DSPE-PEG(2000)-Maliemide	1, 2-distearoyl-sn-glycero-3-phosphoethanolamine-N-[maleimide (polyethylene glycol)-2000]
EGFR	Endothelial growth factor receptor
EGVGE	Ethylene glycol vinyl glycidyl ether
EpCAM	Epithelial cell adhesion molecule
EPR	Enhanced permeability and retention
FGF	Fibroblastic growth factor
GAPDH	Glyceraldehyde 3-phosphate dehydrogenase
Gd	Guodalinium
GFP	Green fluorescent protein
HA	Hyaluronic acid
hEGFR	Human epidermal growth factor receptor
HER2	Human epidermal growth factor receptor 2
hrRNP	Heterogeneous ribonucleoprotein particle
IC50	Inhibitory concentration 50
IGHM	Immunoglobulin m heavy chain
IL	Interleukin
JAK2	Janus kinases
KGF	Keratinocytes growth factor
LPS	Lipopolysaccharide
Luc2	Luciferase 2
miRNA	Micro-RNA
MRI	Magnetic resonance imaging
MS	Mesoporous
MTT	3-(4,5-dimethylthiazol-2-yl)-2,5-diphenyltetrazolium bromide
NCL	Nucleolin
NF-Kb	Nuclear factor kappa-light-chain-enhancer of activated B cells
PCR	Polymerase chain reaction

PDGF	Platelets-derived growth factor
pDNA	Plasmid DNA
PE	Phycoerythrin
PEI	Polyethylenimine
PE-Rhod	L-α-Phosphatidylethanolamine-N-(lissamine rhodamine B sulfonyl)
PHMNP	Porous lagnatite nanoparticles
PLA-b-PEG	Polylactide-block-poly(ethylene glycol)-block-polylactide
PLA-PEG	Poly(lactide)-co-poly(ethlyene glycol)
PLGA	Poly(lactic-co-glycolic acid)
Pol2R	RNA Polymerase II
PSMA	Prostate specific membrane antigen
PTK	Proteine tyrosine kinase 7
PTX	Paclitaxel
QD	Quantum-dots
Q-PCR	PCR quantitative
rRNA	Ribosomal RNA
RT-PCR	Reverse-transcriptase polymerase chain reaction
SELEX	Systematic evolution of ligands by exponential enrichment
siRNA	Small interfering RNA
ssDNA	Single stranded DNA
ssRNA	Single stranded RNA
STAT	Signal transducers and activators of transcription
TCEP	Tris(2-carboxyethyl)phosphine hydrochloride
TCL-SPION	Thermally cross-linked superparamagnetic iron oxide nanoparticle
Tm	Transition temperature
TNBC	Triple negative breast cancer cells
TNF	Tumor nicrosis factor
Trf	Transferrine
UCNPs/MOF	Upconverting lanthanide nanoparticles/ metal-organic framework
VEGF	Vesicular endothelial growth factor

Introduction générale

General introduction

Introduction générale

L'utilisation de nanotechnologies pour le traitement du cancer est en constante progression. Cette stratégie permet d'améliorer les résultats thérapeutiques en diminuant les effets secondaires des chimiothérapies anti-tumorales conventionnelles, et en augmentant leur ciblage vers les tumeurs. Pour améliorer ce ciblage, une approche actuellement en développement consiste à concevoir des nanoparticules chargées en principe actif et fonctionnalisées par des ligands de ciblage, choisis pour leur interaction avec des molécules biologiques ou des récepteurs surexprimés par les cellules cancéreuses. Les aptamères sont des ligands de nature nucléique caractérisés par une forte affinité de fixation et une excellente spécificité vis-à-vis de leurs cibles, et présentant de faibles toxicité et immunogénicité. La fonctionnalisation de nanoparticules par des aptamères représente donc une stratégie de délivrance de principes actifs prometteuse et innovante pour améliorer le ciblage des tumeurs.

Le récepteur CD44 a été décrit comme un biomarqueur tumoral important, particulièrement dans le cas des cellules souches cancéreuses, qui constituent une population cellulaire capable de renouvellement, de prolifération et de différentiation en nombreuses cellules tumorales. Plusieurs études conduites par l'équipe du Pr Elias Fattal ont montré l'intérêt de l'acide hyaluronique comme ligand de ciblage pour l'adressage de petites molécules ou de macromolécules à des cellules surexprimant CD44. Cependant, l'acide hyaluronique exogène peut dans certains cas présenter une activité pro-angiogénique ou inflammatoire, et manquer de spécificité. L'objectif de ce travail est de concevoir un nouveau type de nanovecteur reposant sur l'utilisation d'un aptamère anti-CD44 conjugué à des liposomes PEGylés encapsulant des siRNA modèles, et d'en évaluer l'efficacité in vitro et in vivo.

Ce manuscrit comporte deux parties :

La première partie passe en revue la littérature sur les aptamères et les récentes avancées dans les thérapies ciblées du cancer utilisant les aptamères, notamment les nanoparticules fonctionnalisées par des aptamères et les conjugués entre molécules actives et aptamères.

La seconde partie décrit les résultats expérimentaux obtenus et se divise en trois chapitres :

- *Le premier chapitre décrit la sélection in vitro d'aptamères d'ARN dirigés contre la protéine CD44. Il comprend i) la conception de motifs d'ADN, ii) l'amplification de cet ADN par PCR, iii) la transcription in vitro de la bibliothèque d'ADN en ARN, iv)*

la fixation et l'isolement des aptamères fixés à la protéine CD44, v) le clonage, le séquençage et la caractérisation des séquences d'aptamères fixées, vi) les mesures d'affinité, vii) l'évaluation de la capacité de fixation au niveau cellulaire, et viii) l'évaluation de la stabilité des aptamères. Ce chapitre a été publié dans Journal of Nucleic Acid Therapeutics en 2013.

- *Le deuxième chapitre décrit la fonctionnalisation de surface de liposomes PEGylés par un aptamère anti-CD44 sélectionné au chapitre 1 et leur interaction avec plusieurs modèles cellulaires exprimant CD44. Ce chapitre comprend i) la préparation et la caractérisation des liposomes, ii) l'optimisation de la chimie de greffage de l'aptamère anti-CD44 à la surface des liposomes, iii) les mesures d'affinité vis-à-vis de la protéine CD44 de l'aptamère libre et de l'aptamère conjugué aux liposomes, iv) l'étude de la capture des différents liposomes par les cellules et iv) l'analyse de leur potentiel inflammatoire. Ce chapitre a été fait l'objet d'une publication dans Bioconjugate Chemistry en 2015.*
- *Le troisième chapitre décrit l'efficacité d'extinction génique ds liposomes fonctionnalisés par l'aptamère anti-CD44 sélectionné et chargés en siRNA, in vitro et in vivo. Ce chapitre comprend i) l'encapsulation des siRNA dans les liposomes PEGylés et son optimisation, ii) la fonctionnalisation des liposomes chargés en siRNA avec l'aptamère anti-CD44 par post-insertion, iii) l'évaluation de l'extinction génique in vitro, iv) la mise en place d'un modèle murin de cancer du sein humain par xénogreffe orthotopique, v) l'évaluation de la capacité d'extinction génique in vivo par la mesure de l'activité luciférase en bioluminescence et par Q-PCR. Ce chapitre a été écrit sous la forme d'un article de recherche en vue d'une soumission pour publication.*

À la fin du manuscrit, les résultats obtenus font l'objet d'une discussion génétale et plusieurs perspectives sont proposées.

Cette thèse de doctorat a été réalisée au sein de l'Institut Galien Paris-Sud, sous la direction du Pr Elias Fattal et du Dr Hervé Hillaireau. La partie correspondant à la sélection de l'aptamère a fait l'objet d'une collaboration entre le Pr Said Ismail à l'Université de Jordanie et l'équipe du Pr Elias Fattal. Cette thèse a été financée par la société pharmaceutique ALHIKMA et Campus France en Jordanie.

General introduction

The use of nanotechnology in cancer therapeutics has made tremendous progresses during these last decades. This field now has a meaningful potential to improve the therapeutic outcomes by decreasing the side effects of conventional anticancer therapeutics and by increasing their targeting to tumors. To do so, one important trend is the development of drug-loaded nanoparticles functionalized with targeting ligands selected for their interaction with biological molecules or receptors overexpressed by tumor cells. Aptamers are class of nucleic acid ligands characterized by a high binding affinity and specificity toward their targets, as well as a low toxicity and immunogenicity. Functionalizing nanoparticles with aptamers is thus an attractive targeted drug delivery strategy to improve the targeting of tumors.

The CD44 receptor has been identified as an important biomarker of tumors, especially of cancer stem cells, which are defined as a small population of cells able to renew, proliferate, and differentiate into heterogeneous tumor cells. Such cells are highly resistant against therapeutics and maintain tumor progression. In the group of Pr Elias Fattal, several studies have been carried out using hyaluronic acid as a ligand for CD44, in order to deliver small and large molecules to CD44-expressing cells. However, the use of exogenous hyaluronic acid might induce some undesired effects such as angiogenesis or inflammatory response in some cases, and lacks specificity. The goal of this thesis is therefore to design a new drug nanocarrier based on an anti-CD44 aptamer conjugated to PEGylated liposomes containing an siRNA as a model drug. The purpose is also to evaluate *in vitro* and *in vivo* the reliability of such a platform in terms of targeting and delivery.

This manuscript is composed of two parts.

The first part is a literature review on aptamers, including selection methods and recent therapeutic advances in tumor biology, with a special focus on aptamer-functionalized nanoparticles and aptamer-drug conjugates, and their impact on tumor therapy.

The second part is an experimental section divided into three chapters as follows:

- The first chapter describes the *in vitro* selection of RNA aptamers against the CD44 protein, which includes: i) DNA template design, ii) template amplification by PCR, iii) *in vitro* transcription of the DNA template to produce an RNA library, iv) folding, incubation, and partitioning of bound aptamers to CD44 protein, v) cloning, sequencing, and characterization of bound aptamer sequences, vi) binding affinity, vi)

cellular binding, and viii) aptamer stability evaluation. This chapter has been published in *Journal of Nucleic Acid Therapeutics* in 2013.

- The second chapter describes the functionalization of an anti-CD44 aptamer selected in chapter 1 to the surface of PEGylated liposomes for the targeting of CD44-expressing cancer cell lines, which includes: i) liposome preparation and characterization, ii) optimization of the conjugation chemistry of the anti-CD44 aptamer to the surface of liposomes, iii) binding affinity evaluation of the free aptamer and aptamer-conjugated liposomes toward the CD44 protein and iv) toward CD44-expressing cells, and finally iv) evaluation of the inflammatory potential of aptamer-functionalized liposomes. This chapter has been published in *Journal of Bioconjugate Chemistry* in 2015.
- The third chapter describes the gene silencing efficacy of anti-CD44 aptamer-functionalized liposomes for the targeted delivery of siRNA molecules to CD44-expressing breast cancer cells *in vitro* and *in vivo*, which includes: i) trapping of siRNA into PEGylated liposomes and its optimization, ii) functionalization of siRNA-loaded liposomes with the selected anti-CD44 aptamer by post insertion, iii) investigation of the gene silencing efficacy *in vitro*, iv) development of a mouse orthotopic model of human breast cancer, v) *in vivo* gene silencing efficacy by using bioluminescence imaging and Q-PCR. This chapter is written in the form of a research paper for publication.

The manuscript is concluded by a general discussion about the results obtained and the future perspectives of this work.

This PhD thesis was performed in Institut Galien Paris-Sud at Université Paris-Sud, under the supervision of Professor Elias Fattal and Dr Hervé Hillaireau. The aptamer selection part was done in collaboration between Professor Said Ismail at University of Jordan and the group of Elias Fattal. The thesis was funded by the pharmaceutical company ALHIKMA and Campus France in Jordan.

Travaux antérieurs

Les aptamères dans le ciblage et le traitement des tumeurs

Literature review

Tumor-targeted therapy by mean of aptamers

Travaux Antérieurs

Les aptamères dans le ciblage et le traitement des tumeurs

Résumé

Les aptamères sont des ligands de type nucléique caractérisés par une forte affinité et une forte spécificité pour leurs cibles. Le processus de sélection est maîtrisable, la modification chimique est aisée et leur taille est petite. Par conséquent, les aptamères sont des molécules attrayantes pour le développement de thérapies anticancéreuses innovantes. Ce chapitre se concentre sur les avancées récentes dans l'utilisation des aptamères comme ligands de ciblage pour la fonctionnalisation de nanovecteurs, mais également comme molécules pharmacologiquement actives (agonistes comme antagonistes) pour le traitement des tumeurs.

Literature review

Tumor-targeted therapy by mean of aptamers

Abstract

Aptamers are versatile nucleic acid-based macromolecules characterized by their high affinity and specificity for their targets. Therefore, aptamers are attractive molecules for therapeutic innovations in the targeting tumors. This review chapter focuses on the current advances in using aptamers as targeting moieties for the delivery of therapeutics and imaging agents by conjugation to drugs (small molecules, toxins, nucleic acids) or to nanocarriers (liposomes, micelles, polymeric nanoparticles, in organic nanoparticles), and as anti-tumor therapeutics (agonists or antagonists).

1. Introduction

Cancer remains among the most common causes of death worldwide, although major advances have been made in the understanding of tumor biology and the development of new therapeutics, leading to a reduction of the mortality rate [1]. With regard to the biology of the tumor, it is known that cancer cells are heterogeneous in nature and can develop mechanisms to preserve their survival, such as escaping the immune system and generating resistance to conventional tumor chemotherapy or radiotherapy. Several factors guide the hallmarks of the tumor cells including genetics, epigenetics, and the microenvironment [2]. These factors contribute to increase the risk of therapeutic failure and thereby tumor relapse. At the therapeutic level, conventional chemotherapy lacks specificity and causes high damage to both tumor and normal cells. There is therefore a need for reducing the side effects and increasing the efficacy of most of the antitumor drugs by improving their accumulation inside cancer cells and decreasing their uptake by normal cells [3, 4]. Nanocarriers, of 1-150 nm, are able to deliver their therapeutic payload to cancer cells after extravasation from the tumor aberrant and leaky blood vessels and accumulation in the tumor tissues through the enhanced permeability and retention (EPR) effect [5, 6]. Using such a mechanism, a few antitumor drug-loaded nanocarriers have reached the clinical stage [7]. However, despite these successes, most nanocarriers still present the inconvenient of lacking specificity towards their target cells. This is the reason why a promising field in nanomedicine consists in the design of carriers functionalized by the mean of molecular ligands, targeting, in a specific manner, unique or overexpressed tumor biomarkers. Several types of targeting ligands can be used to guide nanocarriers to tumor cells including receptor binding ligands such as antibodies, and aptamers [8].

Aptamers (ssDNA and ssRNA), also named chemical antibodies, are short oligonucleotides able to bind a target with a high affinity and specificity. In addition to this two remarkable

properties, they are gaining a growing interest in the field of drug targeting due to their low toxicity and immunogenicity as well as their ease of production. This chapter will mainly focus on the different strategies and the recent advances in aptamer conjugation to antitumor drugs and nanocarriers for targeted delivery. It will also cover the delivery of anticancer therapeutic aptamers.

2. Aptamers

2.1. Generalities about aptamers

First discoveries in the field of nucleic acids started in 1869, when the Swiss doctor Friedrich Miesche identified a chemical composition of the cell that he named nuclein (later called deoxyribonucleic acid or DNA). Since then, many discoveries confirmed the functions and the structures of nucleic acids (DNA and ribonucleic acid or RNA) in the cell as a genetic material [9]. In the 1980s, in addition to the determination of their template functions, studies showed that nucleic acids can play structural functions by folding into complex structures and binding to cellular targets, consequently enabling the regulation of several cellular pathways [10-12]. The structural functions of nucleic acids were explored *in vitro* by systematic evolution studies. Modern *in vitro* selection methods enabled the chemical synthesis and preparation of large combinatorial libraries of oligonucleotides comprising nearly 10^6 compounds [13]. By 1990, two independent groups, using *in vitro* selection, succeeded to isolate RNA molecules that bind selected ligand. Tuerk and Gold [14] were able to isolate RNA molecules that bind the T4 DNA polymerase and termed the selection process SELEX (abbreviation of Systematic Evolution of Ligands by EXponentioal enrichment). At the same time, Ellington and Szostak [15] developed different RNA molecules that bind small molecules (organic dyes) and gave the name aptamers for the selected motifs, a term that derived from the Latin word “aptus”, which means “fit”. In 1992, the first DNA aptamer have been isolated to bind small molecules and thrombin [16, 17]. Today, the field of aptamers

continues to grow covering varous chemical modifications. More recently, the introduction of protein-like side chains at positions far away from hydrogen bonds of nucleic acid bases improved the capability of aptamers to bind a wide range of different epitopes [18, 19].

In contrast to linear RNA molecules, such as small interfering RNA (siRNA), micro-RNA (mi-RNA) or antisense oligonucleotides that interrupt the genetic transcription based on the Watson and Crick base baring, aptamers are short, single-stranded DNA or RNA molecules (20-100 bases) that have the ability to fold into complex 3D structures [20, 21]. Since the discovery of the SELEX method and the advancements in nucleic acid amplification methods, many aptamers have been successfully selected to bind a wide range of targets such as ions, small chemical molecules, peptides, proteins, whole living cells and unicellular living organisms, as they are capable to bind their target in a high affinity range (from picomolar to nanomolar) and high selectivity, being moreover able to distinguish very closely related molecules [22]. Aptamers are narrowly close to antibodies in their range of target recognition and variety of applications [23, 24]. Both share common properties in terms of binding and specificity but differ in structure (Figure 1), chemistry, and production methods. Table 1 summarizes the advantages of limitations of each. Compared to aptamers, antibodies display some advantages such as satisfying pharmacokinetic properties, low renal filtration, and are not susceptible to nucleases. On the other hand, Aptamers have superior properties over antibodies in several ways. They are chemically synthesized while antibodies need a very complex biological setup to be produced. Moreover, aptamers have been demonstrated little or no toxicity and immunogenicity, and are smaller in size compared to antibodies [25]. Such properties make aptamers smart binding ligands for many biomedical applications such as therapeutics (antagonists or agonists), regulation of gene expression, diagnostics, drug or biomarker discovery, and targeted drug delivery. Many aptamers targeting different diseases are today in clinical trials for anticancer therapy.

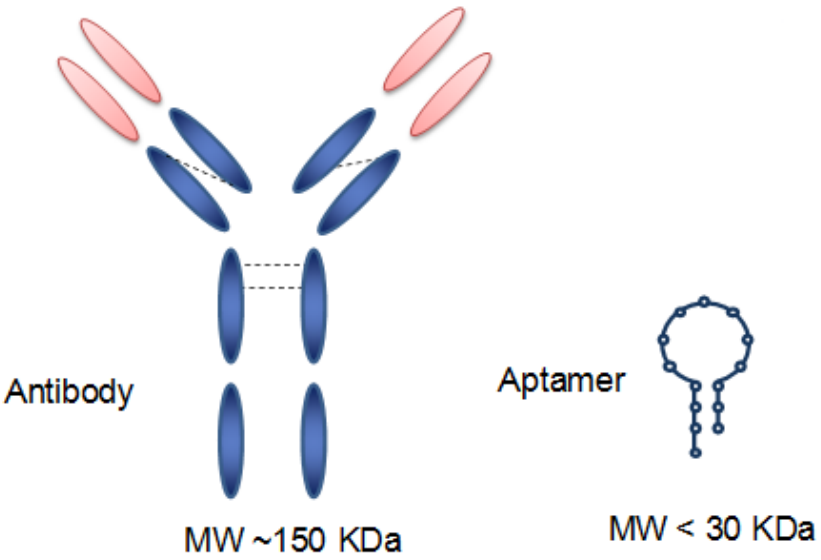

Figure 1: *Structure of an antibody compared to an aptamer*

2.2. Aptamer selection

Aptamers can exist in nature or be selected from a combinatorial library composed of 10^{13} to 10^{15} different sequence molecules (Figure 2). Such complexity can be achieved by designing a template sequence composed of up to 60 bases as a random region, flanked by two fixed regions for primer annealing and amplification. The conventional SELEX method starts by the preparation of the initial single stranded oligonucleotides library using amplification techniques and folding this library into 3D structures. The next step is the incubation of the folded library with the selected target. At this step, conditions such as pH, ionic strength, and temperature can be controlled to consider the target properties and the application purpose, if the aptamers are designed for therapeutic application, and need to be incubated in physiological conditions. After incubation, the unbound aptamer fraction is washed, allowing isolation of the bound fraction and its amplification for another round of selection. The SELEX method can be repeated up to 20 times to ensure the enrichment of highest affinity aptamers to the target. The selected candidates are then cloned, classified and characterized.

Table 1: Summary comparison of the advantages and limitations of aptamers and antibodies.

Aptamers	
Advantages	**Limitations**
• Selection performed *in vitro* and the conditions can be easily controlled to meet the optimal binding • Wide range of targets, starting from ions to whole living cells • High binding affinity (picomolar to nanomolar concentrations) • High specificity • Chemically synthesized and easy to reproduce • Renature easily after denaturation • Long shelf-life • Easy to conjugate to nanoparticles and drugs • Can be expressed intracellularly as intramers • Low toxicity and immunogenicity • Relatively low cost of production • Small compared to antibodies • Availability of antidotes	• Sensitivity to degradation by nucleases that require chemical modifications to ensure better stability • Rapid circulation clearance that require conjugation with other molecules such as PEG to decrease their clearance rate
Antibodies	
Advantages	**Limitations**
• High binding affinity • High binding specificity • Production technology and applications are well established in research and clinic • Low clearance rate from the body	• Immunogenic • Produced only against immunogenic molecules, which limits the range of targets • Denaturation is irreversible • Short biological half-life • Sensitive to conditions such as temperature and pH • High cost and complexity of production

In the case of RNA aptamers an extra step of *in vitro* transcription is added using RNA polymerases promoters (such as T7 and SP6) [20]. Since the invention of SELEX, different modifications have been applied to the conventional method (see [26] for review). For example, the cell-SELEX method is an important step in the selection of aptamers against whole diseased cells. One advantage provided by this method is the selection of aptamers without any previous knowledge regarding the target biomarkers. A second advantage is the selection of aptamers that bind the surface target in a native state, thereby eliminating the risk, after selection, of binding failure compared to the pure protein [27]. In the cell-SELEX process, normal cells or closely related cells, can be used as negative cells for counter-selection to eliminate aptamers that may bind the shared targets on both cells. In addition, in this method, it is possible to select aptamers internalized by receptor endocytosis avoiding those only bound to the cell surface [28].

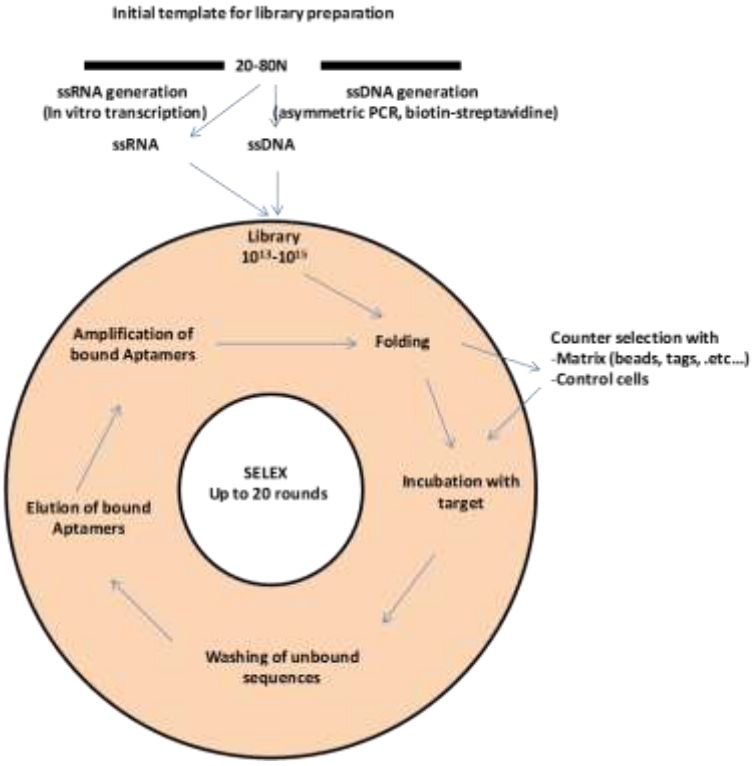

***Figure 2**: Schematic representation of SELEX methodology*

3. Aptamers as targeting moiety

Finding therapeutics able to target diseased cells is a great challenge in medicine. One way to achieve this goal consists in targeting biomarkers that are specifically or differentially expressed by the diseased cells, thereby delivering the drug specifically to these biomarker-expressing cells. In tumors, biomarkers can be expressed through three mechanisms: i) genetic mutations that produce structurally different biomarkers from the normal ones, ii) overexpression of a biomarker that may be beneficial to the tumor progression, and iii) post-translation modifications that may induce changes in the structural-functional properties of the biomarker [29, 30]. Therefore, there is a need for smart molecules that can distinguish between the different biomarkers. Aptamers specificity allows them to distinguish between very closely related molecules [31] and their molecular recognition capabilities have been broadly used in targeting intracellular, extracellular and cell surface tumor markers.

Aptamers can be used as guiding molecules for the delivery of drugs and various macromolecules or nanocarriers to tumor cells (figure 3). Their specific interaction with surface receptors can increase the rate of cellular internalization through receptor-mediated-endocytosis. Therefore, several RNA and DNA aptamers have been successfully selected to potential cancer cell surface receptors. Noteworthy examples include the selection of two 2′-fluorinated-RNA aptamers (A10 and A9) against purified prostate-specific membrane antigen (PSMA) [32, 33] and the selection of DNA aptamers to MUC1 (Mucin 1) cell surface associated protein (called MA3), which is overexpressed on several tumors such as breast, colon, lung, and prostate cancers [34]. The selection of aptamers against tumor cells, in the absence of identification of a target protein, has been applied in several cases using the cell-SELEX method. The studies led to the discovery of biomarkers such as the protein tyrosine kinase 7 (PTK7), which is a transmembrane receptor protein tyrosine kinase-like molecule, present in a series of leukemia cell lines [35, 36]. The aptamer used for the discovery of this

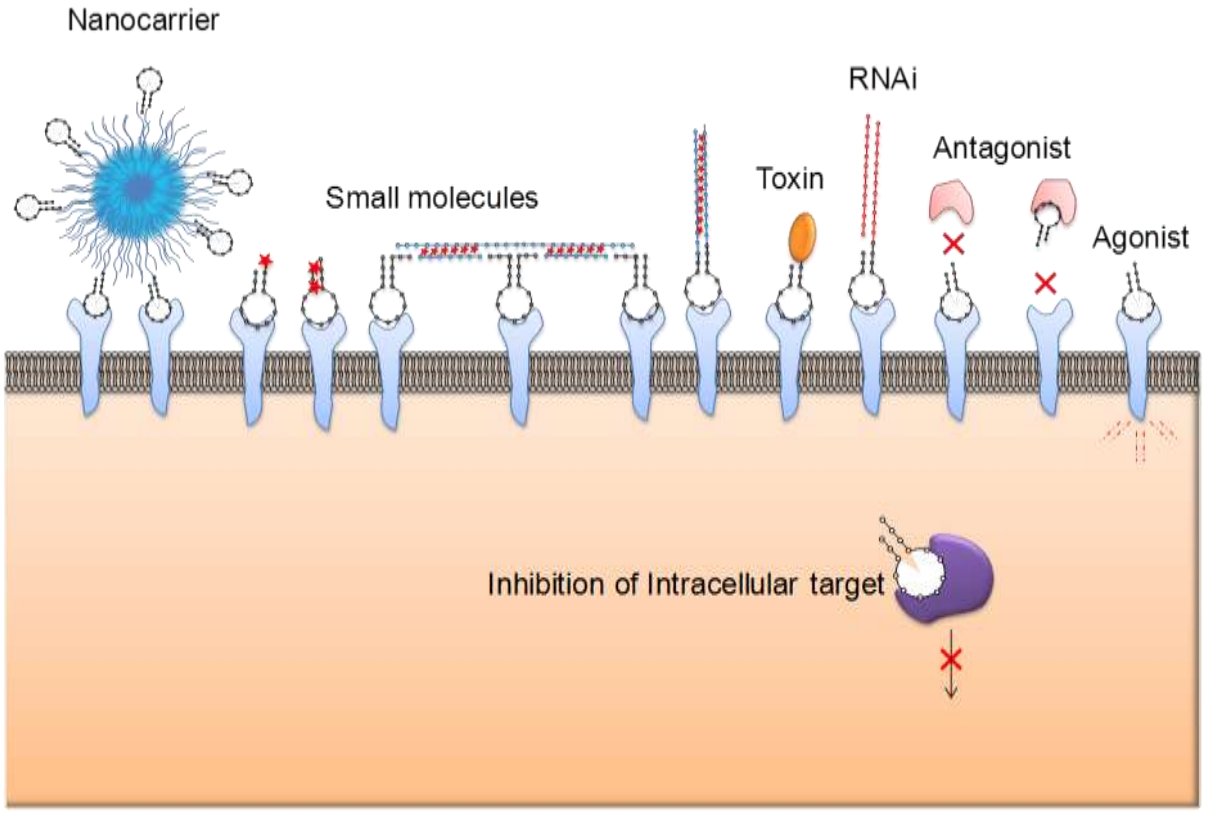

Figure 3: *schematic representation of the mechanism of actions of aptamers for anticancer therapeutic applications, ether as targeting moiety for nanocarriers, small molecules, etc., or as pharmacological active molecules (agonist, antagonist).*

biomarker was called sgc8c, and was also used in further targeting experiments. In another cell-SELEX experiment, the immunoglobulin heavy constant mu chain (IGHM) was discovered on burkitt lymphoma and the aptamer called TDO5, was used as well as a target ligand [37]. Recently, aptamers have been successfully selected to the cancer stem cell biomarkers. Cancer stem cells (CSC) are defined as a small population of cells that are characterized by their ability to renew, proliferate, and differentiate into heterogeneous tumor cells. They are highly resistant against therapeutics and maintain tumor progression. The best described cancer stem cell markers are CD44, CD133, and EpCAM [38]. Therefore, it is not surprising to find several aptamers selected against these markers [39-44].

Moreover, aptamers can exhibit several functions, like the anti-Nucleolin aptamer (AS1411) which can work as a targeting ligand and as a therapeutic molecule (detailed in section 4.1) at the same time. These aptamers have been widely used in the targeting of drugs and nanocarriers to cancer cells. All these aptamers summarized in table 2.

3.1. Aptamer-drug conjugates

3.1.1. Small molecules

The targeting efficacy of aptamer-drug conjugates has been investigated and led to potential successes and promising clinical applications. In comparison to antibodies (~150 kDa), due to their smaller size (<30 kDa), aptamers can penetrate the tumor tissues at a higher extent. Indeed, the tumor accumulation the EpCAM aptamer compared to the anti-EpCAM antibody, given intravenously in a mouse xenograft model of human colorectal cancer, 1.67 and 6.6 fold higher tumor accumulation showed at 3 and 24 hours following administration, respectively, compared to the anti-EpCAM antibody. It was concluded to a better penetration, homogenous distribution, and prolonged retention of the EpCAM aptamer [45]. Therefore, aptamers can mediate better distribution and accumulation of directly loaded chemotherapeutic drugs and macromolecules into tumors compared to their antibodies counterparts.

The loading of therapeutic drugs into aptamers can be performed by non-covalent or covalent attachment. In non-covalent attachments, active molecules such as doxorubicin can be chelated by the CG/GC rich regions of the aptamer sequence or to a nucleic acid sequence attached to the aptamer for this purpose [46]. For example, doxorubicin chelated by anti-MUC-1 aptamer (MA3), showed higher uptake and toxicity towards $MUC1^{+}$ cancer cells compared to the $MUC1^{-}$ cells [47]. One advantage demonstrated by such an approach is the ability of the aptamer to increase the drug antitumor effect towards target cells and, due to a better selectivity, to avoid toxicity towards normal tissues and side effects [47]. TMPyP4

photosensitizer is another type of molecule that has been successfully chelated into G-quadruplex aptamer for tumor imaging [48]. However, in this latest case the low loading capacity has limited the aptamer-drug conjugate potency. Nevertheless, some authors succeeded in increasing this loading capacity, using polyvalent aptamers nucleic acid chimeras linked to aptamers as drug loading domains [49]. For example, a polyvalent aptamer system that is composed of one nucleic acid strand unit with multiple aptamer binding domains has been found to increase the doxorubicin loading capacity and to improve the binding affinity by 40 times compared to the monovalent aptamer [49]. However, non-covalent attachment of drugs to aptamers suffers low stability particularly in biological fluids. Therefore, a stable covalent conjugation of drugs has been addressed in many studies. For instance, the direct conjugation of anti-protein tyrosine kinase 7 (PTK7) aptamer (sgc8c) to doxorubicin was achieved using a hydrazone linker. The sgc8c-doxorubicin conjugate displayed specific binding and high affinity to the acute lymphoblastic leukemia cells (CCRF-CEM) [50]. Although similar drug efficacy was obtained from both free doxorubicin and sgc8c-doxorubicin conjugate, lower toxicity was observed for the non-target cells [50].

3.1.2. Protein toxins

In addition to the conjugation and delivery of small molecules, tumor-targeted delivery of toxic proteins via aptamers has been successfully addressed. One interesting example is the delivery of the ribosomal toxin gelonin. Gelonin is 28 kDa protein known to inhibit protein synthesis by calving the glycosidic bounds in the rRNA. Gelonin is poorly internalized into cells and has little cellular toxicity. The anti-PSMA aptamer (A9) has been conjugated to gelonin toxin for targeting prostate cancer. the A9 aptamer-toxin conjugate showed an IC_{50} of 27 nM and the potency at least 600 fold higher to $PSMA^{+}$ cells compared to $PSMA^{-}$ cells [51]. The ability of aptamers to target this particular therapeutic toxin opens possibilities for the delivery of other proteins using aptamers-guided delivery system.

3.1.3. Nucleic acids

The RNA interference (RNAi) based mechanisms offer an efficient and specific tool for silencing genes inside cells. Molecules of the RNAi machinery, including small interfering RNA (siRNA) and micro RNA (miRNA), have been widely used for silencing genes of interest in different diseases including cancer. However, these molecules suffer poor stability in biological fluids, low and nonspecific cellular uptake [52]. Therefore, specific delivery systems are required to increase the efficacy RNAi in tumor cells [53]. Consequently, high attention has been given to aptamers as specific targeting ligands that can be conjugated to RNAi molecules and guide their delivery into tumor cells [54]. The conjugation of RNAi to aptamers can be performed through streptavidin bridge, sense and antisense complimentary strands extended from both aptamer and RNAi, or by covalent attachment of the RNAi antisense sequence to one ends of the aptamer (for review see [55]). One of the early progress in aptamer-mediated siRNA delivery into cancer cells was made in 2006 by Chu *et al.* [56]. The anti-PSMA aptamer and siRNAs sequences knocking down laminin and glyceraldehyde-3-phosphate dehydrogenase (GAPDH) genes have been modified with biotin and bridged to streptavidin. The aptamer-streptavidin-siRNA chimera was shown to successfully inhibit the targeted genes in $PSMA^+$ cell line [56]. Interestingly, when the aptamer-siRNA chimera was complexed with cationic PEI, low improvement was observed on the cellular uptake which was only around 6 to 8 % [57]. This was explained by the random organization of the whole system hiding the binding domains of aptamers. By contrast, when siRNAs were first complexed with PEI followed by immobilization of the aptamer on the PEI-siRNA complex, the orientation of the aptamer was good enough to improve by 34 % the uptake by the target cells [57].

MicroRNAs (miRNA) are short noncoding RNA molecules that play a role in the regulation of gene expression and cell cycle. They were shown to be involved in tumor progression,

maintenance, and metastasis. miRNA can act as oncogenic or tumor suppressor molecules. Therefore, selective delivery of miRNAs or anti-miRNAs into tumors is of high interest as new antitumor therapeutics. Using aptamers for guided-delivery of anti-miRNA has been successfully applied for the delivery of miRNA-21, an oncogenic miRNA molecule that induces tumorigenicity of several tumors including triple negative breast cancer (TNBC). Shu *et al.* [58] developed a triple-functional system composed of three motifs, the EGFR-RNA aptamer, the anti-miRNA-21 sequence, and one fluorescent probe. This multifunctional RNA conjugate showed intact stability for 8h after systemic administration into a murine MDA-MB-231 orthotopic breast cancer model, a high tumor accumulation and a neglected uptake by healthy tissues [58].

3.2. Aptamers-conjugated nanocarriers

Nanocarriers are nano-sized vehicles (from 1 to around 200 nm) made of organic or inorganic materials (Figure 4) that can carry molecules such as drugs and imaging agents within or on the surface of cells in a target tissue. Nanocarriers offer a high surface area and trapping volume enabling to carry large amounts of payloads into specific areas of the body [7]. Many studies have showed the ability of nanoparticles, preferentially with the size less than 200 nm, to distribute into the tumors using the EPR effect [59, 60] (figure 5). However, it is considered that the smaller they are, the deepest the nanocarrier can diffuse into the tumor [61]. There are many advantages of using nanocarriers as delivery systems: i) they can be loaded with large amounts of therapeutics and imaging molecules and deliver them into tiny sites in the body improving their therapeutic efficiency, ii) they can be loaded with combination of therapeutics, iii) they can be loaded with lipophilic and or hydrophilic drugs, iv) they can carry and protect fragile and unstable molecules such as nucleic acids and proteins, v) they can be functionalized with a variety of ligands that target specific molecules, particularly membrane proteins [8]. However, there are also limitations for the use of

nanocarriers including, i) in some cases, their weak colloidal stability [62], ii) their unsuitability for the entrapment of some molecules particularly the poorly soluble ones and iii) their eventual toxicity that can lead to some damages to the normal cells [63].

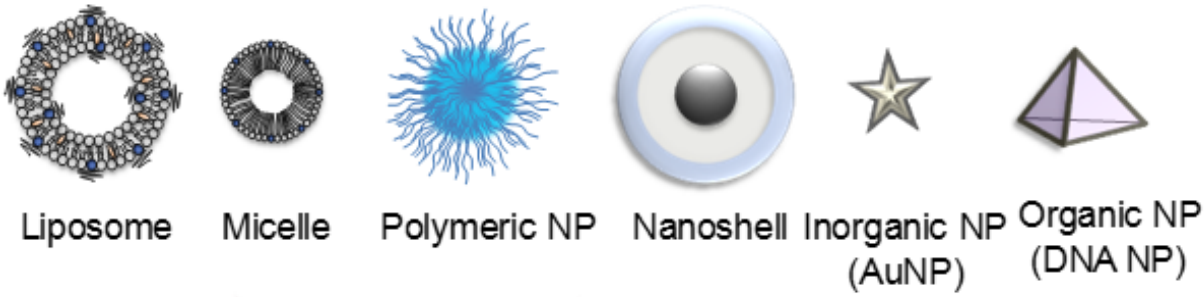

Figure 4*: Schematic representation of different nanocarriers used in drug delivery.*

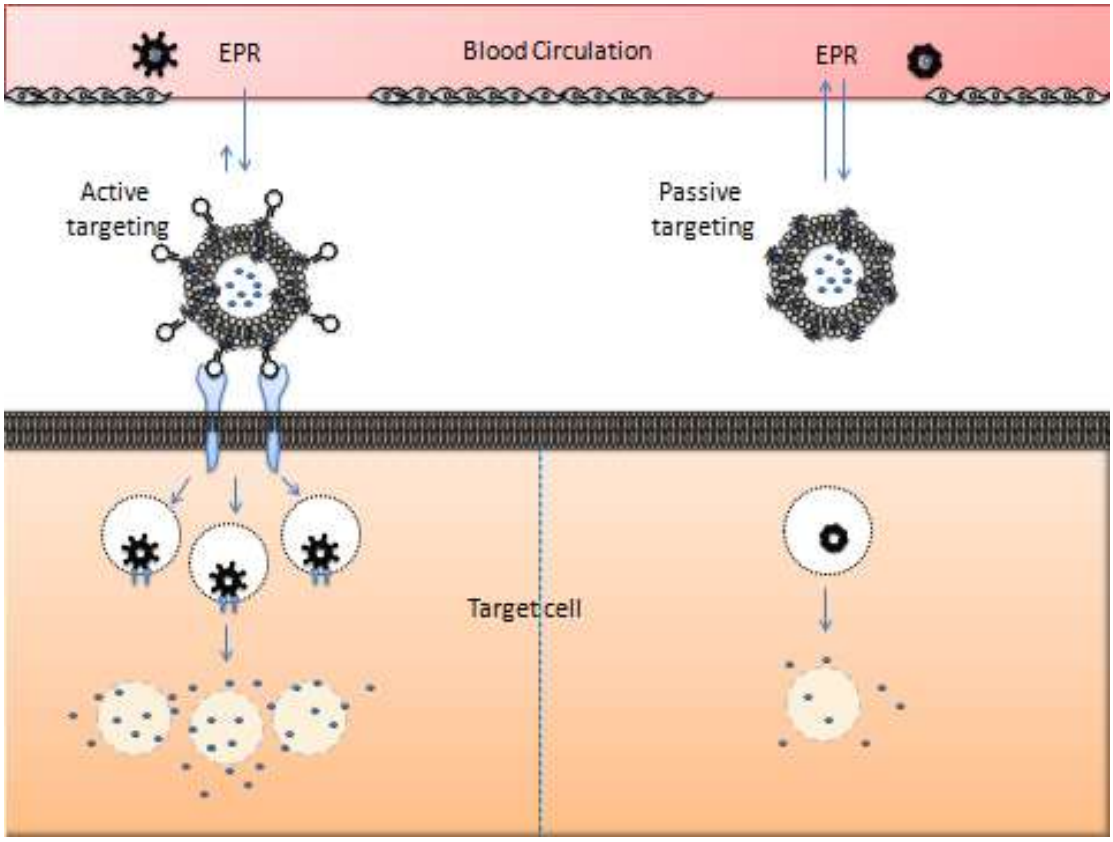

Figure 5: *Schematic representation of enhanced permiability and retention effect and the mechanism of passive and active targeting.*

3.2.1. Liposomes

Liposomes are vesicles composed of two or more lipid bilayers first described in 1962 and widely used in many biomedical applications, specifically as nanocarriers for drugs and imaging agents in cancer therapy. Liposomes are among the most successful drug nanocarriers reaching clinical studies in nanomedicine due to the following main advantages, including i) their biodegradability and biocompatibility, ii) their ability to carry high payloads of small and large molecules iii) both hydrophilic and hydrophobic molecules can be loaded into liposomes, iv) their ease of preparation, v) the possibility of sterical stabilization by the addition of PEG thereby increasing circulation half-life resulting in high accumulation by EPR effect, vi) their ability to be functionalized with active ligands such as antibodies, peptides, small molecules, and aptamers.

Early proof of concept studies related to the functionalization of liposomes with aptamers were performed by Willis *et al.* (1998) [64] who functionalized lipid vesicles with the nuclease-stable anti-VEGF aptamer, using the diacyl-glycerol (DAG) lipid to anchor the aptamers onto the vesicle membrane. Such conjugation to liposomes did not affect the binding affinity of the aptamer. Moreover, the conjugated liposomes reduced the proliferation of endothelial cells and therefore blocked the angiogenesis *in vitro* and *in vivo* [64]. Subsequently, several aptamers have been attached at the surface of different liposomal formulations to deliver payloads such as small chemotherapeutic molecules (cisplatin and doxorubicin), imaging agents (such as gadolinium compounds and ^{225}Ac), and nucleic acids (mostly siRNA). For example, the targeting capabilities of anti-NCL aptamer (AS1411) present on the surface of doxorubicin-loaded liposomes were investigated *in vitro* and *in vivo* [65]. The resulting 200 nm aptamer-functionalized doxorubicin-loaded liposomes (Apt-Dox-Lip) were then tested on MCF7 cells *in vitro* and on a mouse xenograft model of human breast cancer and compared to control liposomes functionalized with nonspecific DNA

aptamer sequence [65]. A higher cytotoxic effect against tumors *in vitro* and *in vivo* was obtained for the Apt-Dox-Lip compared to controls [65]. The same AS1411 aptamer was used to coat similar liposomes loaded with cisplatin [66]. The IC_{50} of free cisplatin on MCF-7 (NCL positive) and LNCaP (NCL negative) was reported to be 28 μM and 5.95 μM, respectively [66]. However, the cytotoxic effect of the aptamer-liposome-cisplatin was increased in MCF-7 cells compared to LNCaP cells, suggesting a decrease of the toxicity versus the non-targeted cells [66]. An originality in this report consisted in the synthesis of a complementary DNA strand to the AS1411 aptamer able to disrupt the 3D structure of the aptamer and thus to work as an antidote to reverse the action of aptamer-mediated targeted drug delivery [66]. This antidote was efficient *in vitro* but, unlike other studies related to aptamers, was not tested *in vivo* [66]. Another interesting aptamer-liposomal-based drug delivery system was reported by Baek *et al.* [67] In this study a tethered linker of complimentary DNA strand to anti-PSMA aptamer (A10) has been conjugated to DSPE-PEG-maleimide by the thiol-maleimide chemistry and then post-inserted into preformed PEGylated liposomes. After that, the anti-PSMA aptamer has been attached to the complementary DNA strand conjugated on the surface of liposome. Such an approach allows a better control of the number of aptamers on liposome surface and gives an interesting versatility to the functionalization method. Doxorubicin was then encapsulated inside liposomes using the pH gradient-driven loading method. The resulting aptamer-liposome targeting efficacy was tested *in vitro* on a $PSMA^+$ cell line (LNCaP) and on a mouse xenograft model of human prostate cancer. A significant decrease in the tumor volume was observed in animals treated with aptamer-liposomes compared to blank liposomes and to free doxorubicin thereby confirming the efficacy of aptamers as targeting ligands *in vivo* [67]. Another interesting approach was the development of AS1411-functionalized thermosensitive liposomes composed of dioleylphosphatidylcholine (DPPC) encapsulating both doxorubicin and ammonium

bicarbonate, for the selective targeting of multi-drug-resistance breast cancer cells (MCF-7/MDR) that overexpress nucleolin. DPPC has a phase transition temperature (Tm) of 41°C, making liposomes based on this phospholipid leaky upon temperature raise. Moreover, the triggered release of doxorubicin inside tumor cells is also enhanced by liposomes permeabilization due to CO_2 bubbles formed from ammonium bicarbonate upon local heating [68]. Such a combination between a better drug release from thermosensitive liposomes and aptamer targeting property increased drug efficacy [68]. This was also the case for entrapped contrast agents such as gadolinium (Gd) derivatives for Magnetic Resonance Imaging (MRI). Indeed, AS1411 functionalized to a surface of thermosensitive liposomes composed of DPPC and loaded with Gd improved the MRI imaging by increasing the liposomes relaxivity 4 times compared to non-functionalized liposomes [69]. Moreover, our group has successfully selected a high affinity RNA aptamer (named Apt1) against CD44 receptor protein [39]. Furthermore, the Apt1 has been functionalized to PEGylated liposomes containing DPPC phospholipids using the thiol-maleimide chemistry. The Apt1-functionalized liposomes showed higher selectivity and uptake by $CD44^+$ cancer cells lines (MDA-MB-231 breast cancer cells and A549 lung cancer cells) compared to $CD44^-$ 3T3 cell line. Moreover, the Apt1 functionalized liposomes have shown no signs of inflammatory response by tumors cells after incubation *in vitro* [70]. In addition to the use of thermosensitive phospholipid (DPPC), it is possible to sensitize liposomes with a thermosensitive polymer for the development of ultrasound-triggered drug delivery as shown by Ninomiya *et al.* [71]. An anti-platelet-derived growth factor receptor aptamer was surface-linked to doxorubicin-liposomes sensitized with poly(NIPMAM-co-NIPAM) as a thermosensitive polymer. The MDA-MB-231 breast cancer cell line was used as target cells. After ultrasound irradiation (generating heat), the cell viability of MDA-MB-231 cells treated with doxorubicin-loaded, aptamer-functionalized liposomes was lower compared to cell viability without ultrasound irradiation or doxorubicin-

loaded liposomes alone. In addition to the delivery of small therapeutic and imaging molecules, aptamer-functionalized liposomes have also been successfully applied to macromolecules such as siRNA. For example, PEGylated cationic liposomes were complexed with siRNA specific for the B-Raf oncoprotein for the treatment of malignant melanomas [72]. The AS1411 aptamer was covalently attached to siRNA-loaded lipoplexes via thiol-maleimide chemistry [72]. In a mouse xenograft model of human melanoma, the knockdown of B-Raf was stronger with targeted liposomes compared to the non-targeted ones [72]. Another example was the delivery of siRNA specific to the green fluorescent protein using a nuclease-stable RNA aptamers against human transferrin (Trf) [73]. The selected aptamers were specific and rapidly internalized Trf-expressing cells [73]. The resulting siRNA delivery system showed a higher efficacy in terms of targeting and delivery of siRNA into Trf–expressing cells [73]. The silencing activity was optimal at a half maximal effective concentration (EC_{50}) of 74 pM whereas the non-targeted liposomes had a very limited silencing effect [73].

A DNA aptamer (sgc8) has been successfully selected against CEM-CCRF acute leukemia cells targeting the protein tryrosine kinase 7 (PTK7) receptor as a biomarker [74]. It was successfully functionalized to the surface of liposomes using the thiol-maleimide chemistry [74]. In this work, liposomes were loaded with FITC-dextran and the sgc8 aptamer fluorescently labeled with tetramethylrhodamine (sgc8-TMR) [74]. The dual-fluorophore labeling of the carrier and the targeting ligand enabled to track the interaction of sgc8 aptamer-liposomes interaction and their content with CEM-CCRF cells [74]. The sgc8 aptamer-liposomes displayed higher uptake by $PTK7^+$ CEM-CCRF cells compared to plain liposomes and a low uptake $PTK7^-$ NB4 promyelocytic leukemia cells, demonstrating that targeting was essential in cell internalization [74].

Angiogenesis is one of the main causes of tumor progression in which the blood vessels are

aberrant and leaky around the tumor. Therefore, targeting biomarkers expressed by the tumor endothelial cells could be promising as well as targeting tumor cells. This is the reason why a thiolated aptamer against E-selectin (ESTA) was successfully used to functionalize PEGylated liposomes using the carbodiimide chemistry [75]. The resulting aptamer-liposomes have been tested *in vitro* for their uptake by human umbilical cord vein endothelial cells (HUVEC) stimulated by TNF-α to induce E-selectin expression [75]. The results showed a higher accumulation of aptamer-liposomes in stimulated HUVEC cells compared to unstimulated ones [75]. Furthermore, after intravenous administration to mice xenograft model of human breast cancer, the aptamer-liposomes were much more retained in the tumor vasculature without any decrease in the circulation half-life of the liposomes conjugated to aptamers [75]. Ara *et al.* [76] used the cell-SELEX method to select a DNA aptamer against mouse tumor endothelial cells (mTECs) named AraHH001 [76]. The anti-mTEC aptamer (AraHH001) showed specificity to bind mTEC cells but not to the normal mouse endothelial cells (skin-ECs) [76]. It was also found to possess an anti-angiogenesis activity as indicated by the inhibition of tube formation by mTEC on matrigel [76]. In a further study, the AraHH001 aptamer was functionalized to PEGylated liposomes using the thiol-maleimide chemistry [77]. The binding of AraHH001 -functionalized liposomes was well characterized for the targeting of tumor endothelial cells involved in the tumor progression [77], demonstrating that the AraHH001-liposomes constitute a promising carrier for the targeted delivery of anti-angiogenesis drugs into tumor endothelial cells.

3.2.2. Micelles

Micelles made of lipids or polymers, designed for drug delivery, are self-assembled colloidal nanoparticles (5-100 nm) composed of a hydrophilic shell and a hydrophobic core. Micelles are considered as potential nanocarriers mostly for poorly water-soluble drugs as well as imaging agents. PEG with a molecular weight of 2-15 kDa is commonly used as the

hydrophilic part of the micelles, while biocompatible or biodegradable materials such as polyesters and polyamides generally compose the hydrophobic part. Several micelle-based nanocarriers are currently in clinical trials such as Genexol®-PM NK911 (Paclitaxel-loaded micelles) in phase II, NK911® (doxorubicin loaded micelles), NK105® (paclitaxel loaded micelles), and SP1049C® (doxorubicin loaded pluronic® based polymer micelles). Several groups are today considering the functionalization of these micelles by aptamers to improve, one step forward drug, efficacy. For example, the TDO5 aptamer, selected by cell SELEX technology to bind the immunoglobulin heavy mu chain receptor on ramose cells (B-cell lymphoma), was successfully conjugated to lipid micelles using PEG as a linker between TD05 and the lipid tail allowing the self-assembly of micelles [78]. These micelles were tested on two cell lines, ramose (target cells) and HL60 cells (negative cells) [78]. The binding affinity constant was 750 times higher for the TDO5-conjugated micelles compared to free TDO5 aptamer, resulting in a 80-fold higher internalization of the TDO5-micelles by ramose cells compared to unconjugated ones [78]. More complexed systems have been described such as pH sensitive polymeric micelles using D-α-tocopheryl polyethylene glycol 1000-block-poly-(β-amino ester) (TPGS-b-PBAE, TP) as pH sensitive copolymer, loaded with paclitaxel, and decorated by AS1411 on the surface [79]. The resulting PTX/Apt-mixed micelles showed a high stability at physiological pH (7.4) and optimal release of PTX at acidic pH (5.5) [79]. A higher cellular uptake by SKOV3 ovarian cancer cells in mice was also observed both *in vitro* and *in vivo* in a xenograft model of human ovarian cancer, with significant cytotoxicity, reduction in tumor growth and myelosupression [79]. Further examples proved the efficacy of active targeting using aptamers-functionalized polymeric micelles, such as the AS1411 aptamer decorated on the surface of multifunctional composite micelles made of Pluronic F127 and beta-cyclodextrin-linked poly(lactide)-co-poly(ethlyene glycol) (PLA-PEG) encapsulating doxorubicin [80], or the anti-PSMA aptamer covering the

surface of doxorubicin-loaded unimolecular micelles composed of hyperbranched polymer molecules (H40 polymer) in the core and PLA-PEG arms on the shell [81].

3.2.3. Polymeric nanocarriers

Polymeric nanoparticles are commonly used nanocarriers in drug delivery. They are produced from synthetic polymers such as polyesters (poly(lactic acid) (PLA), poly(lactic-co-glycolic acid) (PLGA)), and polyalkylcyanoacrylate or from natural polymers such as chitosan, collagen, and PEI.

The polymeric nanoparticles display sizes going from 50 to 200 nm. Polymeric nanoparticles have been designed to release payloads by different methods, including surface or bulk erosion, diffusion through the polymer, diffusion after swelling, or in response to environmental stimuli and many polymeric nanoparticles are today under clinical studies [82]. Several authors have investigated the efficacy of aptamer-functionalized polymeric nanoparticles in targeting tumors. PLGA-b-PEG is one of the commonly used polymer to form these nanoparticles due to its known biodegradability and the capability of such nanoparticles to entrap a variety of small molecules. For example, PLGA-b-PEG nanoparticles have been loaded with doxorubicin with a high encapsulation efficacy (~90%) and functionalized with anti-EpCAM aptamer, showing, in a mouse xenograft model of human small lung cancer, a higher tumor inhibition (60.9%) when compared to the unconjugated PLGA-b-PEG nanoparticles (31.4%) [83]. Targeting CSCs using functionalized nanocarriers constitute a promising approach in cancer therapeutics, by increasing the therapeutic index and decreasing relapse resulting from inherited therapeutic-resistance of CSCs. An RNA aptamer (named A15) selected to bind the CD133 CSC marker, has been successfully conjugated to PLGA-b-PEG nanoparticles encapsulating salinomycin. Salinomycin is an antibiotic that suffers poor water solubility but showed efficacy to kill CSCs. The resulting aptamer-functionalized, salinomycin-loaded PLGA-b-PEG nanoparticles

had a diameter of 150 nm and a drug encapsulation efficacy of 50 % [84]. The *in vitro* cytotoxicity of aptamer-functionalized nanoparticles on $CD133^+$ Saos-2 osteosarcoma CSCs, showed 4.92 and 2.33 fold higher cytotoxicity compared to the non-functionalized nanoparticles and the free salinomycin, respectively [84]. They also displayed a higher therapeutic efficacy in killing $CD133^+$ cells in Saos-2 osteosarcoma xenografted in mice [84]. Moreover, functionalizing PLGA-b-PEG with anti-NCL aptamer did not affect drug encapsulation or release [85].

Similar approaches of aptamer-functionalized PLGA-based nanoparticles have been described for drug delivery in several types of tumors using different aptamers such as anti-NCL aptamer (AS1411) (for targeted delivery of PTX to Glioma) [86], anti-PSMA aptamer (A10) (for targeted delivery docetaxel and paclitaxel to prostate cancer) [87, 88], anti-MUC1 aptamer (for targeted delivery of paclitaxel to Breast cancer) [89], and EpCAM (for targeted delivery of curcumin, and Nutlin-3a to a colorectal adenocarcinoma) [90].

Chitosan is a natural and biocompatible polymer also used to design nanocarriers displaying mean diameters between 100 and 200 nm. Chitosan is also used to coat other nanocarriers to modulate their bioavailability. MUC1-aptamer-decorated chitosan or hyaluronan/chitosan nanoparticles for targeted delivery of SN38 and 5-fluorouracil to MUC1-overexpressing adenocarcinomas successfully improved the cytotoxicity of the drug compared to the unconjugated nanoparticles by increasing the specific cellular delivery [91, 92]. In addition to the delivery of small molecules, plasmid (pDNA) and siRNA have been successfully delivered into tumor cells for gene silencing and therapy using aptamer-guided nanocarriers. The cationic polymer polyethylenimine (PEI) was used to complex pDNA containing the firefly luciferase gene an anti-MUC1 aptamer to target A549 cancer cells *in vitro* and *in vivo* [93]. pDNA/PEI/MUC1 aptamer complexes showed higher gene expression in a mouse xenograft model of human lung cancer, compared to pDNA/PEI/random aptamer sequence

[93]. As for siRNA delivery, anti-CD30 and anti-EpCAM aptamers have been complexed with PEI for the delivery of siRNA against the anaplastic lymphoma kinase (ALK) fusion oncogene and EpCAM proteins for targeting lymphoma and breast cancer [94, 95]. Despite the significant toxicity of PEI, such a combination in using PEI to complex aptamers and siRNA may have advantages including high uptake, tumor cell-selectivity, and cancer gene-specificity. However, this raises concerns about the proper orientation of aptamers upon random complexing with cationic molecules [94, 95].

Dendrimers are synthetic, highly branched (tree-like) macromolecules with nanometric dimensions composed of three components: the core, branches of the interior, and the surface functional groups. Dendrimers can be synthesized by divergent or convergent methods to produce homogenous nanostructures with low polydispersity, unified size and shape, and with polyvalent multiple functional groups on the surface. Dendrimers are characterized by their biocompatibility, high water solubility and sufficient space for loading hydrophobic/ hydrophilic molecules by conjugation or hosting, while the multifunctional groups on the surface offer a high number of sites for conjugation of targeting ligands [96, 97]. Several aptamers have been reported as ligands linked to dendrimers such as the conjugation of the anti-nucleolin aptamer AS1411 to multimolecular hyperbranched dendritic polymer for targeted cancer imaging. The importance of hyperbranched dendritic polymer is to offer more functional groups for aptamers conjugation [98]. An interesting example was the targeted gene delivery system mediated by the second generation of anti-PSMA aptamer (A10-3.2). The PAMAM PEGylated dendrimers have been loaded with the tumor-suppressors/non-coding miR-15a and miR-16-1 and functionalized with anti-PSMA aptamer [99]. They induced apoptosis and selective cell death of prostate cancer cells [99].

Further examples about aptamers-functionalized polymeric nanocarriers are summarized in Table 2.

Table 2: Recent work on aptamer-guided nanocarriers for targeting tumors

Target	Tumors	Aptamer	Therapeutic /Imaging molecule	Nanocarrier	Biological model	Ref
Nucleolin	Breast	AS1411 (DNA)	Cisplatin	PEGylated liposomes	*In vitro*	[66]
	Breast		Doxorubicin	PEGylated liposomes	*In vitro and in vivo*	[65]
	Breast		Gadolinium compounds	PEGylated thermosensitive liposomes	*In vitro*	[69]
	Breast		Doxorubicin	PEGylated thermosensitive liposomes	*In vitro and in vivo*	[68]
	Melanoma		B-RAF/siRNA	PEGylated cationic-liposomes	*In vitro and in vivo*	[72]
	Ovarian cancer		Paclitaxel	Micelles	*In vitro and in vivo*	[79]
	Breast		Doxorubicin	Micelles	*In vitro and in vivo*	[80]
	Glioma		Paclitaxel	PLGA-b-PEG	*In vitro and in vivo*	[100]
	Breast		Paclitaxel	PLGA-lecithin-PEG	*In vitro*	[85]
	Breast		Doxorubicin	EGVGE	*In vitro*	[101]
	Breast		Fluorescein	Hyperbranched dendritic polymer	*In vitro*	[98]
	Cervical carcinoma		NA	DNA pyramids	*In vitro*	[102]
	Breast		Doxorubicin	UCNPs/MOF	*In vitro*	[103]
	Four cancer subcategories		Direct inhibition by AS1411	Gold-nanostars (AuNS)	*In vitro*	[104]
	Breast		TMPyP4	AuNps	*In vitro*	[105]

	Cervical carcinoma		TMPyP4	AuNR@MS@AgNPs	*In vitro*	[106]
	Breast		Doxorubicin	Polyvalent mesoporus nanoparticles	*In vitro*	[107]
	Breast		Gadolinium	Mesoporous strontium hydroxyapatite nanorods	*In vitro and in vivo*	[108]
PSMA	Prostate	A10(F-RNA)	Doxorubicin	PEGylated liposomes	*In vitro and in vivo*	[67]
			^{225}Ac	PEGylated liposomes	*In vitro and in vivo*	[109]
			Doxorubicin	Micelles	*In vitro and in vivo*	[81]
			Docetaxel	PLGA-b-PEG	*In vitro and in vivo*	[87]
			Pt(IV)	PLGA-b-PEG	*In vitro and in vivo*	[110]
			Paclitaxel-	PLA	*In vitro*	[88]
			miR-15a and miR-16-1	PAMAM-PEG	*In vitro*	[99]
			Doxorubicin	QD (CdSe/ZnS core-shell QD490)	*In vitro*	[111]
			Doxorubicin	TCL-SPION	*In vitro and in vivo*	[112]
		A9 (F′-Py-RNA)	Doxorubicin	Plasmid composed of unmethelated CpG	*In vitro and in vivo*	[113]
MUC1	Colorectal adenocarcinoma	DNA	5-fluorouracil	Hyaluronan/chitosan	*In vitro*	[91]

	Breast /metastasis		Fluorescent probes	Silica	*In vitro*	[108]
	Lung		pDNA	Polyethylinamine (PEI)	*In vitro and in vivo*	[93]
	Colon		SN38	Chitosan	*In vitro*	[92]
	Breast		Paclitaxel	PLGA	*In vitro*	[89]
	Breast		Doxorubicin	3D DNA nanoparticles (polyhedra)	*In vitro*	[114]
	Prostate		Daunorubicin	$CuInS_2$ quantum dot	*In vitro*	[115]
	Ovarian		Doxorubicin	QD	*In vitro*	[47]
	Lung		Zn^2+ doped CdTe QDs	Zn-doped CdTe QDs	*In vitro and in vivo*	[116]
PTK7	T-ALL	Sgc8 (DNA)	FITC-Dextran	PEGylated liposomes	*In vitro*	[74]
			Doxorubicin	DNA dendimersY-shaped DNA monomers	*In vitro*	[117]
			Doxorubicin	Polyvalent aptamer system	*In vitro*	[49]
			Doxorubicin	Au-Ag nanorods	*In vitro*	[118]
			NA	Au/MnO (nanoflowers)	*In vitro*	[113]
			Daunorubicin	Single-walled carbon nanotubes	*In vitro*	[119]
			Doxorubicin	Porous lagnatite nanoparticles (PHMNP), PEG	*In vitro*	[120]
		Sgc8c (DNA)	Prophyrines	Protein shell of bacteriophage MS2	*In vitro*	[121]
			Doxorubicin	Au	*in vitro*	[122]

			Daunorubicin	Acoustic droplets	*In vitro*	[123]
			Fluorescent dye	MS2 capsid	*In vitro*	[124]
			Photodynamic therapy and photothermal therapy	AuNR-ASP-Ce6	*In vitro*	[125]
			Daunorubicin	Au	*In vitro*	[126]
IGHM	Burkitt's lymphoma	TDO5 (DNA)	Uptake study	PEGylated micelles	*In vitro (uptake study)*	[78]
			Uptake study	Bivalent aptamer	*In vitro (uptake study)*	[127]
HER2	Breast	DNA aptamer	shRNA	AuNPs	*In vitro*	[128]
		DNA aptamer	Hyperthermia	Dextran-coated ferric oxide	*In vitro*	[129]
		HB5 aptamer	Doxorubicin	Silica-carbon	*In vitro*	[130]
		S6 aptamer	Fe3O4	Plasmonic/magnetic nanoparticles	*In vitro*	[131]
CD44	Breast, Lung	Apt1(F′-Py-RNA)	NA	liposomes	*In vitro*	[70]
CD133	Osteosarcoma CSCs	RNA (A15)	Salinomycin	PLGA-b-PEG	*In vitro and in vivo*	[84]
EpCAM	Lung	EpApt	Doxorubicin	PLGA-b-PEG	*In vitro and in vivo*	[83]
	Colorectal	EpApt	Lecithisn curcumin	PLGA-b-PEG	*In vitro and in vivo*	[132]
	Breast, Ovarian	EpApt	Nutlin-3a /Quantum Dot 605	PLGA-b-PEG	*In vitro spheroid model*	[90]

	Breast	EpApt	EpCAM siRNA	PEI nanoplexes	*In vitro*	[95]
	Hepatocellular carcinoma	EpApt	Doxorubicin	carboxy-methyl cellulose (CMC)-magnatic iron oxide	*In vitro*	[133]
E-Selectin	Breast	ESTA(Thiolated DNA)	Gemcitabine	PEGylated liposomes	*In vitro and in vivo*	[75]
EGFR	Breast	E07 aptamer	Anti-miR-21	Aptamer conjugate	*In vitro and in vivo*	[58]
CD30	Lymphoma	CD 30 (RNA)	siRNA to ALK	PEI	*In vitro*	[94]
Tenascin-C	Glioma	GBI-10	Gadolinium compounds	PEGylated Liposomes	*In vitro*	[134]
	Glioma	GBI-10	CdSe/ZnS	QD–Apt nanoprobes	*In vitro*	[135]
VEGF	Vasicular endothelial cells	F′-Py-RNA	Inhibit the binding of VEGF to receptor	liposomes	*In vitro and n vivo*	[64]
PDGFR	Breast cancer	DNA	Doxorubicin	Thermosensitive liposomes	*In vitro and in vivo*	[71]
Cell-Selex	Breast cancer	SRZ1	Doxorubicin	Cationic-liposomes	*In vitro and in vivo*	[136]
Transferrine	Human cervical cancer	C2	siRNA (eGFP)	PEGylated liposomes	*In vitro*	[73]
mTEC	Human renal cell carcinoma	AraHH001	Uptake study	PEGylated liposomes	*In vitro and in vivo*	[77]
hnRNP	Different cancer cell lines	DNA	Inhibition of hrRNP	Fluorecent carbon nanodots (CDots)	*In vitro*	[137]

3.2.4. Biomimetic carriers

The bacteriophage MS2 display a protein coat with 180 sequences of identical monomers that are arranged as a spherical structure. The protein coat can be expressed and self-assembled readily in *Escherichia coli* to produce a genome-free nanostructure that is robust, non-toxic and biodegradable. The MS2 viral capside has pores enable to trap therapeutics and imaging molecules. For example, the sgc8c aptamer that targets PTK-7 has been conjugated to bacteriophage MS2 produced in *E. coli*. The interior of the virus capside was modified with porphyrins capable of generating cytotoxic singlet oxygen after UV irradiation, and the surface of the capside was then functionalized with sgc8c aptamer for targeting Jurkat leukemia T cells. The capside was able to kill selectively 76% of the targeted tumor cells after illumination for 20 min [121, 124].

DNA nanostructures are nanometric structures made of self-assembled DNA building blocks. Recently there has been an increasing interest in DNA nanostructures by many disciplines. They are biodegradable, biocompatible, allow control of the size, shape, and the position of functional groups for the conjugation of targeting ligands [102]. Aptamers were successfully conjugated to DNA nanostructures such as the AS1411 to DNA pyramids [102]. The construction of AS1411 aptamer into DNA-pyramid nanostructure was found to increase the resistance against nucleases and the selective cellular uptake compared to the single stranded aptamers [102]. In a further interesting approach, the six anti-MUC1 aptamers have been conjugated to 3D DNA icosahedra nanostructure for targeting MCF-7 breast cancer cells and deliver doxorubicin [114]. Around 1200 doxorubicin molecules have been chelated to each icosahedral nanocarriers [114]. One interesting advantage of such a DNA nanostructure is the large chelating ability versus doxorubicin and the possibility of delivering this drug in a selective manner into targeted cancer cells. Moreover, the anti-PSMA aptamer (A9) has been linked to unmethylated CpG motifs and used to functionalize dendrimers followed by

doxorubicin loading [113]. The system was showed to improve the chemoimmunotherapy of prostate cancer cells [113]. Finally, construction of multiple copies of anti-PTK7 aptamer (sgc8) to three armed Y-DNA has been found to improve the binding affinity compared to monovalent aptamer [117].

3.2.5. Inorganic nanoparticles

Inorganic nanoparticles, such as the metal-based ones, usually display a high monodispersity and can be synthesized with chemical groups that can be conjugated to a variety of ligands for targeting purposes. Besides, therapeutics and imaging, metal nanoparticles can be used in a wide range of applications including diagnostic magnetic separation, concentration and detection of analytes. Although metallic nanoparticles are nonspecific and difficult to eliminate from the circulation and can, therefore, induce long-term toxicity to normal tissues, functionalizing these nanoparticles with aptamers was seen by many authors as a promising strategy for the delivery of therapeutics and imaging molecules [138]. For instance, gold nanoparticles functionalized with the AS1411 aptamer were tested on 12 cancer cell lines that represent four cancer subcategories. These construct increased the cell death by 17% compared to free AS1411 aptamer alone. Interestingly, visualizing the active trafficking of AS1411-Au nanoparticles allowed to observed the active transportation into the nucleus, which induced phenotypic changes to the nuclear envelop and leads to cell apoptosis [139]. Moreover, the combination between tracking cancer cells and inducing hyperthermia has been verified by targeting MCF7 cancer cells using multimodal imaging nanoparticles (Gd_2O_3 and Ag nanoparticles) functionalized with the AS1411 aptamer [140]. In another interesting approach, a co-drug delivery platform has been developed by conjugation of the AS141 aptamer tethered with 21 base pairs of $(CGATCGA)_3$ repeats to Au nanoparticles and the photosensitizer TMPyP4. The doxorubicin was chelated into the bases of the AS1411 tethered linker. The photodynamic stimulation of these construct triggered the release of doxorubicin

in cancer cells with higher cytotoxicity compared to free doxorubicin [105]. Several examples proved the potency of using aptamer-functionalized metallic nanoparticles after photothermal and/or photodynamic therapy [106, 125]. For example, the dextran-coated ferric oxide magnetic nanoparticles have been conjugated with the HER2 aptamer and used to induce hyperthermia in SK-BR-3 cells (target cells) and U-87 MG cells (control cells). A 19-fold lower dose was required to achieve 50% cell death in targeted cells by the aptamer conjugated nanoparticles compared to non-conjugated ones, while maintaining 100% cell viability in control cells at all tested doses. Interestingly, a further study has showed that the targeting of HER2 receptor by the HER2 aptamer conjugated to gold (Au) nanoparticles can reduce receptor recycling and induce the degradation of HER2 receptor [128, 129, 141]. In a similar approach, the hnRNP aptamer was conjugated to carbon nanotubes and has been found to bind multiple tumor cell lines and inhibit the tumor proliferation by inhibition of the heterogeneous nuclear ribonucleoprotein (hrRNP) A2/B1 [137].

The conjugation of aptamers to metallic nanoparticles can increase the binding affinity of nanoparticles. For example, the functionalization of sgc8c aptamer to Au-Ag nanorods has increased the binding affinity by 26 times to CCRF-CEM cells compared to the dye-labeled aptamer alone, and increased 300 times the fluorescence signal obtained from flow cytometry compared to the free aptamer [142]. The sgc8c-functionalized Au-Ag nanorods were tested for the selective photothermal therapy in mixed cancer cells. After exposure to a specific laser intensity, 50% of CCRF-CEMM cells were killed compared to 13% cell death in the control cells (NB-4) [142]. Aptamers have also been successfully addressed as a targeting ligands in cell imaging [143], and for the design of multifunctional nanocarriers that mediate drug delivery and cell imaging [111]. For example, the AS1411 aptamer was functionalized to UCNPs/MOF complexes followed by doxorubicin loading to form UCNPs/MOF-Dox-AS1411 multifunctional nanocarriers that mediate drug delivery and cell imaging [103]. In

addition, several aptamers have been guided metallic nanoparticles for doxorubicin delivery and showed higher toxicity to targeted cells and minimized side effects to non-targeted cells such as the conjugation of the PSMA aptamer (A10) with superparamagnetic iron oxide [144]. Other example include the PTK7 aptamer with Au and CaCO3 nanoparticles [145, 146], MUC1 aptamer to pH-responsive quantum dots [147] and EpCAM aptamer to carboxymethyl cellulose (CMC)-magnetic iron oxide nanoparticles [133]. In addition to the doxorubicin, daunorubicin is another antitumor drug widely used in the treatment of acute myeloid leukemia and the childhood cancers that can be chelated into CG rich sequences. Danesh *et al.* [126] loaded daunorubicin into gold nanoparticles functionalized with the PTK7 aptamer (sgc8c) to target T cell acute lymphoblastic leukemia. The resulting Apt-daunorubicin-Au nanoparticles showed a higher internalization and delivery of daunorubicin into cells *in vitro* with a higher release of daunorubicin in response to a decrease in pH [126].

3.2.6. Silica nanoshells

Nanoshells are a class of nanoparticles with magnetic resonances properties. They are composed of a silica core and a metal outer layer and can absorb and scatter resonances at any electromagnetic spectrum including in the near infrared spectrum which is optimal for penetrating tissues without interference. Nanoshells can carry both therapeutics and imaging agents and the radiation absorbance by nanoshells is suitable for hyperthermia-based therapeutics in cancer. Inducing the temperature in the cancer cells after localized irradiation will end with irreversible cellular damage [148]. Therefore, a higher uptake of nanoshells by cancer cells compared to normal tissues could improve the therapeutic and imaging efficacy. Several studies validated the delivery of therapeutic and imaging agents, or combination of both, using a variety of aptamer-functionalized mesoporous nanoparticles [46, 108, 149-152]. For example, the HER2 aptamer (HB5) attached to silica-carbon and loaded with doxorubicin has been constructed for chemo-photothermal therapy of $HER2^{+}$ breast cancer cell line (SK-

BR-3) but not the normal MCF7-10A cell line. The results demonstrated a higher cytotoxicity of the combined therapy compared to chemo- or photo-therapy alone, showing the synergistic effect of both therapeutic modalities [130].

Sealing mesoporous nanoparticles for drug loading and selective delivery into cancer cells is a major concern. Zhang *et al.* [153] have developed redox-responsive mesoporous nanoparticles loaded with doxorubicin and sealed with cytochrome c via disulfide bond followed by conjugation of the AS1411 aptamer for selective targeting. Such nanocarrier exhibits triple therapeutic combination to tumors: doxorubicin induces apoptosis, cytochrome c participates in protease activation, and the AS1411 can destabilize the anti-apoptotic protein BCL-2.

3.3. Optimizing aptamer-based targeting delivery with nanocarriers

Achieving the optimal targeting efficacy and long-time circulation properties require a precise engineering of the nanoparticles. In general, there are several factors that influence the efficacy of nanocarriers as a drug carrier including size, surface charge, shape, sterical stabilization, density of targeting ligands, and density of target receptors [154]. For instance, particles with a diameter larger than 500 nm easily undergo phagocytosis by macrophages [155]. The surface charge of nanoparticles also influences the cellular entry. The cellular membrane being negatively charged, cationic nanoparticles have higher affinity to the cell surface, which can increases their uptake compared to the negatively charged or neutral counterparts. In tumors, cationic nanoparticles favor binding to the epithelium of tumor neovasculature, which alters the deep distribution into tumor tissues and reduces the systemic circulation of these nanoparticles [8].

The density of aptamers on the surface of nanoparticles can affect the stealth properties of nanoparticles. For example, Gu *et al.* [156] have investigated the effect of PSMA aptamer (A10) density on the maximum targeting efficacy with stealth stability when functionalized to PLGA-b-PEG nanoparticles. The findings of this study showed an increase in the

accumulation of targeted nanoparticles at a 5% aptamer/nanoparticle ratio while no further increase in the targeting efficacy was observed beyond this ratio [156]. Interestingly, there was an increase in the accumulation of PLGA-b-PEG nanoparticles in the liver with increasing aptamer density [156]. Such findings can be explained by the reduction of the stealth properties of PLGA-b-PEG nanoparticles due to the high aptamer density [156]. In different studies, Bandekar *et al.* [109] have compared the targeting efficacy of liposomes loaded with ^{225}Ac and functionalized with the PSMA specific ligands (J591 antibody, and A10 aptamer). The average numbers of targeting ligands per liposome were 17 and 9 for J591 and A10 ligands, respectively. The results of this study showed a specific uptake for both J591-labeled liposomes and A10-labeled liposomes by $PSMA^+$ cells compared to $PSMA^-$ cells. On the other hand, a higher cellular uptake of J591-labeled liposomes was obtained compared to A10-labeled liposomes, which can be related to the lower number of aptamers conjugated to each liposome molecules. Moreover, the antibodies have two binding regions for each. Thus, a careful optimization of aptamer density should be performed to conclude the preferences of using targeting ligands [109].

4. Aptamers as tumor therapeutics

4.1. Aptamers as antagonists for extracellular targets

Aptamers can antagonize the functions of extracellular targets in the bloodstream or on the cell surface by direct interaction (figure 3). For instance, aptamers have been selected to a number of growth factors such as vesicular endothelial growth factor (VEGF) [157], basic fibroblastic growth factor (bFGF) [158], platelets-derived growth factor (PDGF) [159], and keratinocytes growth factor (KGF) [160]. These aptamers can bind these growth factors and block the interaction with their receptors, which has been proved as an efficient therapeutic strategy for cancer treatment [161]. Moreover, aptamers can antagonize the function of

receptors by blocking the receptor interaction with the growth factors. For instance, the human epidermal growth factor receptor (hEGFR), a member of receptor tyrosine kinases family, has been found overexpressed and involved in the progression of several tumors such as lung cancer [162]. An RNA aptamer selected to hEGFR was able to block the binding of EGFR to its ligand (the endothelial growth factor, EGF), inhibit the receptor autophosphorylation and reduce the human epidermoid carcinoma cells (A431) proliferation [163].

Aptamers selected against cell surface targets can play dual functions, as antagonist and as targeting ligands. One interesting example is the nucleolin aptamer. Nucleolin (NCL) is a multifunctional protein with molecular weight of 77 kDa, found in different compartments of the cell including nucleus, cytoplasm, and on the cell membrane of eukaryotic cells. NCL plays different roles in each cell compartment to control cell homeostasis such as ribosome biogenesis, cell growth and proliferation, cytokinesis, signal transduction and organization of the chromatin structure [164]. NCL has been found overexpressed and preferentially localized on the cell membrane of many tumors, and involved in cell proliferation and survival (for review see ref. [165]). The G-rich oligonucleotide DNA aptamer named AS1411 (formerly AGRO100) was developed as a direct G-rich aptamer (not derived by SELEX) to bind NCL. AS1411 demonstrated by itself an antiproliferative activity against 80 cancer cells line tested with a growth inhibitory concentrations 50 (GI_{50}) in the micromolar range [166-169].

4.2. Aptamers as antagonists for intracellular targets

The majority of aptamers have been selected to bind extracellular targets for the significance of these targets in tumor biology. Moreover, the access to those targets is straightforward since there is no need to cross the cellular membrane to reach them. Despite the challenge, such barrier did not limit the efforts to select aptamers for potential intracellular targets (figure 3) such as kinases, coenzymes, transcription factors, and anti-apoptotic proteins [170-

172]. However, aptamers, as other nucleic acid-based therapeutic molecules, need a delivery system to reach their intracellular target. There are two mechanisms for the delivery of aptamers, either by cellular transfection or by intracellular expression (so called intramers). An important concern regarding the delivery of aptamers to intracellular targets is maintaining their structural functionality. However, successful delivery of aptamers for intracellular targets has been addressed. For example, Zamay *et al.* [173] have developed a DNA aptamer against vimentin which is an important protein for maintaining cell shape, integrity of the cytoplasm and stability of the cell cytoskeleton. The anti-vimentin aptamer (NAS-24) was complexed with the natural polysaccharide arabinogalactan carrier, and the whole complex was administered intraperitoneally to mice bearing adenocarcinoma as a single dose every day for 5 days. The results showed a higher inhibition obtained by NAS-24-arabinogalactan complexes compared to NAS-24 or arabinogalactan alone. Another interesting example is the delivery of a β-catenin RNA aptamer into the nucleus of HepG2 human cells via gold nanoparticles. The aptamer successfully binds B-catenin and inhibit its interaction with p50 subunit of NF-kB in the nucleus, which induce repression of NF-jB p50-dependent transcription in human cells. In the same study, gold nanoparticles have been used to deliver another RNA aptamer targeted to the p50 subunit of NF-jB into the A549 human cell line, and was sufficient to induce apoptosis of A549 cells [174]. In a further example, Maasch *et al.* [175] reported the selection of L-RNA aptamer (so called Spiegelmers) against the high mobility group A1 (HMGA1) transcription factor that is overexpressed in many cancers. In this study, the best two spiegelmers, NOX-A50 and NOX-F33, were found to inhibit the binding of HMGA1 to its partners. The NOX-A50 was PEGylated and complexed with PEI. The results showed enhanced delivery and improved distribution of NOX-A50 spiegelmer in tumor which has successfully reduced the tumor volume in a muse xenograft model of human pancreatic cancer.

In addition to their delivery using nanocarriers, aptamers were successfully expressed intracellularly as intramers. Several proteins have been targeted with intramers such as the splicing factor B52, the selenocysteine-specific elongation factor SelB, HIV-RT, the guanine nucleotide-exchange protein cytohisine, and the transcription factor NF-kB [176]. For example, an RNA aptamer (named M69) against cytohesin 1 has been delivered by the vaccinia virus vector and successfully expressed in the cytoplasm of Jurkat T cells. The expression of M69 intramer has destabilized the reorganization of the cell cytoskeleton and spreading by inhibition of LFA-1-mediated adhesion [177]. Based on these results, the expression of intramers displays a promising strategy to regulate the cellular pathways and studying the protein functions in normal and diseased cells such as cancer [176]. Moreover, the vaccination of cells such as T cells or stem cells with a stable expression of intramers against pathogenic protein targets or oncogenic proteins could be promising in the future [178]. However, the concerns about the immunogenicity of viral vectors and the specificity of delivery and expression in targeted cells should be carefully addressed and considered.

4.3. Aptamers as agonists

Aptamers can also work as agonists (figure 3) and stimulate signaling pathways. For instance, an RNA aptamer was able to activate the OX40 receptor after binding [179]. The OX40 receptor is a member of the TNF receptors family, expressed on activated T cells. Aptamer-mediated activation of the OX40 receptor on T cells was found to stimulate an antitumor immune response. The mechanism of the OX40 receptor activation requires dimerization of OX40 aptamer while this is impossible with monomeric aptamer. Importantly, activation of OX40 receptor by antibodies against the same receptor was shown to simulate an immune response against the murine antibodies after one single administration [180]. Similarly, the CD30 receptor protein is overexpressed in Hodgkin’s lymphomas and anaplastic large cell

lymphoma. Activation of CD30 through trimerization of the receptor has been found to induce apoptosis in anaplastic large cell lymphoma. Indeed, a polymer of anti-CD30 DNA aptamer has been generated through biotin-streptavidin interaction. These polymers of anti-CD30 aptamer were able to induce activation of CD30 receptor trimerization leading to apoptosis in K299 cells of anaplastic large cell lymphoma. In another interesting study, the activation of human epidermal growth factor receptor 2 (ErB-2/HER2) with an anti-HER2 DNA aptamer reduced the growth of tumor in a model of xenografted human gastric cancer in mice. HER2 is a tyrosine kinase receptor overexpressed in several cancers including breast and gastric tumors. Such tumor growth inhibition may occur when the trimeric anti-HER2 aptamer promotes the translocation of the HER2 from the cell surface into the cytoplasm and induces the lysosomal degradation of the HER2 receptor, thereby losing the proliferative effect of oncogenic HER2 receptor. Such agonist therapeutic effects of aptamers might open up interesting properties in cancer therapeutics.

5. Aptamers in clinic

There are several aptamers involved in clinical trials, either as direct therapeutic molecules or as targeting ligands for selective delivery of other therapeutic molecules. Such clinical trials offer valuable information for more understanding of aptamers behavior in human.

Pegaptanib. Pegaptanib (Macugen) is a 2′-fluoro-pyrimidine-containing RNA aptamer post-modified with 2′-*O*-methyl-purines to induce resistance against nucleases and conjugated to 40 kDa PEG for stealth stability. Pegaptanib can decrease the angiogenesis through binding to VEGF and inhibition of its interaction with VEGFR1 and VEGFR2. Pegaptanip was approved in 2004 by the US food and drug administration (FDA) for the treatment of age-related macular degeneration. Recently pegaptanib sales diminished because of recent marketing of the antibody fragment ranibizumab which can bind all isoformes of VEGF [157, 181].

AS1411. AS1411 is a G-rich DNA aptamer known to bind nucleolin and can inhibit nucleolin

based signaling pathways. AS1411 entered clinical trial phase II for the treatment of acute myeloid leukemia. Moreover, AS1411 showed antitumor activities in a clinical trial phase I in patients with metastatic renal cell carcinoma. However, this trial has been terminated in phase II because of the low level of activity with only 2.9 % of partial response [182].

NOX.A12. NOX.A12 is L-RNA aptamer (Spiegelmer) can bind to the chemokine CXCL12. CXCL12 play roles in cell metastasis, homing, angiogenesis, and proliferation. NOX.A12 inhibits CXCL12 functions in tumors including the attraction of tumor cells to niches in bone marrow, protection of tumor cells from immune cells, attraction of repairing cells to heal tumor cells after tumor therapy such as radiotherapy. NOX.A12 is now in phase II clinical trial in combination with other chemotherapies, bendamustine and rituximab, for the treatment of chronic lymphocytic leukemia and completed phase II clinical trial in combination with bortezomib and dexamethasone for the treatment of relapsed multiple myeloma [183].

Bind014. BIND014 is PLGA-b-PEG nanoparticle loaded with docetaxel and functionalized with A10-PSMA aptamer. BIND-014 is the first aptamer-based targeted drug delivery system for the treatment of patients with solid tumors. It has now entered clinical trials phase II. Preclinical studies had showed 100 fold higher docetaxel plasma concentrations compared to free docetaxel which is related to the prolonged circulation of nanoparticles with a 12 h half-life. Moreover, phase I trial on 45 patients with advanced or metastatic cancer who failed the first-line therapy showed tumor shrinkage at concentrations 5 times lower comparing the concentrations of free docetaxel to obtain the same tumor response. The overall results of the phase I trial on BIND-014 have demonstrated the safety and good tolerance related to higher accumulation of docetaxel in tumor [184].

6. Conclusions and future perspectives

Aptamers are nucleic acid based smart binding ligands which have sophisticated properties suitable for many applications in tumor biology such as therapy, diagnosis and targeting. Aptamers evolved since their discovery in 1990 into a mature filed with tremendous promises for the future. With respect to other targeting ligands used in drug delivery, aptamers-functionalized nanoparticles have succeeded to guide different types of regimens into tumors with high targeting efficacy. Several chemical modifications have been applied to aptamers sequences to increase nuclease resistance and stability *in vitro* and *in vivo*. PEGylation of aptamers increased their circulation half-life and thus allow them to perform biological functions. The conjugation engineering aptamers to different types of nanocarriers is increasingly well established. The first aptamer-functionalized polymeric nanoparticles targeting PSMA-expressing tumor cells have completed clinical phase II trials with promising outcomes.

7. References

[1] The World Cancer Report--the major findings, Cent Eur J Public Health, 11 (2003) 177-179.

[2] A. Kreso, J.E. Dick, Evolution of the cancer stem cell model, Cell Stem Cell, 14 (2014) 275-291.

[3] J.R. Heath, M.E. Davis, Nanotechnology and cancer, Annu Rev Med, 59 (2008) 251-265.

[4] K.Y. Kim, Nanotechnology platforms and physiological challenges for cancer therapeutics, Nanomedicine, 3 (2007) 103-110.

[5] U. Prabhakar, H. Maeda, R.K. Jain, E.M. Sevick-Muraca, W. Zamboni, O.C. Farokhzad, S.T. Barry, A. Gabizon, P. Grodzinski, D.C. Blakey, Challenges and key considerations of the enhanced permeability and retention effect for nanomedicine drug delivery in oncology, Cancer Res, 73 (2013) 2412-2417.

[6] L.Y. Rizzo, B. Theek, G. Storm, F. Kiessling, T. Lammers, Recent progress in nanomedicine: therapeutic, diagnostic and theranostic applications, Curr Opin Biotechnol, 24 (2013) 1159-1166.

[7] D. Peer, J.M. Karp, S. Hong, O.C. Farokhzad, R. Margalit, R. Langer, Nanocarriers as an emerging platform for cancer therapy, Nat Nanotechnol, 2 (2007) 751-760.

[8] N. Bertrand, J. Wu, X. Xu, N. Kamaly, O.C. Farokhzad, Cancer nanotechnology: the impact of passive and active targeting in the era of modern cancer biology, Adv Drug Deliv Rev, 66 (2014) 2-25.

[9] R. Dahm, Discovering DNA: Friedrich Miescher and the early years of nucleic acid research, Human Genetics, 122 (2008) 565-581.

[10] T.R. Cech, Ribozymes, the first 20 years, Biochemical Society Transactions, 30 (2002) 1162-1166.

[11] S. Jones, D.T.A. Daley, N.M. Luscombe, H.M. Berman, J.M. Thornton, Protein-RNA interactions: a structural analysis, Nucleic Acids Research, 29 (2001) 943-954.

[12] S. Jones, P. van Heyningen, H.M. Berman, J.M. Thornton, Protein-DNA interactions: A structural analysis, Journal of Molecular Biology, 287 (1999) 877-896.

[13] D.S. Wilson, J.W. Szostak, In vitro selection of functional nucleic acids, Annual Review of Biochemistry, 68 (1999) 611-647.

[14] C. Tuerk, L. Gold, Systematic evolution of ligands by exponential enrichment: RNA ligands to bacteriophage T4 DNA polymerase, Science, 249 (1990) 505-510.

[15] A.D. Ellington, J.W. Szostak, In vitro selection of RNA molecules that bind specific ligands, Nature, 346 (1990) 818-822.

[16] A.D. Ellington, J.W. Szostak, Selection in vitro of single-stranded DNA molecules that fold into specific ligand-binding structures, Nature, 355 (1992) 850-852.

[17] L.C. Bock, L.C. Griffin, J.A. Latham, E.H. Vermaas, J.J. Toole, Selection of single-stranded DNA molecules that bind and inhibit human thrombin, Nature, 355 (1992) 564-566.

[18] L. Gold, SELEX: How It Happened and Where It will Go, Journal of Molecular Evolution, (2015).

[19] J.C. Rohloff, A.D. Gelinas, T.C. Jarvis, U.A. Ochsner, D.J. Schneider, L. Gold, N. Janjic, Nucleic Acid Ligands With Protein-like Side Chains: Modified Aptamers and Their Use as Diagnostic and Therapeutic Agents, Mol Ther Nucleic Acids, 3 (2014) e201.

[20] T. Fitzwater, B. Polisky, A SELEX primer, Methods Enzymol, 267 (1996) 275-301.

[21] S.K. Piasecki, B. Hall, A.D. Ellington, Nucleic acid pool preparation and characterization, Methods Mol Biol, 535 (2009) 3-18.

[22] R. Stoltenburg, C. Reinemann, B. Strehlitz, SELEX--a (r)evolutionary method to generate high-affinity nucleic acid ligands, Biomol Eng, 24 (2007) 381-403.

[23] K. Groff, J. Brown, A.J. Clippinger, Modern Affinity Reagents: Recombinant Antibodies and Aptamers, Biotechnol Adv, (2015).

[24] S.D. Jayasena, Aptamers: an emerging class of molecules that rival antibodies in diagnostics, Clin Chem, 45 (1999) 1628-1650.

[25] S.M. Nimjee, C.P. Rusconi, B.A. Sullenger, Aptamers: an emerging class of therapeutics, Annu Rev Med, 56 (2005) 555-583.

[26] M. Darmostuk, S. Rimpelova, H. Gbelcova, T. Ruml, Current approaches in SELEX: An update to aptamer selection technology, Biotechnology Advances, 33 (2015) 1141-1161.

[27] S. Catuogno, C.L. Esposito, V. de Franciscis, Developing Aptamers by Cell-Based SELEX, Methods Mol Biol, 1380 (2016) 33-46.

[28] A. Yan, M. Levy, Cell internalization SELEX: in vitro selection for molecules that internalize into cells, Methods Mol Biol, 1103 (2014) 241-265.

[29] F. Cavallo, C. De Giovanni, P. Nanni, G. Forni, P.L. Lollini, 2011: the immune hallmarks of cancer, Cancer Immunol Immunother, 60 (2011) 319-326.

[30] D. Hanahan, R.A. Weinberg, Hallmarks of cancer: the next generation, Cell, 144 (2011) 646-674.

[31] S. Jeong, S.R. Han, Y.J. Lee, J.H. Kim, S.W. Lee, Identification of RNA aptamer specific to mutant KRAS protein, Oligonucleotides, 20 (2010) 155-161.

[32] A. Ghosh, W.D. Heston, Tumor target prostate specific membrane antigen (PSMA) and its regulation in prostate cancer, J Cell Biochem, 91 (2004) 528-539.

[33] S.E. Lupold, B.J. Hicke, Y. Lin, D.S. Coffey, Identification and characterization of nuclease-stabilized RNA molecules that bind human prostate cancer cells via the prostate-specific membrane antigen, Cancer Res, 62 (2002) 4029-4033.

[34] C.S.M. Ferreira, C.S. Matthews, S. Missailidis, DNA aptamers that bind to MUC1 tumour marker: Design and characterization of MUC1-binding single-stranded DNA aptamers, Tumor Biology, 27 (2006) 289-301.

[35] L. Cerchia, F. Duconge, C. Pestourie, J. Boulay, Y. Aissouni, K. Gombert, B. Tavitian, V. de Franciscis, D. Libri, Neutralizing aptamers from whole-cell SELEX inhibit the RET receptor tyrosine kinase, Plos Biology, 3 (2005) 697-704.

[36] D. Shangguan, Z. Cao, L. Meng, P. Mallikaratchy, K. Sefah, H. Wang, Y. Li, W. Tan, Cell-specific aptamer probes for membrane protein elucidation in cancer cells, Journal of proteome research, 7 (2008) 2133-2139.

[37] D. Shangguan, Y. Li, Z.W. Tang, Z.H.C. Cao, H.W. Chen, P. Mallikaratchy, K. Sefah, C.Y.J. Yang, W.H. Tan, Aptamers evolved from live cells as effective molecular probes for cancer study, Proceedings of the National Academy of Sciences of the United States of America, 103 (2006) 11838-11843.

[38] H. Clevers, The cancer stem cell: premises, promises and challenges, Nature Medicine, 17 (2011) 313-319.

[39] N. Ababneh, W. Alshaer, O. Allozi, A. Mahafzah, M. El-Khateeb, H. Hillaireau, M. Noiray, E. Fattal, S. Ismail, In Vitro Selection of Modified RNA Aptamers Against CD44 Cancer Stem Cell Marker, Nucleic Acid Therapeutics, 23 (2013) 401-407.

[40] A. Somasunderam, V. Thiviyanathan, T. Tanaka, X. Li, M. Neerathilingam, G.L.R. Lokesh, A. Mann, Y. Peng, M. Ferrari, J. Klostergaard, D.G. Gorenstein, Combinatorial Selection of DNA Thioaptamers Targeted to the HA Binding Domain of Human CD44, Biochemistry, 49 (2010) 9106-9112.

[41] J. Iida, R. Clancy, J. Dorchak, R.I. Somiari, S. Somiari, M.L. Cutler, R.J. Mural, C.D. Shriver, DNA Aptamers against Exon v10 of CD44 Inhibit Breast Cancer Cell Migration, Plos One, 9 (2014).

[42] S. Shigdar, J. Lin, Y. Yu, M. Pastuovic, M. Wei, W. Duan, RNA aptamer against a cancer stem cell marker epithelial cell adhesion molecule, Cancer Science, 102 (2011) 991-998.

[43] S. Shigdar, L. Qiao, S.F. Zhou, D.X. Xiang, T. Wang, Y. Li, L.Y. Lim, L.X. Kong, L.H. Li, W. Duan, RNA aptamers targeting cancer stem cell marker CD133, Cancer Letters, 330 (2013) 84-95.

[44] Y.L. Song, Z. Zhu, Y. An, W.T. Zhang, H.M. Zhang, D. Liu, C.D. Yu, W. Duan, C.J. Yang, Selection of DNA Aptamers against Epithelial Cell Adhesion Molecule for Cancer Cell Imaging and Circulating Tumor Cell Capture, Analytical Chemistry, 85 (2013) 4141-4149.

[45] D. Xiang, C. Zheng, S.-F. Zhou, S. Qiao, P.H.-L. Tran, C. Pu, Y. Li, L. Kong, A.Z.

Kouzani, J. Lin, K. Liu, L. Li, S. Shigdar, W. Duan, Superior Performance of Aptamer in Tumor Penetration over Antibody: Implication of Aptamer-Based Theranostics in Solid Tumors, Theranostics, 5 (2015) 1083-1097.

[46] Z. Liu, J.-H. Duan, Y.-M. Song, J. Ma, F.-D. Wang, X. Lu, X.-D. Yang, Novel HER2 Aptamer Selectively Delivers Cytotoxic Drug to HER2-positive Breast Cancer Cells in Vitro, Journal of Translational Medicine, 10 (2012) 148-148.

[47] Y. Hu, J. Duan, Q. Zhan, F. Wang, X. Lu, X.-d. Yang, Novel MUC1 Aptamer Selectively Delivers Cytotoxic Agent to Cancer Cells In Vitro, In Vitro, 7 (2012).

[48] K. Wang, M. You, Y. Chen, D. Han, Z. Zhu, J. Huang, K. Williams, C.J. Yang, W. Tan, Self-assembly of a bifunctional DNA carrier for drug delivery, Angewandte Chemie - International Edition, 50 (2011) 6098-6101.

[49] Z. Zhang, M.M. Ali, M.a. Eckert, D.K. Kang, Y.Y. Chen, L.S. Sender, D.a. Fruman, W. Zhao, A polyvalent aptamer system for targeted drug delivery, Biomaterials, 34 (2013) 9728-9735.

[50] Y.-F. Huang, D. Shangguan, H. Liu, J.A. Phillips, X. Zhang, Y. Chen, W. Tan, Molecular assembly of an aptamer-drug conjugate for targeted drug delivery to tumor cells, Chembiochem, 10 (2009) 862-868.

[51] T.C. Chu, J.W. Marks, L.a. Lavery, S. Faulkner, M.G. Rosenblum, A.D. Ellington, M. Levy, J.W.M. Iii, L.a. Lavery, S. Faulkner, M.G. Rosenblum, A.D. Ellington, M. Levy, Aptamer:toxin conjugates that specifically target prostate tumor cells, Cancer Res, 66 (2006) 5989-5992.

[52] G. Lambert, E. Fattal, P. Couvreur, Nanoparticulate systems for the delivery of antisense oligonucleotides, Adv Drug Deliv Rev, 47 (2001) 99-112.

[53] E. Fattal, A. Bochot, Ocular delivery of nucleic acids: antisense oligonucleotides, aptamers and siRNA, Adv Drug Deliv Rev, 58 (2006) 1203-1223.

[54] C.L. Esposito, S. Catuogno, V. de Franciscis, Aptamer-mediated selective delivery of short RNA therapeutics in cancer cells, J RNAi Gene Silencing, 10 (2014) 500-506.

[55] J. Zhou, J.J. Rossi, Aptamer-targeted cell-specific RNA interference, Silence, 1 (2010) 4.

[56] T.C. Chu, K.Y. Twu, A.D. Ellington, M. Levy, Aptamer mediated siRNA delivery, Nucleic Acids Res, 34 (2006) e73.

[57] V. Bagalkot, X. Gao, SiRNA-aptamer chimeras on nanoparticles: preserving targeting functionality for effective gene silencing, ACS Nano, 5 (2011) 8131-8139.

[58] D. Shu, H. Li, Y. Shu, G. Xiong, W.E. Carson, 3rd, F. Haque, R. Xu, P. Guo, Systemic Delivery of Anti-miRNA for Suppression of Triple Negative Breast Cancer Utilizing RNA Nanotechnology, ACS Nano, 9 (2015) 9731-9740.

[59] T.M. Allen, P.R. Cullis, Drug delivery systems: entering the mainstream, Science, 303

(2004) 1818-1822.

[60] K. Greish, Enhanced permeability and retention (EPR) effect for anticancer nanomedicine drug targeting, Methods Mol Biol, 624 (2010) 25-37.

[61] S.D. Perrault, C. Walkey, T. Jennings, H.C. Fischer, W.C.W. Chan, Mediating tumor targeting efficiency of nanoparticles through design, Nano Lett, 9 (2009) 1909-1915.

[62] F. Gambinossi, S.E. Mylon, J.K. Ferri, Aggregation kinetics and colloidal stability of functionalized nanoparticles, Adv Colloid Interface Sci, 222 (2015) 332-349.

[63] G. Bhabra, A. Sood, B. Fisher, L. Cartwright, M. Saunders, W.H. Evans, A. Surprenant, G. Lopez-Castejon, S. Mann, S.A. Davis, L.A. Hails, E. Ingham, P. Verkade, J. Lane, K. Heesom, R. Newson, C.P. Case, Nanoparticles can cause DNA damage across a cellular barrier, Nat Nano, 4 (2009) 876-883.

[64] M.C. Willis, B.D. Collins, T. Zhang, L.S. Green, D.P. Sebesta, C. Bell, E. Kellogg, S.C. Gill, a. Magallanez, S. Knauer, R.a. Bendele, P.S. Gill, N. Janjić, B.D. Collins, Liposome-anchored vascular endothelial growth factor aptamers, Bioconjugate chemistry, 9 (1998) 573-582.

[65] H. Xing, L. Tang, X. Yang, K. Hwang, W. Wang, Q. Yin, N.Y. Wong, L.W. Dobrucki, N. Yasui, J.A. Katzenellenbogen, W.G. Helferich, J. Cheng, Y. Lu, Selective Delivery of an Anticancer Drug with Aptamer-Functionalized Liposomes to Breast Cancer Cells and, J Mater Chem B Mater Biol Med, 1 (2013) 5288-5297.

[66] Z. Cao, R. Tong, A. Mishra, W. Xu, G.C. Wong, J. Cheng, Y. Lu, Reversible cell-specific drug delivery with aptamer-functionalized liposomes, Angew Chem Int Ed Engl, 48 (2009) 6494-6498.

[67] S.E. Baek, K.H. Lee, Y.S. Park, D.-K. Oh, S. Oh, K.-S. Kim, D.-E. Kim, RNA aptamer-conjugated liposome as an efficient anticancer drug delivery vehicle targeting cancer cells in vivo, Journal of Controlled Release, 196 (2014) 234-242.

[68] Z.X. Liao, E.Y. Chuang, C.C. Lin, Y.C. Ho, K.J. Lin, P.Y. Cheng, K.J. Chen, H.J. Wei, H.W. Sung, An AS1411 aptamer-conjugated liposomal system containing a bubble-generating agent for tumor-specific chemotherapy that overcomes multidrug resistance, J Control Release, 208 (2015) 42-51.

[69] K. Zhang, M. Liu, X. Tong, N. Sun, L. Zhou, Y. Cao, J. Wang, H. Zhang, R. Pei, Aptamer-Modified Temperature-Sensitive Liposomal Contrast Agent for Magnetic Resonance Imaging, Biomacromolecules, 16 (2015) 2618-2623.

[70] W. Alshaer, H. Hillaireau, J. Vergnaud, S. Ismail, E. Fattal, Functionalizing Liposomes with anti-CD44 Aptamer for Selective Targeting of Cancer Cells, Bioconjugate Chemistry, 26 (2015) 1307-1313.

[71] K. Ninomiya, T. Yamashita, S. Kawabata, N. Shimizu, Targeted and ultrasound-triggered drug delivery using liposomes co-modified with cancer cell-targeting aptamers and a thermosensitive polymer, Ultrasonics Sonochemistry, 21 (2014) 1482-1488.

[72] L. Li, J. Hou, X. Liu, Y. Guo, Y. Wu, L. Zhang, Z. Yang, Nucleolin-targeting liposomes guided by aptamer AS1411 for the delivery of siRNA for the treatment of malignant melanomas, Biomaterials, 35 (2014) 3840-3850.

[73] S.E. Wilner, B. Wengerter, K. Maier, M. de Lourdes Borba Magalhães, D.S. Del Amo, S. Pai, F. Opazo, S.O. Rizzoli, A. Yan, M. Levy, An RNA Alternative to Human Transferrin: A New Tool for Targeting Human Cells, Molecular Therapy — Nucleic Acids, 1 (2012) e21-e21.

[74] H. Kang, M.B. O'Donoghue, H. Liu, W. Tan, A liposome-based nanostructure for aptamer directed delivery, Chemical communications (Cambridge, England), 46 (2010) 249-251.

[75] A.P. Mann, R.C. Bhavane, A. Somasunderam, B. Liz Montalvo-Ortiz, K.B. Ghaghada, D. Volk, R. Nieves-Alicea, K.S. Suh, M. Ferrari, A. Annapragada, D.G. Gorenstein, T. Tanaka, Thioaptamer conjugated liposomes for tumor vasculature targeting, Oncotarget, 2 (2011) 298-304.

[76] M.N. Ara, M. Hyodo, N. Ohga, K. Hida, H. Harashima, Development of a Novel DNA Aptamer Ligand Targeting to Primary Cultured Tumor Endothelial Cells by a Cell-Based SELEX Method, PLoS One, 7 (2012).

[77] M.N. Ara, T. Matsuda, M. Hyodo, Y. Sakurai, H. Hatakeyama, N. Ohga, K. Hida, H. Harashima, An aptamer ligand based liposomal nanocarrier system that targets tumor endothelial cells, Biomaterials, 35 (2014) 7110-7120.

[78] Y. Wu, K. Sefah, H. Liu, R. Wang, W. Tan, DNA aptamer-micelle as an efficient detection/delivery vehicle toward cancer cells, Proc Natl Acad Sci U S A, 107 (2010) 5-10.

[79] J. Zhang, R. Chen, X. Fang, F. Chen, Y. Wang, M. Chen, Nucleolin targeting AS1411 aptamer modified pH-sensitive micelles for enhanced delivery and antitumor efficacy of paclitaxel, Nano Research, 8 (2015) 201-218.

[80] X. Li, Y. Yu, Q. Ji, L. Qiu, Targeted delivery of anticancer drugs by aptamer AS1411 mediated Pluronic F127/cyclodextrin-linked polymer composite micelles, Nanomedicine, 11 (2015) 175-184.

[81] W. Xu, I.a. Siddiqui, M. Nihal, S. Pilla, K. Rosenthal, H. Mukhtar, S. Gong, Aptamer-conjugated and doxorubicin-loaded unimolecular micelles for targeted therapy of prostate cancer, Biomaterials, 34 (2013) 5244-5253.

[82] R.H. Prabhu, V.B. Patravale, M.D. Joshi, Polymeric nanoparticles for targeted treatment in oncology: current insights, Int J Nanomedicine, 10 (2015) 1001-1018.

[83] M. Alibolandi, M. Ramezani, F. Sadeghi, K. Abnous, F. Hadizadeh, Epithelial cell adhesion molecule aptamer conjugated PEG–PLGA nanopolymersomes for targeted delivery of doxorubicin to human breast adenocarcinoma cell line in vitro, International Journal of Pharmaceutics, 479 (2015) 241-251.

[84] M.Z. Ni, M. Xiong, X.C. Zhang, G.P. Cai, H.W. Chen, Q.M. Zeng, Z.C. Yu, Poly(lactic-

co-glycolic acid) nanoparticles conjugated with CD133 aptamers for targeted salinomycin delivery to CD133(+) osteosarcoma cancer stem cells, International Journal of Nanomedicine, 10 (2015) 2537-2554.

[85] A. Aravind, P. Jeyamohan, R. Nair, S. Veeranarayanan, Y. Nagaoka, Y. Yoshida, T. Maekawa, D.S. Kumar, AS1411 aptamer tagged PLGA-lecithin-PEG nanoparticles for tumor cell targeting and drug delivery, Biotechnol Bioeng, 109 (2012) 2920-2931.

[86] J. Guo, X. Gao, L. Su, H. Xia, G. Gu, Z. Pang, X. Jiang, L. Yao, J. Chen, H. Chen, Aptamer-functionalized PEG-PLGA nanoparticles for enhanced anti-glioma drug delivery, Biomaterials, 32 (2011) 8010-8020.

[87] J. Cheng, B.a. Teply, I. Sherifi, J. Sung, G. Luther, F.X. Gu, E. Levy-Nissenbaum, A.F. Radovic-Moreno, R. Langer, O.C. Farokhzad, Formulation of functionalized PLGA-PEG nanoparticles for in vivo targeted drug delivery, Biomaterials, 28 (2007) 869-876.

[88] R. Tong, L. Yala, T.M. Fan, J. Cheng, The formulation of aptamer-coated paclitaxel-polylactide nanoconjugates and their targeting to cancer cells, Biomaterials, 31 (2010) 3043-3053.

[89] C. Yu, Y. Hu, J. Duan, W. Yuan, C. Wang, H. Xu, X.D. Yang, Novel aptamer-nanoparticle bioconjugates enhances delivery of anticancer drug to MUC1-positive cancer cells in vitro, PLoS One, 6 (2011) e24077.

[90] M. Das, W. Duan, S.K. Sahoo, Multifunctional nanoparticle–EpCAM aptamer bioconjugates: A paradigm for targeted drug delivery and imaging in cancer therapy, Nanomedicine: Nanotechnology, Biology and Medicine, 11 (2015) 379-389.

[91] Z. Ghasemi, R. Dinarvand, F. Mottaghitalab, M. Esfandyari-Manesh, E. Sayari, F. Atyabi, Aptamer decorated hyaluronan/chitosan nanoparticles for targeted delivery of 5-fluorouracil to MUC1 overexpressing adenocarcinomas, Carbohydrate Polymers, 121 (2015) 190-198.

[92] E. Sayari, M. Dinarvand, M. Amini, M. Azhdarzadeh, E. Mollarazi, Z. Ghasemi, F. Atyabi, MUC1 aptamer conjugated to chitosan nanoparticles, an efficient targeted carrier designed for anticancer SN38 delivery, International Journal of Pharmaceutics, 473 (2014) 304-315.

[93] T. Kurosaki, N. Higuchi, S. Kawakami, Y. Higuchi, T. Nakamura, T. Kitahara, M. Hashida, H. Sasaki, Self-assemble gene delivery system for molecular targeting using nucleic acid aptamer, Gene, 491 (2012) 205-209.

[94] N. Zhao, H.G. Bagaria, M.S. Wong, Y. Zu, A nanocomplex that is both tumor cell-selective and cancer gene-specific for anaplastic large cell lymphoma, Journal of nanobiotechnology, 9 (2011) 2-2.

[95] N. Subramanian, J.R. Kanwar, P. Athalya, N. Janakiraman, V. Khetan, R.K. Kanwar, S. Eluchuri, S. Krishnakumar, EpCAM aptamer mediated cancer cell specific delivery of EpCAM siRNA using polymeric nanocomplex, Journal of Biomedical Science, 22 (2015) 4-4.

[96] E. Abbasi, S.F. Aval, A. Akbarzadeh, M. Milani, H.T. Nasrabadi, S.W. Joo, Y. Hanifehpour, K. Nejati-Koshki, R. Pashaei-Asl, Dendrimers: synthesis, applications, and properties, Nanoscale Res Lett, 9 (2014) 247.

[97] B. Klajnert, M. Bryszewska, Dendrimers: properties and applications, Acta Biochim Pol, 48 (2001) 199-208.

[98] S. Yu, R. Dong, J. Chen, F. Chen, W. Jiang, Y. Zhou, X. Zhu, D. Yan, Synthesis and self-assembly of amphiphilic aptamer-functionalized hyperbranched multiarm copolymers for targeted cancer imaging, Biomacromolecules, 15 (2014) 1828-1836.

[99] X. Wu, B. Ding, J. Gao, H. Wang, W. Fan, X. Wang, W. Zhang, X. Wang, L. Ye, M. Zhang, X. Ding, J. Liu, Q. Zhu, S. Gao, Second-generation aptamer-conjugated PSMA-targeted delivery system for prostate cancer therapy, Int J Nanomedicine, 6 (2011) 1747-1756.

[100] A. Aravind, S.H. Varghese, S. Veeranarayanan, A. Mathew, Y. Nagaoka, S. Iwai, T. Fukuda, T. Hasumura, Y. Yoshida, T. Maekawa, D.S. Kumar, Aptamer-labeled PLGA nanoparticles for targeting cancer cells, Cancer Nanotechnol, 3 (2012) 1-12.

[101] S.S. Oh, B.F. Lee, F.A. Leibfarth, M. Eisenstein, M.J. Robb, N.A. Lynd, C.J. Hawker, H.T. Soh, Synthetic aptamer-polymer hybrid constructs for programmed drug delivery into specific target cells, J Am Chem Soc, 136 (2014) 15010-15015.

[102] P. Charoenphol, H. Bermudez, Aptamer-targeted DNA nanostructures for therapeutic delivery, Mol Pharm, 11 (2014) 1721-1725.

[103] K. Deng, Z. Hou, X. Li, C. Li, Y. Zhang, X. Deng, Z. Cheng, J. Lin, Aptamer-Mediated Up-conversion Core/MOF Shell Nanocomposites for Targeted Drug Delivery and Cell Imaging, Scientific Reports, 5 (2015) 7851-7851.

[104] D.H.M. Dam, K.S.B. Culver, T.W. Odom, Grafting aptamers onto gold nanostars increases in vitro efficacy in a wide range of cancer cell types, Molecular Pharmaceutics, 11 (2014) 580-587.

[105] Y.-S. Shiao, H.-H. Chiu, P.-H. Wu, Y.-F. Huang, Aptamer-Functionalized Gold Nanoparticles As Photoresponsive Nanoplatform for Co-Drug Delivery, ACS applied materials & interfaces, (2014).

[106] Z. Zhang, C. Liu, J. Bai, C. Wu, Y. Xiao, Y. Li, J. Zheng, R. Yang, W. Tan, Silver Nanoparticle Gated, Mesoporous Silica Coated Gold Nanorods (AuNR@MS@AgNPs): Low Premature Release and Multifunctional Cancer Theranostic Platform, ACS applied materials & interfaces, (2015) 150311083009002-150311083009002.

[107] L.L. Li, Q. Yin, J. Cheng, Y. Lu, Polyvalent mesoporous silica nanoparticle-aptamer bioconjugates target breast cancer cells, Adv Healthc Mater, 1 (2012) 567-572.

[108] L. Cai, Z.Z. Chen, M.Y. Chen, H.W. Tang, D.W. Pang, MUC-1 aptamer-conjugated dye-doped silica nanoparticles for MCF-7 cells detection, Biomaterials, 34 (2013) 371-381.

[109] a. Bandekar, C. Zhu, R. Jindal, F. Bruchertseifer, a. Morgenstern, S. Sofou, Anti-Prostate-Specific Membrane Antigen Liposomes Loaded with 225Ac for Potential Targeted Antivascular -Particle Therapy of Cancer, Journal of Nuclear Medicine, 55 (2013) 107-114.

[110] S. Dhar, F.X. Gu, R. Langer, O.C. Farokhzad, S.J. Lippard, Targeted delivery of cisplatin to prostate cancer cells by aptamer functionalized Pt(IV) prodrug-PLGA-PEG nanoparticles, Proc Natl Acad Sci U S A, 105 (2008) 17356-17361.

[111] V. Bagalkot, L. Zhang, E. Levy-Nissenbaum, S. Jon, P.W. Kantoff, R. Langer, O.C. Farokhzad, Quantum dot - Aptamer conjugates for synchronous cancer imaging, therapy, and sensing of drug delivery based on Bi-fluorescence resonance energy transfer, Nano Letters, 7 (2007) 3065-3070.

[112] M.K. Yu, D. Kim, I.H. Lee, J.S. So, Y.Y. Jeong, S. Jon, Image-guided prostate cancer therapy using aptamer-functionalized thermally cross-linked superparamagnetic iron oxide nanoparticles, Small, 7 (2011) 2241-2249.

[113] I.H. Lee, S. An, M.K. Yu, H.K. Kwon, S.H. Im, S. Jon, Targeted chemoimmunotherapy using drug-loaded aptamer-dendrimer bioconjugates, Journal of Controlled Release, 155 (2011) 435-441.

[114] M. Chang, C.S. Yang, D.M. Huang, Aptamer-conjugated DNA icosahedral nanoparticles as a carrier of doxorubicin for cancer therapy, ACS Nano, 5 (2011) 6156-6163.

[115] Z. Lin, Q. Ma, X. Fei, H. Zhang, X. Su, A novel aptamer functionalized CuInS2 quantum dots probe for daunorubicin sensing and near infrared imaging of prostate cancer cells, Anal Chim Acta, 818 (2014) 54-60.

[116] C. Zhang, X. Ji, Y. Zhang, G. Zhou, X. Ke, H. Wang, P. Tinnefeld, Z. He, One-Pot Synthesized Aptamer-Functionalized CdTe : Zn 2 + Quantum Dots for Tumor-Targeted Fluorescence Imaging in Vitro and in Vivo, (2013).

[117] H. Zhang, Y. Ma, Y. Xie, Y. An, Y. Huang, Z. Zhu, C.J. Yang, A Controllable Aptamer-Based Self-Assembled DNA Dendrimer for High Affinity Targeting, Bioimaging and Drug Delivery, Scientific Reports, 5 (2015) 10099-10099.

[118] E.W. Orava, N. Cicmil, J. Gariepy, Delivering cargoes into cancer cells using DNA aptamers targeting internalized surface portals, Biochim Biophys Acta, 1798 (2010) 2190-2200.

[119] S.M. Taghdisi, P. Lavaee, M. Ramezani, K. Abnous, Reversible Targeting and controlled release delivery of daunorubicin to cancer cells by aptamer-wrapped carbon nanotubes, European Journal of Pharmaceutics and Biopharmaceutics, 77 (2011) 200-206.

[120] T. Chen, M.I. Shukoor, R.W. Wang, Z.L. Zhao, Q. Yuan, S. Bamrungsap, X.L. Xiong, W.H. Tan, Smart Multifunctional Nanostructure for Targeted Cancer Chemotherapy and Magnetic Resonance Imaging, Acs Nano, 5 (2011) 7866-7873.

[121] N. Stephanopoulos, G.J. Tong, S.C. Hsiao, M.B. Francis, Dual-surface modified virus capsids for targeted delivery of photodynamic agents to cancer cells, ACS Nano, 4 (2010)

6014-6020.

[122] S.T. Kang, Y.L. Luo, Y.F. Huang, C.K. Yeh, DNA-Conjugated Gold Nanoparticles for Ultrasound Targeted Drug Delivery, 2012 Ieee International Ultrasonics Symposium (Ius), (2012) 1866-1868.

[123] C.H. Wang, S.T. Kang, Y.H. Lee, Y.L. Luo, Y.F. Huang, C.K. Yeh, Aptamer-conjugated and drug-loaded acoustic droplets for ultrasound theranosis, Biomaterials, 33 (2012) 1939-1947.

[124] G.J. Tong, S.C. Hsiao, Z.M. Carrico, M.B. Francis, Viral Capsid DNA Aptamer Conjugates as Multivalent Cell Targeting Vehicles, Jacs, 131 (2010) 11174-11178.

[125] J. Wang, G. Zhu, M. You, E. Song, M.I. Shukoor, K. Zhang, M.B. Altman, Y. Chen, Z. Zhu, C.Z. Huang, W. Tan, Assembly of Aptamer Switch Probes and Photosensitizer on Gold Nanorods for Targeted Photothermal and Photodynamic Cancer Therapy, ACS nano, 6 (2012) 5070-5077.

[126] N.M. Danesh, P. Lavaee, M. Ramezani, K. Abnous, S.M. Taghdisi, Targeted and controlled release delivery of daunorubicin to T-cell acute lymphoblastic leukemia by aptamer-modified gold nanoparticles, International Journal of Pharmaceutics, 489 (2015) 311-317.

[127] J. Zhou, B. Soontornworajit, Y. Wang, A Temperature-Responsive Antibody-Like Nanostructure, (2010) 2087-2093.

[128] S.C. Lee, V. Gedi, N.R. Ha, J.H. Cho, H.C. Park, M.Y. Yoon, Development of receptor-based inhibitory RNA aptamers for anthrax toxin neutralization, Int J Biol Macromol, 77 (2015) 293-302.

[129] K. Pala, A. Serwotka, F. Jeleń, P. Jakimowicz, J. Otlewski, Tumor-specific hyperthermia with aptamer-tagged superparamagnetic nanoparticles, Int J Nanomedicine, 9 (2014) 67-76.

[130] K. Wang, H. Yao, Y. Meng, Y. Wang, X. Yan, R. Huang, Specific aptamer-conjugated mesoporous silica–carbon nanoparticles for HER2-targeted chemo-photothermal combined therapy, Acta Biomaterialia, 16 (2015) 196-205.

[131] Z. Fan, M. Shelton, A.K. Singh, D. Senapati, S.A. Khan, P.C. Ray, Multifunctional plasmonic shell-magnetic core nanoparticles for targeted diagnostics, isolation, and photothermal destruction of tumor cells, ACS Nano, 6 (2012) 1065-1073.

[132] L. Li, D. Xiang, S. Shigdar, W. Yang, Q. Li, J. Lin, K. Liu, W. Duan, Epithelial cell adhesion molecule aptamer functionalized PLGA-lecithin-curcumin-PEG nanoparticles for targeted drug delivery to human colorectal adenocarcinoma cells, Int J Nanomedicine, 9 (2014) 1083-1096.

[133] C. Pilapong, S. Sitthichai, S. Thongtem, T. Thongtem, Smart magnetic nanoparticle-aptamer probe for targeted imaging and treatment of hepatocellular carcinoma, International Journal of Pharmaceutics, 473 (2014) 469-474.

[134] M.J. Gu, K.F. Li, L.X. Zhang, H. Wang, L.S. Liu, Z.Z. Zheng, N.Y. Han, Z.J. Yang, T.Y. Fan, In vitro study of novel gadolinium-loaded liposomes guided by GBI-10 aptamer for promising tumor targeting and tumor diagnosis by magnetic resonance imaging, Int J Nanomedicine, 10 (2015) 5187-5204.

[135] X.C. Chen, Y.L. Deng, Y. Lin, D.W. Pang, H. Qing, F. Qu, H.Y. Xie, Quantum dot-labeled aptamer nanoprobes specifically targeting glioma cells, Nanotechnology, 19 (2008).

[136] X.L. Song, Y. Ren, J. Zhang, G. Wang, X.D. Han, W. Zheng, L.L. Zhen, Targeted delivery of doxorubicin to breast cancer cells by aptamer functionalized DOTAP/DOPE liposomes, Oncology Reports, 34 (2015) 1953-1960.

[137] Y. Zhang, Z. Yu, F. Jiang, P. Fu, J. Shen, W. Wu, J. Li, Two DNA aptamers against avian influenza H9N2 virus prevent viral infection in cells, PLoS One, 10 (2015) e0123060.

[138] V.V. Mody, R. Siwale, A. Singh, H.R. Mody, Introduction to metallic nanoparticles, J Pharm Bioallied Sci, 2 (2010) 282-289.

[139] D.H. Dam, K.S. Culver, T.W. Odom, Grafting aptamers onto gold nanostars increases in vitro efficacy in a wide range of cancer cell types, Mol Pharm, 11 (2014) 580-587.

[140] J. Li, J. You, Y. Dai, M. Shi, C. Han, K. Xu, Gadolinium oxide nanoparticles and aptamer-functionalized silver nanoclusters-based multimodal molecular imaging nanoprobe for optical/magnetic resonance cancer cell imaging, Anal Chem, 86 (2014) 11306-11311.

[141] L. Yang, Y.-T. Tseng, G. Suo, L. Chen, J. Yu, W.-J. Chiu, C.-C. Huang, C.-H. Lin, Photothermal Therapeutic Response of Cancer Cells to Aptamer–Gold Nanoparticle-Hybridized Graphene Oxide under NIR Illumination, ACS applied materials & interfaces, 7 (2015) 5097-5106.

[142] Y.-F. Huang, K. Sefah, S. Bamrungsap, H.-T. Chang, W. Tan, Selective photothermal therapy for mixed cancer cells using aptamer-conjugated nanorods, Langmuir, 24 (2008) 11860-11865.

[143] C. Zhang, X. Ji, Y. Zhang, G. Zhou, X. Ke, H. Wang, P. Tinnefeld, Z. He, One-pot synthesized aptamer-functionalized CdTe:Zn2+ quantum dots for tumor-targeted fluorescence imaging in vitro and in vivo, Anal Chem, 85 (2013) 5843-5849.

[144] T.-s.-a. Dox, Thermally cross-linked superparamagnetic iron oxide nanoparticle-A10 RNA aptamer-doxorubicin conjugate, 6-9.

[145] Y.-L. Luo, Y.-S. Shiao, Y.-F. Huang, Release of photoactivatable drugs from plasmonic nanoparticles for targeted cancer therapy, ACS Nano, 5 (2011) 7796-7804.

[146] C. Zhou, T. Chen, C. Wu, G. Zhu, L. Qiu, C. Cui, W. Hou, W. Tan, Aptamer CaCO ₃ Nanostructures: A Facile, pH-Responsive, Specific Platform for Targeted Anticancer Theranostics, Chemistry - An Asian Journal, 10 (2015) 166-171.

[147] R. Savla, O. Taratula, O. Garbuzenko, T. Minko, Tumor targeted quantum dot-mucin 1

aptamer-doxorubicin conjugate for imaging and treatment of cancer, J Control Release, 153 (2011) 16-22.

[148] J.G. Morton, E.S. Day, N.J. Halas, J.L. West, Nanoshells for photothermal cancer therapy, Methods Mol Biol, 624 (2010) 101-117.

[149] F.J. Hernandez, L.I. Hernandez, A. Pinto, T. Schäfer, V.C. Özalp, Targeting cancer cells with controlled release nanocapsules based on a single aptamer, Chemical communications (Cambridge, England), 49 (2013) 1285-1287.

[150] X. Yang, X. Liu, Z. Liu, F. Pu, J. Ren, X. Qu, Near-infrared light-triggered, targeted drug delivery to cancer cells by aptamer gated nanovehicles, Advanced Materials, 24 (2012) 2890-2895.

[151] Z. Li, Z. Liu, M. Yin, X. Yang, Q. Yuan, J. Ren, X. Qu, Aptamer-capped multifunctional mesoporous strontium hydroxyapatite nanovehicle for cancer-cell-responsive drug delivery and imaging, Biomacromolecules, 13 (2012) 4257-4263.

[152] T. Chen, M.I. Shukoor, R. Wang, Z. Zhao, Q. Yuan, S. Bamrungsap, X. Xiong, W. Tan, Smart Multifunctional Nanostructure for Targeted Cancer Chemotherapy and Magnetic Resonance Imaging, ACS Nano, 5 (2011) 7866-7873.

[153] J. Zhu, H. Huang, S. Dong, L. Ge, Y. Zhang, Progress in aptamer-mediated drug delivery vehicles for cancer targeting and its implications in addressing chemotherapeutic challenges, Theranostics, 4 (2014) 931-944.

[154] F. Zhao, Y. Zhao, Y. Liu, X. Chang, C. Chen, Y. Zhao, Cellular uptake, intracellular trafficking, and cytotoxicity of nanomaterials, Small, 7 (2011) 1322-1337.

[155] H. Hillaireau, P. Couvreur, Nanocarriers' entry into the cell: relevance to drug delivery, Cell Mol Life Sci, 66 (2009) 2873-2896.

[156] F. Gu, L. Zhang, B.A. Teply, N. Mann, A. Wang, A.F. Radovic-Moreno, R. Langer, O.C. Farokhzad, Precise engineering of targeted nanoparticles by using self-assembled biointegrated block copolymers, Proc Natl Acad Sci U S A, 105 (2008) 2586-2591.

[157] J. Ruckman, L.S. Green, J. Beeson, S. Waugh, W.L. Gillette, D.D. Henninger, L. Claesson-Welsh, N. Janjic, 2'-Fluoropyrimidine RNA-based aptamers to the 165-amino acid form of vascular endothelial growth factor (VEGF165). Inhibition of receptor binding and VEGF-induced vascular permeability through interactions requiring the exon 7-encoded domain, J Biol Chem, 273 (1998) 20556-20567.

[158] D. Jellinek, L.S. Green, C. Bell, C.K. Lynott, N. Gill, C. Vargeese, G. Kirschenheuter, D.P. McGee, P. Abesinghe, W.A. Pieken, et al., Potent 2'-amino-2'-deoxypyrimidine RNA inhibitors of basic fibroblast growth factor, Biochemistry, 34 (1995) 11363-11372.

[159] L.S. Green, D. Jellinek, R. Jenison, A. Ostman, C.H. Heldin, N. Janjic, Inhibitory DNA ligands to platelet-derived growth factor B-chain, Biochemistry, 35 (1996) 14413-14424.

[160] N.C. Pagratis, C. Bell, Y.F. Chang, S. Jennings, T. Fitzwater, D. Jellinek, C. Dang,

Potent 2'-amino-, and 2'-fluoro-2'-deoxyribonucleotide RNA inhibitors of keratinocyte growth factor, Nat Biotechnol, 15 (1997) 68-73.

[161] E.W. Ng, A.P. Adamis, Anti-VEGF aptamer (pegaptanib) therapy for ocular vascular diseases, Ann N Y Acad Sci, 1082 (2006) 151-171.

[162] O. Hamid, Emerging treatments in oncology: focus on tyrosine kinase (erbB) receptor inhibitors, J Am Pharm Assoc (2003), 44 (2004) 52-58.

[163] N. Li, H.H. Nguyen, M. Byrom, A.D. Ellington, Inhibition of cell proliferation by an anti-EGFR aptamer, PLoS One, 6 (2011) e20299.

[164] H. Ginisty, H. Sicard, B. Roger, P. Bouvet, Structure and functions of nucleolin, J Cell Sci, 112 (Pt 6) (1999) 761-772.

[165] C.M. Berger, X. Gaume, P. Bouvet, The roles of nucleolin subcellular localization in cancer, Biochimie, 113 (2015) 78-85.

[166] P.J. Bates, J.B. Kahlon, S.D. Thomas, J.O. Trent, D.M. Miller, Antiproliferative activity of G-rich oligonucleotides correlates with protein binding, J Biol Chem, 274 (1999) 26369-26377.

[167] X. Xu, F. Hamhouyia, S.D. Thomas, T.J. Burke, A.C. Girvan, W.G. McGregor, J.O. Trent, D.M. Miller, P.J. Bates, Inhibition of DNA replication and induction of S phase cell cycle arrest by G-rich oligonucleotides, J Biol Chem, 276 (2001) 43221-43230.

[168] V. Dapic, P.J. Bates, J.O. Trent, A. Rodger, S.D. Thomas, D.M. Miller, Antiproliferative activity of G-quartet-forming oligonucleotides with backbone and sugar modifications, Biochemistry, 41 (2002) 3676-3685.

[169] P.J. Bates, D.A. Laber, D.M. Miller, S.D. Thomas, J.O. Trent, Discovery and development of the G-rich oligonucleotide AS1411 as a novel treatment for cancer, Exp Mol Pathol, 86 (2009) 151-164.

[170] S.D. Seiwert, T.S. Nahreini, S. Aigner, N.G. Ahn, O.C. Uhlenbeck, RNA aptamers as pathway-specific MAP kinase inhibitors, Chemistry & Biology, 7 (2000) 833-843.

[171] H.H. Salamanca, M.A. Antonyak, R.A. Cerione, H. Shi, J.T. Lis, Inhibiting Heat Shock Factor 1 in Human Cancer Cells with a Potent RNA Aptamer, Plos One, 9 (2014).

[172] D.E. Huizenga, J.W. Szostak, A DNA Aptamer That Binds Adenosine and Atp, Biochemistry, 34 (1995) 656-665.

[173] T.N. Zamay, O.S. Kolovskaya, Y.E. Glazyrin, G.S. Zamay, S.a. Kuznetsova, E.a. Spivak, M. Wehbe, A.G. Savitskaya, O.a. Zubkova, A. Kadkina, X. Wang, D. Muharemagic, A. Dubynina, Y. Sheina, A.B. Salmina, M.V. Berezovski, A.S. Zamay, DNA-Aptamer Targeting Vimentin for Tumor Therapy In Vivo, Nucleic Acid Therapeutics, 24 (2014) 160-170.

[174] S.M. Ryou, J.M. Kim, J.H. Yeom, S. Hyun, S. Kim, M.S. Han, S.W. Kim, J. Bae, S. Rhee, K. Lee, Gold nanoparticle-assisted delivery of small, highly structured RNA into the nuclei of human cells, Biochemical and Biophysical Research Communications, 416 (2011) 178-183.

[175] C. Maasch, A. Vater, K. Buchner, W.G. Purschke, D. Eulberg, S. Vonhoff, S. Klussmann, Polyetheylenimine-polyplexes of Spiegelmer NOX-A50 directed against intracellular high mobility group protein A1 (HMGA1) reduce tumor growth in vivo, Journal of Biological Chemistry, 285 (2010) 40012-40018.

[176] M. Famulok, M. Blind, G. Mayer, Intramers as promising new tools in functional proteomics, Chem Biol, 8 (2001) 931-939.

[177] G. Mayer, M. Blind, W. Nagel, T. Bohm, T. Knorr, C.L. Jackson, W. Kolanus, M. Famulok, Controlling small guanine-nucleotide-exchange factor function through cytoplasmic RNA intramers, Proc Natl Acad Sci U S A, 98 (2001) 4961-4965.

[178] K.H. Choi, M.W. Park, S.Y. Lee, M.Y. Jeon, M.Y. Kim, H.K. Lee, J. Yu, H.J. Kim, K. Han, H. Lee, K. Park, W.J. Park, S. Jeong, Intracellular expression of the T-cell factor-1 RNA aptamer as an intramer, Mol Cancer Ther, 5 (2006) 2428-2434.

[179] C.M. Dollins, S. Nair, D. Boczkowski, J. Lee, J.M. Layzer, E. Gilboa, B.A. Sullenger, Assembling OX40 aptamers on a molecular scaffold to create a receptor-activating aptamer, Chem Biol, 15 (2008) 675-682.

[180] A.D. Weinberg, C. Thalhofer, N. Morris, J.M. Walker, D. Seiss, S. Wong, M.K. Axthelm, L.J. Picker, W.J. Urba, Anti-OX40 (CD134) administration to nonhuman primates: immunostimulatory effects and toxicokinetic study, J Immunother, 29 (2006) 575-585.
[181] E.S. Gragoudas, A.P. Adamis, E.T. Cunningham, Jr., M. Feinsod, D.R. Guyer, V.I.S.i.O.N.C.T. Group, Pegaptanib for neovascular age-related macular degeneration, N Engl J Med, 351 (2004) 2805-2816.

[182] J.E. Rosenberg, R.M. Bambury, E.M. Van Allen, H.A. Drabkin, P.N. Lara, Jr., A.L. Harzstark, N. Wagle, R.A. Figlin, G.W. Smith, L.A. Garraway, T. Choueiri, F. Erlandsson, D.A. Laber, A phase II trial of AS1411 (a novel nucleolin-targeted DNA aptamer) in metastatic renal cell carcinoma, Invest New Drugs, 32 (2014) 178-187.

[183] S.G. Sayyed, H. Hagele, O.P. Kulkarni, K. Endlich, S. Segerer, D. Eulberg, S. Klussmann, H.J. Anders, Podocytes produce homeostatic chemokine stromal cell-derived factor-1/CXCL12, which contributes to glomerulosclerosis, podocyte loss and albuminuria in a mouse model of type 2 diabetes, Diabetologia, 52 (2009) 2445-2454.

[184] V. Sanna, N. Pala, M. Sechi, Targeted therapy using nanotechnology: focus on cancer, Int J Nanomedicine, 9 (2014) 467-483.

Experimental work

Travaux expérimentaux

Chapitre 1

Sélection in vitro d'aptamères d'ARN modifiés dirigés contre CD44, marqueur des cellules souches cancéreuses

Experimental work

Chapter 1

***In vitro* selection of modified RNA aptamers against CD44 cancer stem cell marker**

Travaux expérimentaux

Chapitre 1

Sélection in vitro d'aptamères d'ARN modifiés dirigés contre CD44, marqueur des cellules souches cancéreuses

Résumé

Les cellules souches cancéreuses (CSCs) sont une sous-population de cellules tumorales possédant la capacité d'auto-renouvellement et de différentiation en diverses cellules qui constituent la masse tumorale. La glycoprotéine de surface CD44 est l'un des marqueurs les plus communément employés pour identifier les CSCs. Les aptamères sont des oligonucléotides synthétiques sélectionnés à partir de pools de séquences aléatoires et qui peuvent se lier à un large éventail de cibles avec une affinité et une spécificité élevées. Dans cette étude, la technique d'évolution systématique des ligands par enrichissement exponentielle (SELEX) a été employée pour isoler des aptamères d'ARN à partir d'une bibliothèque d'environ 10^{14} ARN modifiés par des 2-F-pyrimidines, en utilisant une protéine CD44 recombinante humaine complète. Après 11 tours itératifs de SELEX, les aptamères sélectionnés ont été clonés et séquencés, conduisant à l'identification de trois séquences différentes. L'affinité et la spécificité de liaison de l'aptamère majoritaire ont été évaluées sur plusieurs modèles cellulaires représentatifs du cancer du sein exprimant CD44 : MDA-MB-231, MCF7 et T47D. L'aptamère sélectionné (Apt1) est capable de se fixer spécifiquement à ces cellules cancéreuses comme l'ont montré les analyses en cytométrie en flux et en microscopie de fluorescence, avec une intensité corrélée au niveau d'expression du CD44 à la surface de ces cellules. Cet aptamère peut donc être utilisé pour le ciblage des cellules $CD44^{+}$, y compris les cellules souches cancéreuses, en vue de la détection, du tri, et de l'enrichissement cellulaire, ainsi que pour la fonctionnalisation de nanovecteurs de principes actifs.

Ce chapitre a été puplié dans Journal of Nucleic Acis Theraputics en 2013 comme authers.

Authors Nidaa Ababneh,Walhan Alshaer, Omar Allozi, Azmi Mahafzah, Mohammed El-Khateeb, Herve´ Hillaireau, Magali Noiray, Elias Fattal, and Said Ismail.

Experimental work

Chapter 1

In vitro selection of modified RNA aptamers against CD44 cancer stem cell marker

Abstract

Cancer stem cells (CSCs) are a subset of tumor cells that has the ability to self-renew and to generate the diverse cells that comprise the tumor mass. The cell-surface glycoprotein CD44 is one of the most common surface markers used to identify CSCs. Aptamers are synthetic oligonucleotides selected from pools of random sequences that can bind to a wide range of targets with high affinity and specificity. In this study, the systematic evolution of ligands by exponential enrichment (SELEX) technology was used to isolate RNA aptamers using human recombinant fulllength CD44 protein and 2'-F-pyrimidine modified RNA library with a complexity of around 10^{14} different molecules. Following 11 iterative rounds of SELEX, the selected aptamers were cloned and sequenced. Three different sequences were identified. The binding specificities for one of these RNA aptamers was assessed using representative breast cancer cell lines expressing CD44; namely, MDA-MB-231, MCF7, and T47D. The selected RNA aptamer (Apt1) was found to interact specifically with such cancer cells when analyzed by flow cytometry and fluorescent microscopy, with different intensities of fluorescence reflecting the level of CD44 expression on the surface of these cells. It can be concluded that the selected aptamers can be used to target CD44 positive cells, including cancer stem cells, for detection, sorting, and enrichment and for drug delivery purposes.

This chapter has been published in journal of nucleic acids therapeutics in 2013, with Nidaa Ababneh,Walhan Alshaer, Omar Allozi, Azmi Mahafzah, Mohammed El-Khateeb, Herve´ Hillaireau, Magali Noiray, Elias Fattal, and Said Ismail as authors.

1. Introduction

Cancer stem cells (CSCs) are a subset of tumor cells that has the ability to self-renew and to generate the diverse cells that comprise the tumor [1]. Cancer stem cells (CSCs) were first observed in hematological malignancies [2] but have now been identified in solid tumors of breast, prostate, brain, colon, and pancreas [3]. Cancer stem cells are thought to be resistant to conventional chemotherapy, which makes them potential targets for cancer research and drug development [3, 4]. Several cluster of differentiation (CD) markers have been identified specifically on cancer stem cells [5] The most commonly used surface markers to identify CSCs include CD44, EPCAM, and CD133 [6]. CD44 is a cell-surface glycoprotein expressed on lymphocytes, monocytes, and granulocytes, which have been identified as a stem cell marker in some solid tumors, including breast and head and neck cancers [7]. CD44 is the receptor for hyaluronan (HA), which is a major component of the extracellular matrix [8]. It is a multistructural and multifunctional cell-surface molecule involved in cell proliferation, cell differentiation, cell migration, angiogenesis, and presentation of cytokines, chemokines, and growth factors to the corresponding receptors [9]. Hyalronan binding of CD44 seems to prevent apoptosis of tumor cells, rather than promote their migration or invasiveness [10]. The CD44, which is also called metastasis-associated protein, is a reliable indicator of tumor load and disease activity [11]. It also plays an important role in the invasion of a variety of tumor cells, including breast, prostate, and mesotheliomas, and has been positively correlated with the number of circulating prostate cancer cells in the bloodstream [12, 13]. Aptamers are an interesting class of high affinity ligands [14]. They are short, single-stranded (ss) DNA or RNA oligonucleotides, typically isolated from combinatorial libraries by a process of in vitro evolution, termed SELEX (systematic evolution of ligands by exponential enrichment) [15]. The SELEX procedure is a selection process that allows the isolation of aptamers with unique binding properties from a large library of oligonucleotides through iterative cycles of

interaction with the target molecule, separation of bound from unbound aptamer species, elution of bound aptamers, and polymerase chain reaction (PCR) amplification of the binding aptamers for further selection rounds [16]. The present study describes the development of RNA nuclease-resistant aptamer capable of specifically binding to CD44, not only as a purified protein but also by binding on representative breast cancer cells lines.

2. Materials and Methods

2.1. Pool design and library synthesis

An ssDNA library (5'-GGGATGGATCCAAGCTTACTGG(45N)GGGAAGCTTCGATAGG AATTCGG-3') was synthesized with a 45-nucleotide random region, with the following forward primer (APT-FT7 5'-GCTAATACGACTCACTATAGGGATGGATCCAAGCTTA CTGG-3' and reverse primer APT-R 5'-CCGAATTCCTATCGAAGCTTCCC-3'). The forward primer APT-FT7 contains a T7 promoter sequence (underlined) for *in vitro* transcription. The PCR mix contained 10 micrograms of ssDNA library, 5 x Gotaq green buffers (Promega), 200 µM of each dNTPs mix, 1 µM of each primer, 2.5 mM $MgCl_2$, and 2.5 U of Taq DNA polymerase. The PCR program starts with 5 minutes at 95 °C. The cycling begins with a short denaturation step for 15 seconds at 95 °C; the primers are annealed for 20 seconds at 55 °C followed by an extension time of 20 seconds at 72 °C. These cycles were repeated six times, followed by a final elongation step of 5 minutes at 72 °C. The PCR products were purified using 6% PAGE using crush and soak elution method. Following purification, 10 µg of double-stranded DNA were *in vitro* transcribed into RNA library using Dura-Scribe T7 Transcription Kit (Epicentre Technologies) according to the manufacturer's instructions and incubated overnight at 37 °C, then treated with 10 units of DNase 1 at 37 °C for 30 minutes. RNA transcripts were analyzed by 4% agarose gel and purified using 6% PAGE using crush and soak method.

2.2. *In vitro* selection

The 2'-F-modified random RNA library was heated at 70 °C for 5 minutes in the binding buffer (4.2 mM Na_2HPO_4, 2mM K2HPO_4, 140 mM NaCl, 10 mM KCl, 2.5 mM $MgCl_2$), then rapidly cooled on ice for 5 minutes, after which it was equilibrated at room temperature for about 10 minutes. The RNA library was then incubated with the Glutathione S-Transferase (GST)-tagged CD44 recombinant proteins (Abnova Corporation) for 1 hour at 37 °C, followed by the separation of nonbounded sequences using GST magnetic beads as negative selection. The selected sequences were eluted from the target, reverse transcribed by SuperScript 3 reverse transcriptase (Invitrogen), amplified by RT-PCR, and then transcribed as described previously to produce RNA transcripts. After 11 iterative rounds, the resultant aptamers were cloned using the pGEM-T Easy vector (Promega). Around 25 of the isolated clones were subsequently sequenced by Macrogen Inc. Sequences analysis and alignments were carried out using the software ClustalW from the website. The most stable secondary structures for the aptamer were predicted using the *Mfold* program (Figure 1).

2.3. Synthesis of modified and fluorescein-labeled RNA aptamers

One of the resulted RNA aptamer sequences (Apt1) was synthesized via chemical synthesis using cyanoethylphosphoroamitide chemistry (Midland) on a 50-nanomole scale. The first three nucleotides on each end of the aptamer were synthesized with 2′-O-methyl modification (indicated by lower case letters) to enhance its resistance to nucleases, fluorescein isothiocyanate (FITC)-labeled at the 5′ end and purified by HPLC. To rule out nonspecific cell binding, a control ssDNA random library was synthesized and labeled with FITC as a negative control.

2.4. Cellular assays

The human breast adenocarcinoma cell lines MDA-MB-231 and MCF7 and the human ductal breast epithelial tumor cell line T47D were obtained from ATCC (American Type Culture

Collection) and cultured in Dulbecco's modified Eagle medium (DMEM): nutrient mixture F-12 (Lonza) supplemented with 10% heat inactivated fetal bovine serum (FBS; Invitrogen), 100 IU/mL penicillin-streptomycin (Invitrogen), and 5 mM L-glutamine (Lonza). The cells were maintained at 37 °C in a 5% CO2 atmosphere. Cells were passaged when grown to ~80% confluency with 1x trypsin (0.05%, Lonza), then cultured in 12-well culture plates containing glass coverslips at a density of 60,000 cells per well, and were grown under standard culture conditions. After 24 hours of incubation, the wells were washed by decanting the culture media and rinsing three times with 1mL cold 1· phosphate-buffered saline (PBS) per well. Cells were then fixed using 1 mL 4% paraformaldehyde for 10 minutes at room temperature. After fixation, the cells were rinsed two times in 1x PBS, after which nonspecific binding was blocked using 3% bovine serum albumin in PBS for 30 minutes. Cells were then incubated with folded Apt1CD44 aptamer probe (200 nM) in 300 µL of binding buffer (DPBS containing 5 mM MgCl2, 0.1 mg/ml tRNA, and 0.1mg/mL salmon sperm DNA) in the dark at room temperature for 30 minutes. An ssDNA library labeled with FITC was used as a negative control. After incubation, the cells were washed twice with binding buffer to remove unbound sequences and to reduce the fluorescent background after which coverslips were transferred to slides and dipped in mounting media containing 6-diamidino-2-phenylindole dihydrochloride (DAPI) solution (Cytocell) for nuclear counterstaining. The images were then acquired by flourescent microscopy (Carl Zeiss) with filters for FITC (excitation BP450–490, emission BP515–565) and DAPI (excitation D360/40, emission D460/50). The objective used for imaging was a 60x oil-immersion objective. Cells of the selected cell lines were cultured until they reached 80% confluency. They were detached with trypsin, centrifuged, and resuspended in 1mL permeabilizing solution for 10 minutes, then washed twice with binding buffer (DPBS containing 5 mM $MgCl_2$, 0.1 mg/mL tRNA, and 0.1 mg/mL salmon sperm DNA) [17]. The cells were then

resuspended in 5 mL assay buffer (DPBS supplemented with 5 mM $MgCl_2$, 0.1 mg/mL tRNA, 0.1 mg/mL salmon sperm DNA, 0.2% sodium azide, and 5% FBS) and incubated for 30 minutes at 4°C, after which cells were washed twice, and 10^5 cells of each cell line were incubated with 200 nM of FITC-labeled aptamer in a total volume of 200 µL. The binding was carried out in the dark at room temperature for 30 minutes. The same amounts of cells were incubated with phycoerythrin (PE)-labeled anti-CD44 antibody separately as a positive control, and 200 nM ssDNA FITC-labeled library was used as a negative control. Finally, the cells were washed three times and resuspended in 250 µL of assay buffer with 2.5 mM $MgCl_2$ extra concentration and analyzed using the FACS-Calibur flowcytometer (Becton Dickinson). Typically 10,000 events were counted per sample, and the data was analyzed using Cell Quest version 3.3 (BD Biosciences) and WinMDI version 2.8 software.

2.5. Binding affinity

The binding affinity constant (Kd) of Apt1 was determined by incubating FITC-labeled Apt1 (350 nM) with CD44 protein (from 45 to 450 nM) for 1 hour at 37°C in 100 µL binding buffer. After incubation, The Apt1-CD44 complexes were immobilized on GST magnetic beads (Promega) for 20 minutes at room temperature and then washed three times with 100 µL of binding buffer to remove unbound Apt1. The Apt1-CD44 complexes were then eluted from the beads using 100 µL elution buffer and incubated for 30minutes. The fraction of bound Apt1was quantified by the detection of fluorescence (excitation 494 nm, emission 517 nm) in the elution buffer using a FP-750 spectrofluorimeter (JASCO). The same quantity of FITC-labeled Apt1 (350 nM) was incubated with the GST beads without CD44 protein and used as a negative control to determine the nonspecific binding background. The binding data were analyzed to get a saturating curve by performing a regression analysis fitting model for one binding site.

2.6. Cytotoxicity assays

Cellular toxicity of RNA aptamer was assessed using the Cell Titer 96-Cell Proliferation Assay (Promega) according to the manufacturer's instructions. Cells of selected cell lines, with a density of 1 x 10^4 cells per well, were cultured in 96-well microtiter plates in 200 µL DMEM-F12 complete growth medium overnight for attachment, and during the next day, various RNA aptamers concentrations (50, 100, 250, 500, 1000, 2500 ng) were added in duplicates for 72 hours at the same culture conditions. After that, 100 µL of the media was removed from each well, and 15 µL of (3-(4,5-dimethylthiazol-2-yl)-2,5-diphenyltetrazolium bromide (MTT) solution was added, mixed by agitating the plate, and incubated for 4 hours at 37 °C in the dark. Four hours later, 100 µL of stop solution was added for each well to stop the reaction. Plates were read using an enzyme-linked immunosorbent assay reader, and absorbance was measured at 570nm (background wavelength is 630 nm). The viability of cells was calculated based on a comparison of untreated cells and those treated with MTT under the same conditions. Cells were incubated for 72 hours prior to counting the number of viable cells.

2.7. RNA aptamer stability assay

Cell culture media with 10% FBS was used to detect RNA stability by incubation of 12 µg of each of the O-methyl-modified aptamers with 0.5 mL of cell culture media at 37 °C. Samples of 50 µL were taken out and collected after 0, 0.5, 1, 1.5, 2, 3, 4, 6, and 24 hours. RNA was reverse transcribed as described above, and 2 µL complementary DNA were amplified using GoTaq-QPCR Master (Promega), and 25 pmole of forward and reverse primers. The conditions for the PCR were 95 °C for 10 minutes as initial denaturation, 95 °C for 20 seconds, 55 °C for 20 seconds, and 72 °C for 30 seconds, for 40 cycles.

3. Results

3.1. SELEX results, folding prediction, and binding affinity

Following 1 iterative SELEX rounds and successful cloning and sequencing of the selected aptamers, the sequence homology was determined. Based on the sequencing analysis, three sequences were represented more than once in the 25 clones were analyzed. Full-length sequences and frequencies of the three selected aptamers are shown in Table 1. One of the sequences (Apt1) was synthesized and used in the cellular assays. Apt1 was synthesized and labeled with FITC, and the first three nucleotides on each end of the aptamer sequence were modified with 2'O-methyl group for better nuclease resistance. Secondary structures of the selected aptamers were predicted using the Mfold software (Figure 1). Each sequence showed different free energy values (dG) that reflect the stability of folding structures. The results showed that all selected sequences can form hairpin loop structures with the random region forming the loop and the primer regions making up the stem regions. We also tested the binding affinity for the dominant aptamer Apt1 to CD44 protein using GST magnetic beads separation technique. The results clearly demonstrate the ability of Apt1 to bind CD44 with high affinity (Kd = 81.3 ± 30.6 nM) as shown in Figure 2.

Table 1: Full sequences of the three selected aptamers

Name of	*Frequency of sequence (%)*	*No. of clones*	*Sequence*
Apt1	76	19	GGGAUGGAUCCAAGCUUACUGGCAUCUGGAUUUGCGCGUGCCAGAAU AAAGAGUAUAACGUGUGAAUGGGAAGCUUCGAUAGGAAUUCGG
Apt2	12	3	GGGAUGGAUCCAAGCUUACUGGGGAGUAUGCGCUUGGCCGUAAUAAU GUCGAGGCUGCCCAGGUUGUGGGAAGCUUCGAUAGGAAUUCGG
Apt3	12	3	GGGAUGGAUCCAAGCUUACUGGGGAGUACGACUUGGCUGUGUUCUUU CGGUGCUUCUGCGUAGGCCGGGGAAGCUUCGAUAGGAAUUCGG

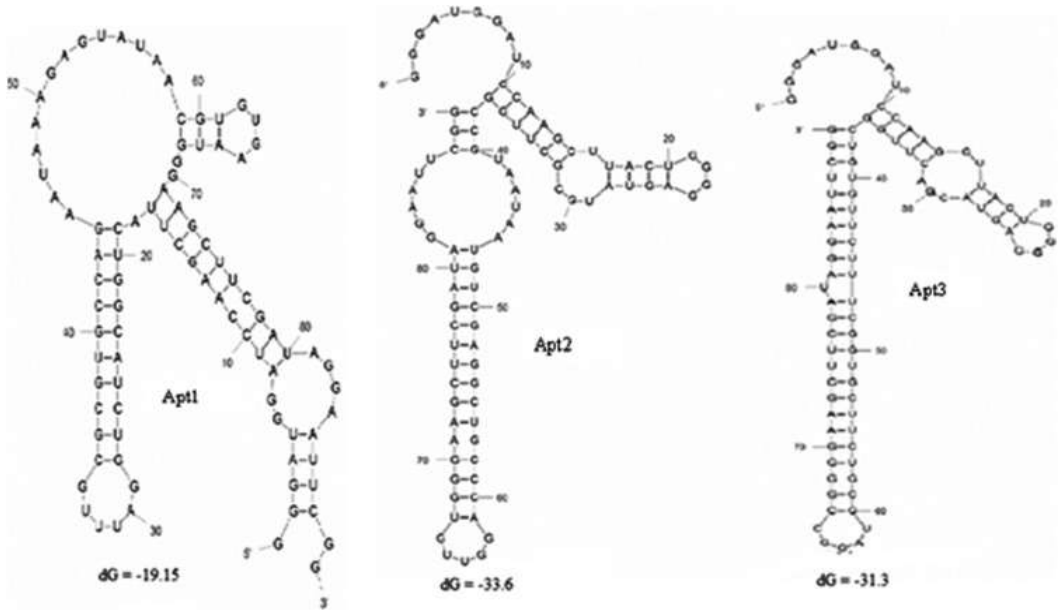

Figure 1: *The secondary structures of three selected aptamers predicted by the Mfold program.*

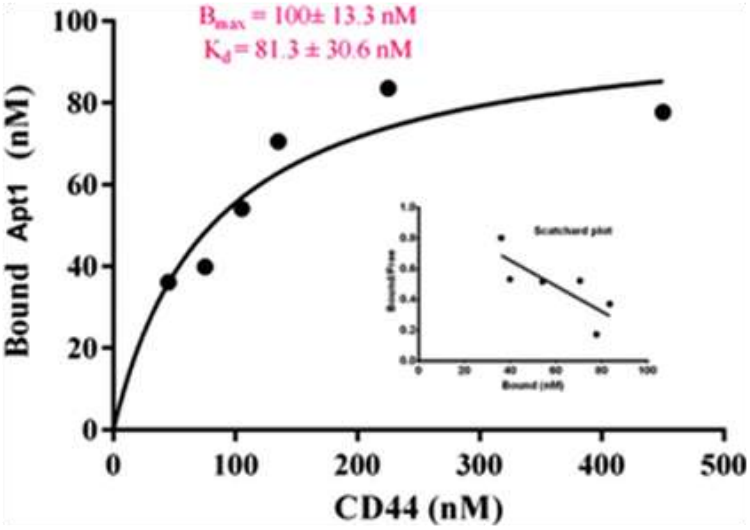

Figure 2: *Fitting curve to measure the affinity binding of fluorescein isothiocyanate (FITC)-labeled Apt1 to cell surface glycoprotein (CD44). The data were fit with regression analysis for one binding site using GraphPad Prism 6 software. The figure insert shows schatchared plot.*

3.2. Cellular assays

The binding specificity of the selected aptamers was evaluated using the Apt1 FITC-labeled RNA aptamer and CD44 + human cancer cell lines. The main cell line was the breast adenocarcinoma-derived cell line MDA-MB-231, which expresses a large amount of CD44 molecules on the cell surface [18]. The MCF7 cell line and the ductal breast epithelial tumor-derived cell line T47D, which have lower levels of CD44 expression, were also used [18]. The fluorescence intensities of all cell lines were compared using the fluorescent microscope (Figure 3).

The MDA-MB-231 cells clearly showed higher FITC fluorescence intensities as compared to MCF7 and T47D. It is worth mentioning here that the synthesized aptamer had no effect on cell growth and proliferation as assessed by the MTT assay.

3.3. Flow cytometry analysis

Flow cytometry was used to confirm that the interaction observed between Apt1 and human cancer cells and to rule out nonspecific binding of RNA aptamers to cultured cells. The binding specificity of Apt1 was evidenced by comparing the measured fluorescence intensities on the histograms shown in Figure 4. The Histogram analysis of the reacted sequences was specific with an observed higher affinity to Apt1 binding. The randomized FITC-labeled ssDNA probe, used as a negative control had little to no binding capacity to the used cancer cells. Unstained cells showed background fluorescence due to autofluorescence. Aptamer modification and stability For effective potential use in therapeutic or diagnostic applications, aptamers must resist the degradation by exo- and endonucleases. To achieve adequate in vivo stability of aptamers, 2′-O-methyl modifications have been incorporated. To test the stability of 2′-O-methyl-modified Apt1, stability assays was carried out by incubating the modified aptamers in growth media containing 10 % Fetal Bovine Serum (FBS) for 36 hours. Real time PCR results confirmed that the modified RNA aptamers was very stable

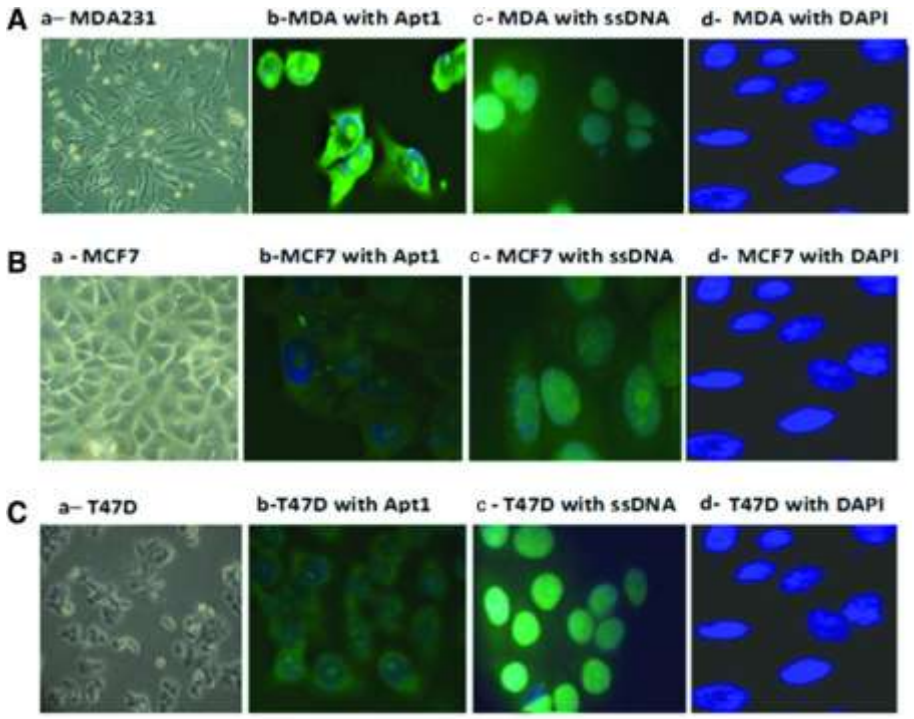

Figure 3: *Detection of CD44 by fluorescence microscopy using FITC-Apt1. Figures A–C represent results for MDA-MB-231, MCF7, and T47D cell lines, respectively. Frames a–d for each cell line represent the following: (a) light microscopy (20×) view of cultured cells before aptamer binding, (b) the binding of Apt1 to the cultured cells, (c) the binding of FITC labeled non-specific single-stranded (ss) DNA library, and (d) the DAPI nuclear DNA counter stain. These 60× fluorescent photographs (b–d, clearly show the higher expression of CD44 by MDA-MB-231 cells as compared with MCF7 and T47D cells.*

When incubated at 37 °C for more than 24 hours, as there was a little difference between cycle thresholds for the amplified aptamers at different time points (Figure 5).

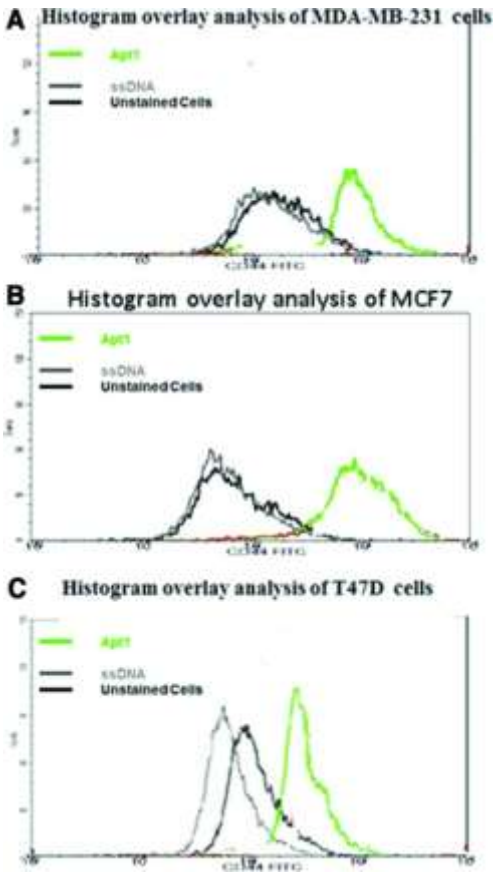

Figure 4: *FAC scan histogram analysis of the binding of Apt1 to breast cancer cell lines. (A) Histogram analysis for the binding of selected aptamer to MDA-MB231 cells, (B) MCF7 cells, and (C) T47D cells. Green curve represents the binding of Apt1 FITC-labeled aptamers to the cells. Unselected ssDNA library was used as a negative control (gray), and unstained cells were used as a fluorescence background (black).*

4. Discussion

In this study, the SELEX methodology was used to select modified RNA aptamers capable of targeting the CD44 receptor protein. To the best of our knowledge, the three aptamers described here are the first RNA aptamers developed against the cancer stem cell marker CD44. These aptamers were selected with the eventual future goal of using them for targeted delivery of therapeutic drugs to cancer cells expressing CD44. Fluorescent microscopy showed that Apt1 CD44 aptamer probes did bind specifically to CD44 expressing cells, which was demonstrated by the staining of the cell membranes of the representative cancer cell lines. The MDA-MB-231 cell line demonstrated the highest fluorescence when bound to Apt1, whereas MCF7 and T47D showed lower fluorescence intensity. Such results reflect the previously reported differential levels of CD44 expression on the surface of these cell lines [18]. It should be emphasized here that not all aptamer sequences developed by SELEX against purified form of their target proteins would automatically bind to their targets in their cellular context. It was noticed that the Apt1 CD44 aptamer probes stained the cell membranes and, more diffusely, the cytoplasm of these cancer cell lines. This staining pattern may be due to the better penetration and more efficient reaction of aptamer probes within the fixed cells. Successful cellular internalization has been reported for a number of aptamers, including anti-PSMA, which targets PSMA in prostate cancer cells, and Sgc8, which targets PTK7 in acute leukemia, cells [19-21]. Twenty five- base-long, synthetic single stranded DNA aptamers were derived to bind to known internalized tumor markers such as CD33, CEA, MUC1, and Tn antigens [22] and were imported through these surface portals into cancer cells. Zhang et al. reported the development of a cancer-cell-specific DNA aptamer

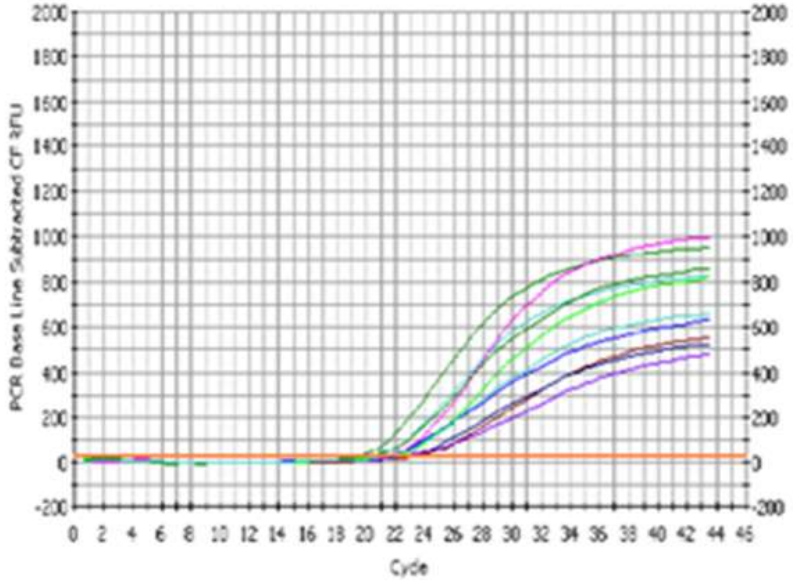

Figure 5: *RNA stability determination for Apt1 by real time polymerase chain reaction (PCR) at different times (0–24 hours). The starting quantity of DNA template is proportional to the threshold cycles. Real time PCR results also confirmed that the Apt1 RNA aptamer was very stable, as there was little difference between cycle thresholds at different time points.*

probe, KMF2-1a, using the cell-SELEX method that was successfully internalized to the endosome of target breast cancer cells [23].These results further support the finding that aptamers can serve as promising agents for cell-type-specific intracellular delivery with both diagnostic and therapeutic implications. The selected aptamers were labeled with FITC and modified with 2′-O-methyl group to inhibit their degradation by nucleases. It has been established that aptamers can be directly modified at either the 5¢ or 3¢ end using several fluorescent dyes without interfering with the aptamer folding and its ability to bind its target [24]. Fluorescein-labeled aptamers have been used for imaging studies of cultured cells by fluorescence microscopy, as well as by flow cytometry for a variety of cell types, including leukemia, lung, liver, ovarian, and colorectal cancer cells, as well as virus-infected cells [24]. Somasunderam et al. (2010) [25] reported the selection of ssDNA thioaptamers that can bind

hyaluronic acid binding domain of the CD44 receptor. The results of this study showed that the selected thioaptamers did bind the CD44 protein with a higher affinity (180–295 nM) compared with hyaluronic acid (Kd > 61 μM). Moreover, the specificity of the selected aptamers confirmed by its ability to bind positive human ovarian cancer cell lines (SKOV3, IGROV, and A2780) while failing to bind the CD44 negative NIH3T3 cell line. In our study, flow cytometry analysis of FITC-labeled CD44 RNA aptamers with breast cancer cells showed that there is an evident binding between Apt1 and cancer cells, in terms for specificity as shown by histogram analysis. This also confirms the specific binding of CD44 aptamers to CD44-positive cancer cells. These results demonstrate the potential application of the selected aptamers to distinguish between normal and tumor tissue sections. Aptamers, especially RNA-based ones, are susceptible to degradation by environmental nucleases, largely limiting their clinical value. In this study, the selected aptamers were modified with 2′-O-methyl group to improve the nuclease resistance of the RNA-based aptamers, which significantly increased the stability of these aptamers making them less susceptible to nuclease degradation. These features improve the capabilities of aptamers when used for diagnostic and therapeutic applications.

5. Conclusions

On the basis of the findings of this study, it is concluded that the isolated RNA aptamers bind specifically to CD44 molecules on the representative cell lines expressing this marker. With further characterization, the developed CD44 aptamers might be exploited in therapeutic applications as vehicles for targeted delivery of cytotoxic drugs against cancer stem cells, as well as in diagnostic assays aimed at detecting such cells in cancer patients. Such further characterization would include first establishing the binding affinities for selected aptamers, and truncating the aptamers to reach the smallest functional sequence.

6. References

[1] J.E. Visvader, G.J. Lindeman, Cancer stem cells in solid tumours: accumulating evidence and unresolved questions, Nat Rev Cancer, 8 (2008) 755-768.

[2] E.M. Hurt, W.L. Farrar, Cancer stem cells: the seeds of metastasis?, Mol Interv, 8 (2008) 140-142.

[3] C. Tang, B.T. Ang, S. Pervaiz, Cancer stem cell: target for anti-cancer therapy, FASEB J, 21 (2007) 3777-3785.

[4] M.P. Deonarain, C.A. Kousparou, A.A. Epenetos, Antibodies targeting cancer stem cells: a new paradigm in immunotherapy?, MAbs, 1 (2009) 12-25.

[5] J.L. Williams, Cancer stem cells, Clin Lab Sci, 25 (2012) 50-57.

[6] A. Jaggupilli, E. Elkord, Significance of CD44 and CD24 as Cancer Stem Cell Markers: An Enduring Ambiguity, Clin Dev Immunol, (2012).

[7] V. Orian-Rousseau, CD44, a therapeutic target for metastasising tumours, Eur J Cancer, 46 (2010) 1271-1277.

[8] S.J. Wang, L.Y. Bourguignon, Role of hyaluronan-mediated CD44 signaling in head and neck squamous cell carcinoma progression and chemoresistance, Am J Pathol, 178 (2011) 956-963.

[9] D. Naor, S. Nedvetzki, I. Golan, L. Melnik, Y. Faitelson, CD44 in cancer, Crit Rev Cl Lab Sci, 39 (2002) 527-579.

[10] A. Afify, P. Purnell, L. Nguyen, Role of CD44s and CD44v6 on human breast cancer cell adhesion, migration, and invasion, Exp Mol Pathol, 86 (2009) 95-100.

[11] J. Liu, G. Jiang, CD44 and hematologic malignancies, Cell Mol Immunol, 3 (2006) 359-365.

[12] R. Marhaba, P. Klingbeil, T. Nuebel, I. Nazarenko, M.W. Buechler, M. Zoeller, CD44 and EpCAM: Cancer-Initiating Cell Markers, Current Molecular Medicine, 8 (2008) 784-804.

[13] M. Baumann, M. Krause, CD44: a cancer stem cell-related biomarker with predictive potential for radiotherapy, Clin Cancer Res, 16 (2010) 5091-5093.

[14] S.D. Jayasena, Aptamers: an emerging class of molecules that rival antibodies in diagnostics, Clin Chem, 45 (1999) 1628-1650.

[15] B. Soontornworajit, Y. Wang, Nucleic acid aptamers for clinical diagnosis: cell detection and molecular imaging, Analytical and Bioanalytical Chemistry, 399 (2011) 1591-1599.

[16] R. Stoltenburg, C. Reinemann, B. Strehlitz, SELEX--a (r)evolutionary method to generate high-affinity nucleic acid ligands, Biomol Eng, 24 (2007) 381-403.

[17] S. Shigdar, A.C. Ward, A. De, C.J. Yang, M. Wei, W. Duan, Clinical applications of aptamers and nucleic acid therapeutics in haematological malignancies, Br J Haematol, 155 (2011) 3-13.

[18] S. Ricardo, A.F. Vieira, R. Gerhard, D. Leitao, R. Pinto, J.F. Cameselle-Teijeiro, F. Milanezi, F. Schmitt, J. Paredes, Breast cancer stem cell markers CD44, CD24 and ALDH1: expression distribution within intrinsic molecular subtype, Journal of Clinical Pathology, 64 (2011) 937-946.

[19] S.E. Lupold, B.J. Hicke, Y. Lin, D.S. Coffey, Identification and characterization of nuclease-stabilized RNA molecules that bind human prostate cancer cells via the prostate-specific membrane antigen, Cancer Research, 62 (2002) 4029-4033.

[20] Z. Xiao, D. Shangguan, Z. Cao, X. Fang, W. Tan, Cell-specific internalization study of an aptamer from whole cell selection, Chemistry, 14 (2008) 1769-1775.

[21] J. Zhou, J.J. Rossi, The therapeutic potential of cell-internalizing aptamers, Curr Top Med Chem, 9 (2009) 1144-1157.

[22] E.W. Orava, N. Cicmil, J. Gariepy, Delivering cargoes into cancer cells using DNA aptamers targeting internalized surface portals, Biochim Biophys Acta, 1798 (2010) 2190-2200.

[23] K. Zhang, K. Sefah, L. Tang, Z. Zhao, G. Zhu, M. Ye, W. Sun, S. Goodison, W. Tan, A novel aptamer developed for breast cancer cell internalization, ChemMedChem, 7 (2012) 79-84.

[24] D. Lopez-Colon, E. Jimenez, M. You, B. Gulbakan, W. Tan, Aptamers: turning the spotlight on cells, Wiley Interdiscip Rev Nanomed Nanobiotechnol, 3 (2011) 328-340.

[25] A. Somasunderam, V. Thiviyanathan, T. Tanaka, X. Li, M. Neerathilingam, G.L. Lokesh, A. Mann, Y. Peng, M. Ferrari, J. Klostergaard, D.G. Gorenstein, Combinatorial selection of DNA thioaptamers targeted to the HA binding domain of human CD44, Biochemistry, 49 (2010) 9106-9112.

Travaux expérimentaux

Chapitre 2

Fonctionnalisation de liposomes avec un aptamère anti-CD44 pour le ciblage sélectif des cellules cancéreuses

Experimental work

Chapter 2

Functionalizing liposomes with anti-CD44 aptamer for selective targeting of cancer cells

Travaux expérimentaux

Chapitre 2

Fonctionnalisation de liposomes avec un aptamère anti-CD44 pour le ciblage sélectif des cellules cancéreuses

Résumé

Dans cette étude, l'aptamère Apt1 à base d'ARN modifié par des 2'-F-pyrimidines, précédemment sélectionné pour son affinité pour CD44, a été conjugué à la surface de liposomes PEGylés en utilisant une réaction de type thiol-maléimide. Cette conjugaison a été confirmée par le changement de taille et de potentiel zéta et par électrophorèse sur gel d'agarose, et a été quantifiée en utilisant un dérivé fluorescent d'Apt1. L'affinité d'Apt1 pour CD44 a été améliorée par la conjugaison aux liposomes par rapport à l'aptamère libre. La capture cellulaire les liposomes fonctionnalisés a été évaluée par cytométrie en flux et par microscopie confocale sur deux lignées cellulaires $CD44^+$, A549 (cancer du poumon humain) et MDA-MB-231 (cancer du sein humain), et a été comparée à une lignée cellulaire $CD44^-$ de fibroblastes embryonnaires de souris (NIH/3T3). Les résultats ont montré une capture cellulaire doublée des liposomes fonctionnalisés par rapport aux liposomes nus, mais seulement sur les cellules $CD44^+$. En conclusion, nous démontrons la possibilité de conjuguer un aptamère anti-CD44 à la surface de liposomes, permettant d'augmenter préférentiellement leur capture par des cellules cancéreuses exprimant CD44. De tels liposomes constituent des nanovecteurs prometteurs pour le ciblage actifs de tumeurs surexprimant CD44.

Ce chapitre a été puplié dans Bioconjugate Chemistry en 2014, avec comme authers Walhan ALSHAER, Hervé HILLAIREAU, Juliette VERGNAUD, Said ISMAIL, Elias FATTAL.

Experimental work

Chapter2

Functionalizing liposomes with anti-CD44 aptamer for selective targeting of cancer cells

Abstract

In this chapter, we describe the conjugation of the 2′-F-pyrimidine-containing RNA aptamer Apt1, previously selected to bind CD44, to the surface of PEGylated liposomes using a thiol-maleimide "click" reaction. The conjugation of Apt1 to the surface of liposomes was confirmed by a change in size and zeta potential and by migration on agarose gel electrophoresis, and was quantified using a fluorescently-labeled Apt1 derivative. The binding affinity of Apt1 was improved after conjugation to liposomes compared to the free Apt. The cellular uptake for the resulting Apt1 liposomes (Apt1-lip) was tested by flow cytometry and confocal imaging using two $CD44^+$ cell lines, human lung cancer cells (A549) and human breast cancer cells (MDA-MB-231), and was compared to a $CD44^-$ cell line, mouse embryonic fibroblast cells (NIH/3T3). The results showed a 2-fold higher uptake of Apt1-lip compared to blank liposomes, but only in the case of $CD44^+$ cells. In conclusion we demonstrate the successful conjugation of an anti-CD44 aptamer to the surface of liposomes, resulting in a preferential uptake by CD44-expressing cancer cells, which shows the promising potency of Apt1-functionnalized liposomes as a targeted drug delivery system.

This chapter has been published in Bioconjugate Chemistry in 2014, with Walhan ALSHAER, Hervé HILLAIREAU, Juliette VERGNAUD, Said ISMAIL, and Elias FATTAL as authors.

1. Introduction

Most of current conventional anti-tumor treatments aim to restrain proliferation and metastasis of tumor cells. However, many of these therapeutics fail to eradicate tumors, as indicated by some poorly understood clinical events including drug resistance and tumor relapse [1, 2]. One of the main hypotheses that explain such events states that malignancies depend on a small population of stem-like cells that are highly resistant to conventional tumor therapeutics and are able to maintain and propagate tumors [3, 4]. Those cells, to which the name Cancer Stem Cells (CSC) was given, are characterized by the ability of self-renewal, tumor initiation and proliferation, and differentiation into other tumor cells [5-7]. Therefore, targeting CSCs as well as the bulk tumor cells could be of high therapeutic potency in eliminating tumors and decreasing tumor relapse [8, 9]. Many CSCs surface markers had been identified such as CD133, EpCAM, and CD44 [10-13]. These markers constitute potent targets for specific and selective targeting of antitumor therapeutics into CSCs [13]. Among all CSC surface markers, CD44 has been characterized as the most common biomarker, being overexpressed by many tumors including colon, breast, pancreatic, head and neck cancers [10, 14-16]. CD44 is a multi-structural and functional cell surface glycoprotein known to play a role in cell communication between the adjacent cells and between the extracellular matrix. CD44 is the main receptor of hyaluronic acid (HA) and collaborate with other cellular proteins to regulate cell adhesion, proliferation, homing, migration, motility, growth, survival, angiogenesis and differentiation [17].

Aptamers are synthetic single stranded oligonucleotides or peptides that can be selected against almost any target including ions, small chemical molecules, peptides, proteins and enzymes, and even whole living cells such as bacteria and tumor cells [18]. Aptamers can be selected from a combinatorial library consisting of 10^{13} to 10^{15} different sequences by a method named Systematic Evolution of Ligands by EXponential enrichment (SELEX) [19,

20]. The principle of molecular binding is based on the ability of the aptamer to fold into complex three dimensional structures and shapes and then fit and bind with the selected target with high affinity and specificity. Aptamers hold several advantages over their long established competitors, monoclonal antibodies, such as their low toxicity and immunogenicity, easy chemical modifications, efficient reproduction with long shelf-life, and reasonable coast. Therefore, aptamers constitute promising molecules with high potential in biomedical applications including therapeutics, diagnostics, biomarkers discovery and specific targeting ligands [21, 22]. They can be clinically used since Macugen® was the first successful aptamer-based therapeutics which was approved in 2006 by FDA for the treatment of Age Macular Degeneration (AMD). Moreover, many aptamers are in clinical trials now[23]. Among all nanoparticle-based drug delivery systems, liposomes are considered as one of the most successful in clinical use due to advantages including biocompatibility, stability, easy to synthesize, low batch-to-batch variation, high drug payload with one or more of different therapeutic molecules [24]. Many liposome formulations have been approved for drug delivery by passive ways based on the concept of enhanced permeability and retention. However, such passive targeting does not discriminate between normal and diseased cells. Therefore, cell-specific targeting liposomes have been developed to increase the accumulation of drugs in diseased cells, mostly cancer stem cells in the case of CD44 targeting, and thus decreasing the toxic side effects to normal cells [25]. Therefore, active targeting could increase the accumulation of therapeutics around the targeted cells, compared to untargeted cells. Antibodies and hyaluronic acid (HA) have been widely and successfully used in the development of drug nanocarrier systems that target CD44-expressing tumor cells [26, 27]. However, there are significant challenges in the utilization of antibodies and HA for targeting. Antibodies showed to be immunogenic and rapidly immune clearance from the peripheral circulation [28, 29]. While, low molecular weight HA showed to be inflammatory,

angiogenic, and immunostimulatory [30]. Therefore, anti-CD44 aptamer are attractive alternative to functionalize liposomes for selective targeting of therapeutics into CD44-expressing tumor cells.

In previous work we succeeded in selecting a modified RNA aptamer, named Apt1, against the standard isoform of human CD44 receptor protein using the SELEX method [31]. The selected aptamer was modified with 2'-F-pyrimidine to increase stability against nucleases for biological applications. In the present work, we developed an aptamer-functionalized-liposome (Apt1-Lip) as a model of drug delivery system that selectively target CD44-expressing tumor cells. Such functionalization was performed by thiol-maleimide conjugation chemistry between 3'-thiol modified Apt1 and the maleimide functionalized to the surface of the liposomes as shown in scheme 1. The targeted liposomes were shown to express high affinity for CD44 positive cells without triggering any inflammatory response within these cells.

Scheme 1: Apt1-Liposome functionalization using Thiol-Maleimide click-reaction.

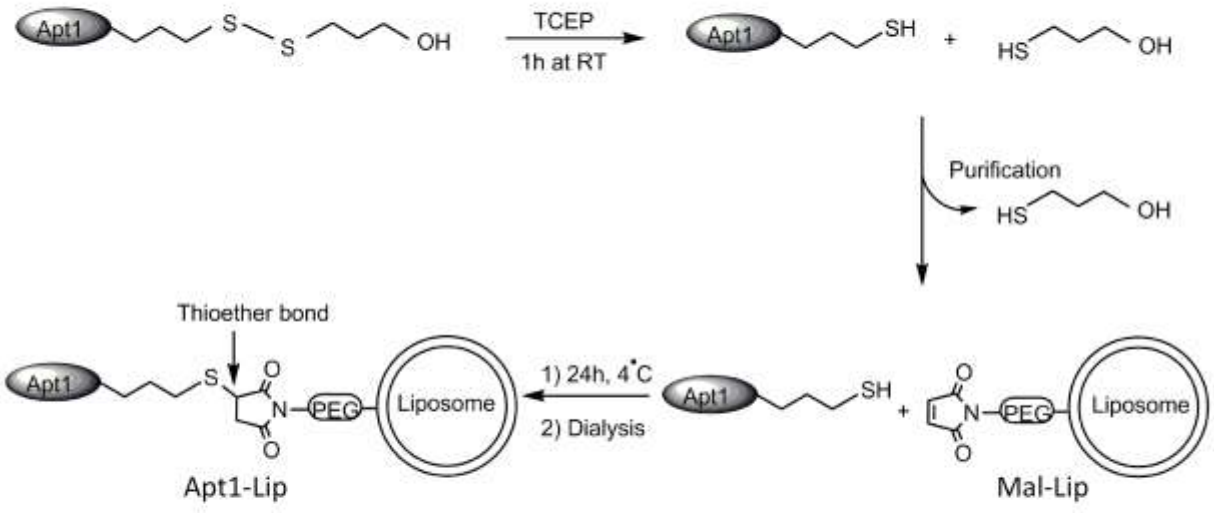

2. Materials and methods

2.1. Materials

The lipids 1, 2-dihexadecanoyl-*sn*-glycero-3-phosphocholine (DPPC) was purchased from Corden pharma (Germany), while 1, 2-distearoyl-*sn*-glycero-3-phosphoethanolamine-N-[maleimide (polyethylene glycol)-2000] (DSPE-PEG(2000)-Maliemide) and L-α-Phosphatidylethanolamine-N-(lissamine rhodamine B sulfonyl) (PE-Rhod) were purchased from Avanti Polar Lipids (Alabaster, USA). Cholesterol was obtained from Sigma-Aldrich. Tris(2-carboxyethyl)phosphine hydrochloride (TCEP) was from Thermo Fisher Scientific (MA, USA).

Apt1 with 2'-F-pyrimidines (sequence: 5' -GGGAUGGAUCCAAGCUUACUGGCAUCU GGAUUUGCGCGUGCCAGAAUAAAGAGUAUAACGUGUGAAUGGGAAGCUUCGA UAGGAAUUCGG-3') have been chemically synthesized by cyanoethyl phosphoramidite chemistry (Midland Certified Reagent, Texas, USA). Apt1 was modified with C6-thiol SS (protected form) at the 3' end and labeled with FITC at the 5' end. All other materials were obtained from different resources.

2.2. Cell lines

Human lung cancer cells (A549) and mouse embryonic fibroblast cell line (NIH/3T3) were obtained from the American Type Culture Collection (ATCC). Human breast cancer cells (MDA-MB-231) were obtained from the European Collection of Cell Culture (ECACC). A549 and NIH/3T3 cells were cultured in RPMI-1 and DMEM medium (Lonza, Switzerland), respectively, supplemented with 10% fetal bovine serum, and 10,000 unit/ml of penicillin and 10 mg/mL of streptomycin (Lonza, Switzerland). MDA-MB-231 cells were cultured in Leibovitz's L-15 medium (Lonza, Switzerland) supplemented with 15% fetal bovine serum, 2 mM L-glutamine, 20 mM sodium bicarbonate and 10,000 unit/ml of penicillin and 10mg/mL of streptomycin. All cell lines have been incubated in humidified incubator supplied with 5%

CO_2 and maintained at 37 °C. Characterization of all cell lines for the expression of CD44 was tested using FITC-labeled anti-CD44 antibodies (Immunotech, Beckman-Coulter, USA).

2.3. Preparation of maleimide-functional liposome

Liposomes with maleimide active group (Mal-Lip) were prepared by the thin lipid film-hydration method.[33] Stock solution of DPPC, cholesterol, and DSPE-PEG(2000)-Mal in a 62:35:3 molar ratio were mixed and dissolved in 5 ml of chloroform. A thin film was obtained by evaporation of chloroform using rotary evaporator for 30 min at 50 °C with decreased pressure. This film was then hydrated with 5 mL of PBS and vortexed for 30 min followed by extrusion 13 times through 100 nm polycarbonate membrane (Millipore) to obtain liposomes with a size around 100 nm. Rhodamine-containing liposomes have been prepared as described above with DPPC:cholesterol:DSPE-PEG(2000)-MAL:PE-Rhod at molar ratio 61:35:3:1. These liposomes were also used as blank liposomes.

2.4. Conjugation of Apt1 to liposomes

Functionalizing Mal-Lip with Apt1 was performed using thiol-maleimide cross linking reaction to form thioether bond. Before conjugation, C6-thiol-modified Apt1 (Apt1-(CH2)3-S-S-(CH2)3-OH) has been deprotected in free nuclease water by 100 mM TCEP (pH 6.5) for 1 hour at room temperature to produce Apt1-SH and then purified by precipitation using 3 volumes of absolute ethanol and 0.1 volume of 3 M sodium acetate. After precipitation, Apt1-SH was resuspended in binding buffer (2.5 mM $MgCl_2$, 1X PBS, pH 7.4) and folded by heating at 70°C for 10 minutes followed by rapid cooling on ice for 10 minutes. The resulting deprotected Apt1 was conjugated to Mal-Lip at a 0.5:1 molar ratio by incubation overnight at 4°C followed by dialysis to remove free Apt1 from the Apt1-Lip suspension.

2.5. Characterization of Apt1-Lip

Size and zeta potential

The size and zeta potential of Apt1-Lip and Mal-liposomes were measured at 25ºC by

Dynamic Light Scattering (DLS) using nano ZS (Malvern instruments, UK). Apt1-Lip or Mal-liposomes in 1X PBS were diluted in free nuclease water to obtain 8 mM sodium chloride final concentration (pH 7.4).

Agarose gel electrophoresis

Agarose gel electrophoresis was performed to confirm the successful conjugation of Apt1 to the surface of liposomes. Samples of Apt1-lip (before and after dialysis), blank liposomes and free Apt1 were loaded into 2% Agarose gel (Promega, USA) supplemented with 5 μL of 2.5 mg/mL ethidium bromide followed by running electrophoresis in 1X TAE buffer (pH 8.2) at 120 V for 20 minutes. Images for analysis were obtained using MF-ChemiBIS gel imaging system (DNR Bio-Imaging Systems).

Determination of Apt1 density at the surface of liposomes

To quantify the amount of Apt1 conjugated to the surface of liposome, a fraction of conjugated Apt1 was quantified by detection of fluorescence intensity obtained from FITC-Apt1-Lip (excitation 494 nm, emission 517 nm) and compared to a standard curve using a Spectrofluorometer LS 50B (PerkinElmer, USA). The number of liposomes was calculated based on the equation S1. Using those two values, it was possible to divide the amount of Apt1 by the number of liposomes to obtain the density of Apt1 on the liposome surface.

2.6. Binding experiments

Binding affinities

The change in the binding affinity of Apt1 before and after conjugation was investigated using magnetic separation beads. The dissociation constants (K_d) have been determined for Apt1-Lip and free Apt1 by binding to GST-tagged CD44 protein immobilized on magnetic separation beads (Promega, USA). An amount of 50 pmol of C6-thiol Apt1 were labeled at 5'-end with radioactive phosphate of [γ-^{33}P]ATP (PerkinElmer) using T4 Polynucleotide Kinase (Promega, USA), and then reduced and conjugated following the same method described

before. The binding affinity constant (K_d) were determined by incubating variable concentrations (1 to 50 nM) for both free-Apt1 and Apt1-Lip with immobilized CD44 protein (10 nM) for 1 h at 37°C in 40 µL binding buffer. After incubation, unbound complexes removed by washing three times with 100 µL of binding buffer. The CD44–Apt1-Lip or CD44-Apt1 complexes were then eluted from the beads using 100 µL of elution buffer (50 nM glutathione, 50 nM Tris-HCl, 1% Triton 100). Radiaoactivity was counted in gold scintillation liquid using Scintillation Counter (LS 6000, Beckman, USA). For non specific binding, the same concentrations of Apt1-Lip and free-Apt1 were incubated with CD44-negative GST-tagged magnetic separation beads. The specific binding was fitted using Hill equation:

$$Y = \frac{B_{max} * X^h}{(K_d^h + X^h)}$$

While Y is the specific binding, B_{max} is the maximum specific binding, h is the Hill slop, X is the Apt1 concentration, and K_d is the dissociation constant.

Flow cytometry

Apt1-Lip binding specificity and uptake by cells were assessed by measuring the mean fluorescence intensity using a flow cytometer (Accuri C6, BD Biosciences, and USA). Approximately 1×10^5 cells of each selected cell line were seeded in 12-well plates and incubated for 24 h at 37 ºC to reach 80% confluency. After incubation, cells were washed by PBS and incubated in 200 µL of fresh medium supplemented with 2.5 mM $MgCl_2$. Then, 400 nM Apt1-Lip-Rhod were incubated with cells for 3 h at 37 °C. The unbound Apt1-Lip were washed three times by PBS and detached by 100 µL of EDTA-accutase for 5 min. After detachment, cells were resuspended in 200 µL of binding buffer and 10,000 events were counted for each sample. Blank Mal-Lip-Rhod and the negative CD44 cell line NIH/3T3 have been used as negative controls.

Confocal laser scanning microscopy

Around 5×10^4 cells have been seeded into 12-well plates containing glass cover slip and incubated under standard conditions. After 24 h of incubation, cells were washed with PBS and 200 µL of fresh medium supplemented with 2.5 mM $MgCl_2$ was added. Cells were then incubated with 400 nM Apt1-Lip-Rhod for 2 h at 37 ºC. After incubation, the cells were washed three times with 500 µL of binding buffer then fixed by 4% paraformaldehyde for 10 min at room temperature in the dark. The cells were then washed three times by PBS and the coverslip transferred onto a glass slide and dipped in mounting medium. Blank lip-Rhod was used as control for comparison. The images were then acquired by a fluorescent microscope LSM 510 (Zeiss-Meta) using the same exposure sittings by 63x/1.5 oil lens.

2.7. Inflammatory cytokines release

To examine the inflammatory cytokines that may be released as a result of treating A549 and MDA-MB-231 cells with Mal-Lip or Apt1-Lip, 2×10^4 cells were seeded in 24-well plates for 48 h to reach 80% confluency. The supernatants were then discarded and replaced with 1 mL of fresh medium. The cells were treated with 10 µg of lipopolysaccharide (LPS) as control and with Mal-Lip or Apt1-Lip at 400 nM final concentrations. After 24 h exposure, the supernatant was collected and the cells washed with 1X PBS treated with 1X Trypsine and counted by flow cytometry. Human inflammatory cytokines IL-12p70, TNF, IL-10, IL-6, IL-1β, and IL-8 were quantified using Cytometric Beads Array (CBA) detection kit (BD Biosciences, USA) and the results were normalized to pg/10^5 cells.

3.8. Statistical analysis

All measurement points were repeated in three times. The values were expressed by the mean ± standard deviation. Multiple comparisons by tow-way ANOVA have been used to assess the statistical significant differences between the means ($p < 0.05$).

3. Results and discussion

3.1. Conjugation of Apt1 to Liposomes

Several aptamers have been successfully functionalized to different nanoparticles for selective targeting and drug delivery [32]. In this work liposomes functionalized with an anti-CD44 2'-F-pyrimidine RNA aptamer were developed as drug delivery system able to selectively bind CD44-expressing tumor cells. Maleimide-functionalized liposomes (Mal-Lip) composed of DPPC:Cholesterol:DSPE-PEG-Maleimide have been prepared by the thin lipid film hydration method [33] followed by extrusion through 100 nm polycarbonate membrane. Conjugation of Apt1 to Mal-Lip was carried out using thiol-Maliemide crosslinking chemistry which is one of efficient strategies to conjugate 3'-thiol-modefied aptamers to the maleimide-functionalized polyethylene glycol (PEG) [34].

Table 1: Hydrodynamic diameter and zeta potential charecterization of liposomes before and after Apt1 conjugation (mean ± SD, *n=6*).

	Lip	**Apt1-Lip**
Mean hydrodynamic diameter (nm ± SD)	129 ± 5	140 ± 6
Polydispersity Index (PDI ± SD)	0.09 ± 0.02	0.11 ± 0.03
ζ-potential (mV ± SD)	−17.5 ± 0.9	−31.05 ± 2.3

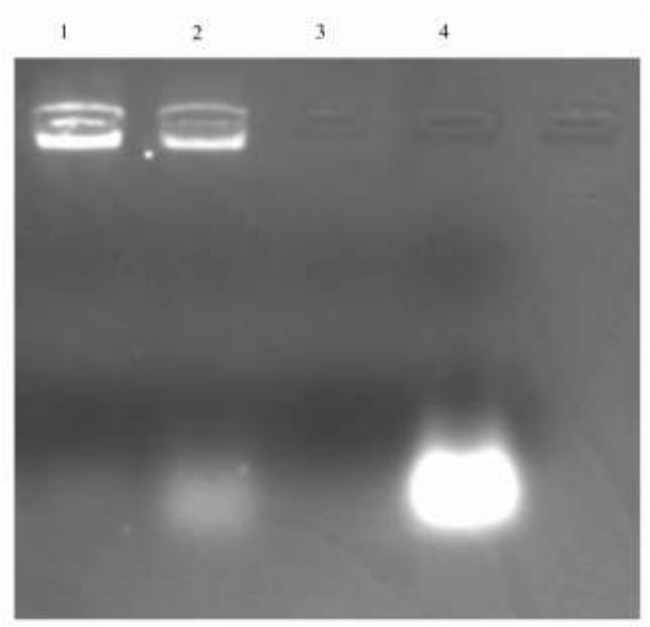

Figure 1: *Characterization of liposomes before and after Apt1 conjugation using agarose gel electrophoresis. Lanes: 1, Apt1-Lip after dialysis; 2, Apt1-Lip before dialysis; 3, Mal-Lip; 4, free Apt1.*

The efficiency and effect of Apt1 conjugation on the size and zeta potential of liposomes was investigated and data were compared to blank liposomes (Table 1). The size of Apt1-Lip showed slight increase in the hydrodynamic diameter (140 ± 6 nm, *n*=6) compared to blank Mal-Lip (129 ± 5 nm, *n*=6). Further characterization to different liposomes was performed by detection of zeta potential of both Mal-Lip (−17.5 ± 0.9 mV, *n*=6) and Apt1-Lip (−31.0 ± 2.3, *n*=6) in a diluted PBS buffer (8 mM NaCl, pH 7.4). The increase in liposome size (≈11 nm) and decrease in zeta potential (≈ −12.5 mV) is consistent with a successful conjugation of the negatively charged macromolecule Apt1 to the surface of liposomes. Additional information about the successful conjugation was obtained by the analysis of Apt1-Lip on agarose gel electrophoresis (Figure 1). Apt1-Lip appears trapped in the well where no signal was obtained for blank Mal-lip. Moreover, electrophoresis showed the efficacy of dialysis in removing unreacted free Apt1 from the Apt1-Lip. Therefore, Apt1 functionalization could be achieved

by covalently attachment to the surface of liposomes by establishing thioether bonds and not by adsorption.

Apt1 density has been determined using the fluorescent signal obtained from FITC-Apt conjugated to the surface of liposomes. The average amount of Apt1 conjugated molecules was calculated to be 6.06 nmole of Apt1 per mg of lipids and to an aptamer surface density of ≈ 422 of Apt1 molecule per one liposome which corresponds to a conjugation efficiency of ≈ 73 ± 3 % (mean ± SD, *n=3*).

3.2. Binding Affinity to CD44 protein

Binding affinity of functionalized liposomes is an important factor that impacts the efficacy of delivery system. Therefore, we investigated whether the conjugation of Apt1 may affect the affinity of binding to CD44 by performing a binding experiment for the free Apt1 and the Apt1-Lip with CD44 protein immobilized on magnetic beads. The binding of Apt1-Lip showed higher binding affinity (K_d = 6.2 ± 1.6 nM) compared to the affinity of free Apt1 (K_d = 21.5 ± 3.3 nM) (Figure 2). This shows that the conjugation did not negatively affect the binding affinity to CD44 receptor model. Moreover, such higher binding affinity of Apt1-Lip can be explained by multivalent-binding of conjugated Apt1 to CD44 on the surface of the beads. However, free Apt1 showed superior maximum-binding saturation (B_{max} = 374 ± 45 fmole) compared to Apt1-Lip (B_{max} = 106 ± 13 fmole). This can be due to the binding of Apt1-Lip covering of large areas on the beads resulting in steric hindrance of the remaining free binding sites compared to free Apt1 as appears in figure 2(A).

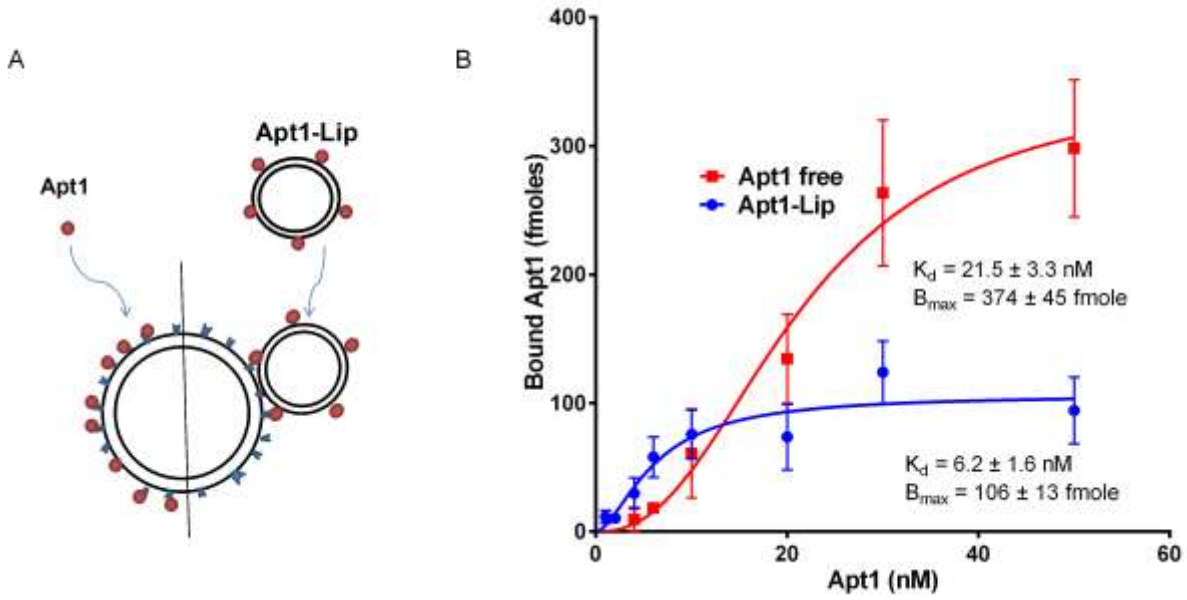

Figure 2: *Binding affinity curves of free Apt1 and Apt1-Lip to CD44. (A) Different concentrations of radiolabeled Apt1 (free or conjugated) have been incubated with fixed concentration of CD44 protein immobilized on magnetic beads. (B) Specific binding was obtained after subtracting non specific interaction with negative beads. The data are fitted using one binding site with hill equation (mean ± SD, n=3).*

3.3. Cellular Uptake

To investigate the binding specificity and selectivity to CD44 expressing cells, three cell lines have been selected for cellular uptake. The human lung cancer cells (A549) and the human breast cancer cells (MDA-MB-231) known to have high CD44 expression. $*p < 0.05$ compared to untreated cells and Lip-Rhod. Mouse embryonic fibroblast cell line (NIH/3T3) was used as negative cells for CD44. All cell lines have been confirmed for the expression or the absence of CD44 by flow cytometry using FITC-anti-CD44 antibodies. Both A549 cells and MDA-MB-231 cells had shown high CD44 expression level while NIH/3T3 cells were negative for CD44 expression (Figure S1). The same concentrations of Apt1-Lip-Rhod and Lip-Rhod were incubated with all selected cell lines and the mean fluorescent intensity was detected by flow cytometry.

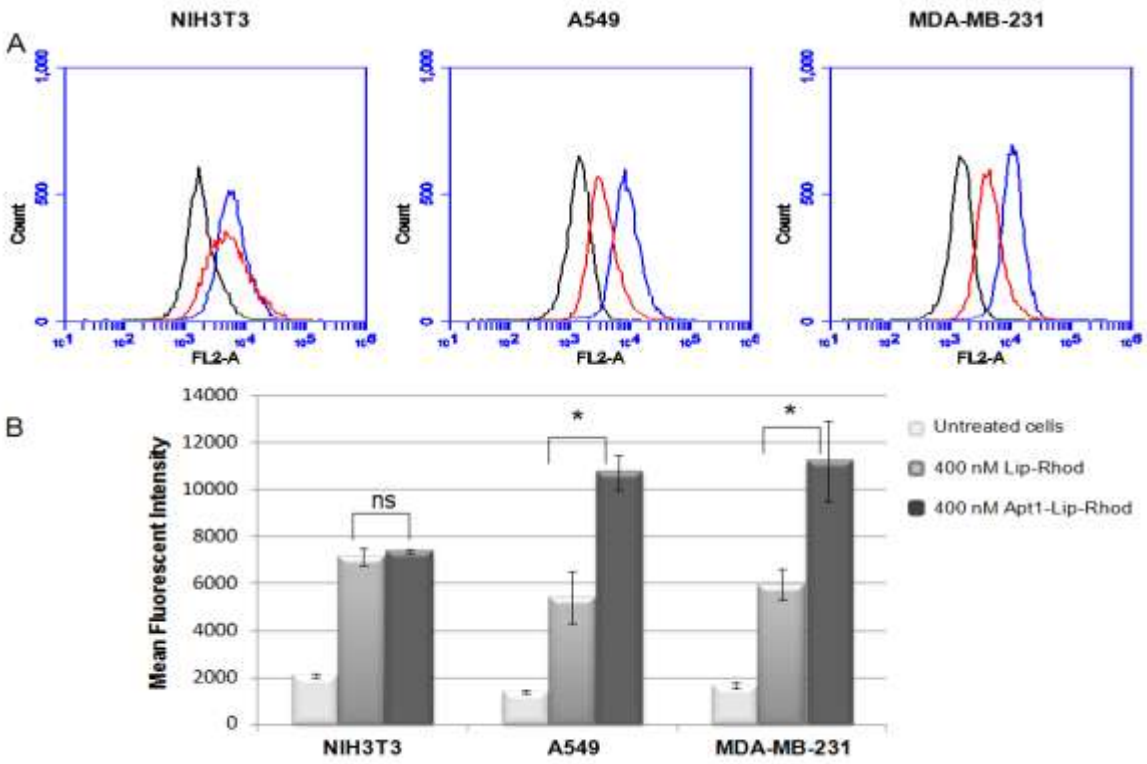

Figure 3: *Cellular uptake of Apt1-Lip-Rhod and Mal-Lip-Rhod. (A) Flow cytometry analysis of the three cell lines after incubation with 400 nM of Apt1-Lip-Rhod (blue) and Mal-Lip-Rhod (red), untreated cells (Black). (B) Mean Fluorescent Intensity (MFI) obtained from flow cytometry analysis after treatment of cells with 400 nM of Apt1-Lip-Rhod and Mal-Lip-Rhod (mean ± SD, n = 3, *p <0.05 compared to Lip-Rhod cells, ns: non significant).*

Both A549 and MDA-MB-231 cells showed higher mean fluorescent intensity when treated with Apt1-Lip-Rhod compared to Lip-Rhod. No significant difference in the mean fluorescent intensity was seen between Apt1-Lip-Rhod and Lip-Rhod was obtained with NIH/3T3 negative cells (Figure 3). These results demonstrate the preference of Apt1-Lip-Rhod to bind to CD44 positive cells and such binding preference is indicated by the higher selectivity and uptake sensitivity of CD44 positive cells to Apt1-Lip-Rhod compared to Lip-Rhod CD44-negative cells. Furthermore, the cellular uptake was analyzed using confocal microscopy and the results demonstrated higher accumulation of Apt1-Lip in cytoplasm of $CD44^{+}$ cells

compared to $CD44^{-}$ cells, therefore supporting the results obtained from flow cytometry (Figure 4).

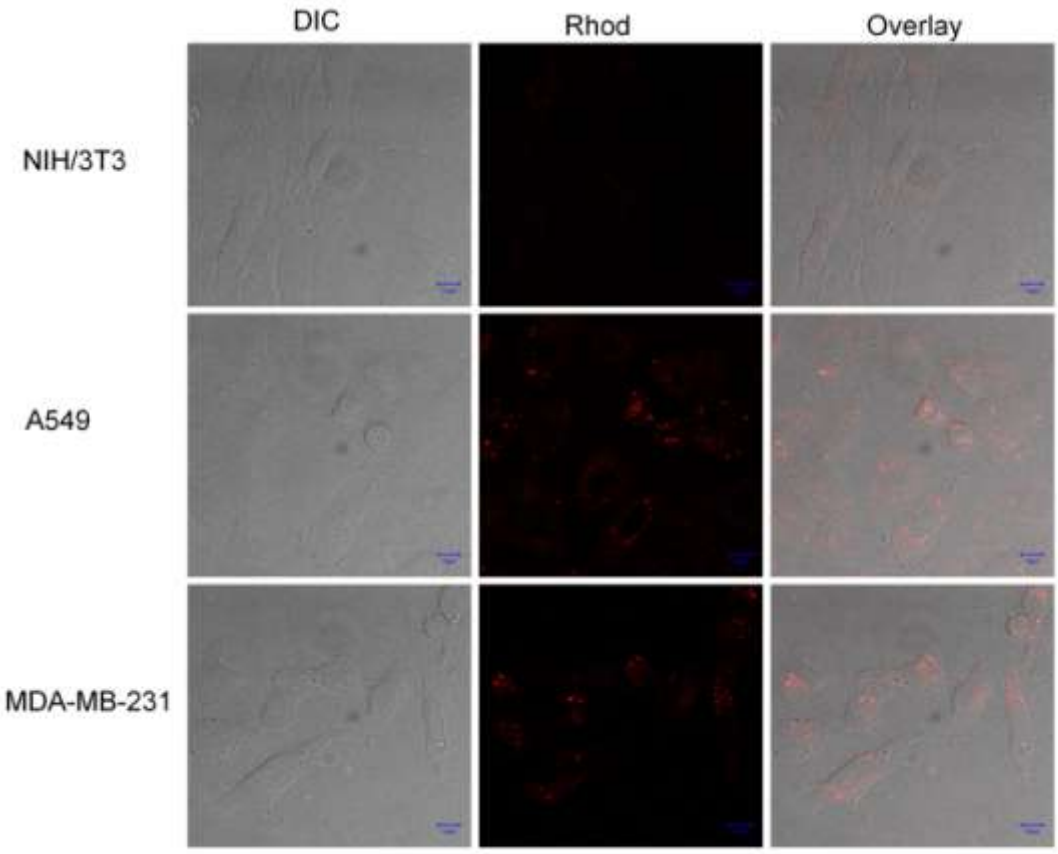

Figure 4: *Confocal microscope imaging for the selected cell lines treated with 400 nM of Apt1-Lip-Rhod.*

3.4. Inflammatory response

Considerable amount of evidence illustrate the link between inflammatory cytokines and the development of tumors. There are several inflammatory cytokines that are associated with chronic inflammation including IL-1β, IL-6, and IL-8. These cytokines are found to activate signaling pathways and positive feedback loops involved in tumor maintenance, invasion, metastasis, and drug resistance [35]. Therefore, investigation of inflammatory response against drug delivery systems such as liposomes could be carefully examined thereby

enabling the control of unwanted signals which resulted from inflammatory cytokines. In this study, the inflammatory response of A549 and MDA-MB-231 cells have been investigated by detection of the inflammatory cytokines IL-12p70, TNF, IL-10, IL-6, IL-1β, and IL-after exposure to Apt1-Lip.

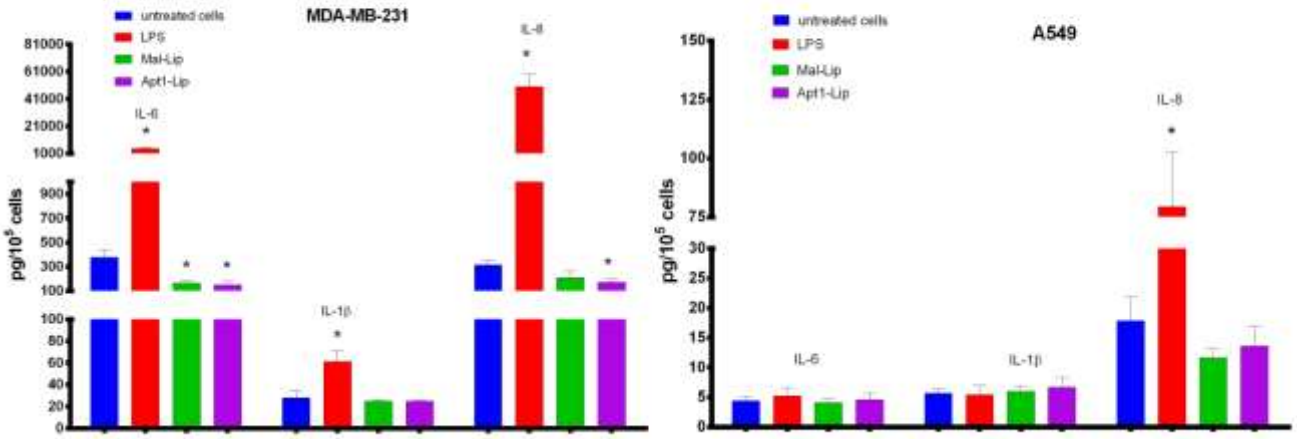

Figure 5: *Inflammatory cytokines secretions IL-6, IL-1β, and IL-8. After exposure to Mal-Lip, Apt1-Lip, and 10 μg/mL LPS (mean ± SD, n = 3, *p <0.05 compared to untreated cells)*

The results showed a significant increase in the secretion of IL-6, IL-1β, and IL-8 by MDA-MB-231 and IL-8 by A549 cell lines after treatment with LPS as shown in figure 5 while no increase were detected in the cytokines IL-12p70, TNF, IL-10 (figure S2). These results highlight the importance of the cytokines IL-6, IL-1β, and IL-8 in the maintaining and proliferation of tumor cells. Furthermore, there was no increase in the secretion of the inflammatory cytokines IL-12p70, TNF, IL-10, IL-6, IL-1β, and IL-8 after treatment with Apt1-Lip at 400 nM concentration compared to Mal-Lip and untreated cells. These results

conclude that Apt1-Lip fails to induce inflammatory response by tumor cells realizing the safe and efficient drug delivery system for therapeutic applications. Moreover, previous researches described other molecules to target CD44 receptor such as hyaluronan and specific anti-CD44 antibodies. However, some challenges face the application of these molecules for specific drug delivery purposes. For example, low molecular hyaluronan ($<10^6$ Da) and the monoclonal antibodies (NIH4-1) were shown to induce tumor cell survival, resistance and the escape from the immune system and induce inflammation. Therefore, choosing specific ligands such as aptamers that target CD44 receptor without further stimulation of the receptor could be of higher therapeutic potency [36, 37].

4. References

[1] M. Dean, T. Fojo, S. Bates, Tumour stem cells and drug resistance, Nat Rev Cancer, 5 (2005) 275-284.

[2] J.E. Visvader, Cells of origin in cancer, Nature, 469 (2011) 314-322.

[3] L. Vermeulen, F. de Sousa e Melo, D.J. Richel, J.P. Medema, The developing cancer stem-cell model: clinical challenges and opportunities, Lancet Oncol, 13 (2012) e83-89.

[4] L. Vermeulen, M.R. Sprick, K. Kemper, G. Stassi, J.P. Medema, Cancer stem cells--old concepts, new insights, Cell Death Differ, 15 (2008) 947-958.

[5] H. Clevers, The cancer stem cell: premises, promises and challenges, Nat Med, 17 (2011) 313-319.

[6] J.A. Magee, E. Piskounova, S.J. Morrison, Cancer stem cells: impact, heterogeneity, and uncertainty, Cancer Cell, 21 (2012) 283-296.

[7] W. Alshaer, H. Hillaireau, J. Vergnaud, S. Ismail, E. Fattal, Functionalizing Liposomes with anti-CD44 Aptamer for Selective Targeting of Cancer Cells, Bioconjug Chem, 26 (2015) 1307-1313.

[8] R.J. Jones, W.H. Matsui, B.D. Smith, Cancer stem cells: are we missing the target?, J Natl Cancer Inst, 96 (2004) 583-585.

[9] C.Y. Park, D. Tseng, I.L. Weissman, Cancer stem cell-directed therapies: recent data from the laboratory and clinic, Mol Ther, 17 (2009) 219-230.

[10] L. Ricci-Vitiani, D.G. Lombardi, E. Pilozzi, M. Biffoni, M. Todaro, C. Peschle, R. De

Maria, Identification and expansion of human colon-cancer-initiating cells, Nature, 445 (2007) 111-115.

[11] M. Al-Hajj, M.S. Wicha, A. Benito-Hernandez, S.J. Morrison, M.F. Clarke, Prospective identification of tumorigenic breast cancer cells, Proc Natl Acad Sci U S A, 100 (2003) 3983-3988.

[12] A. Eramo, F. Lotti, G. Sette, E. Pilozzi, M. Biffoni, A. Di Virgilio, C. Conticello, L. Ruco, C. Peschle, R. De Maria, Identification and expansion of the tumorigenic lung cancer stem cell population, Cell Death Differ, 15 (2008) 504-514.

[13] Y. Hu, L. Fu, Targeting cancer stem cells: a new therapy to cure cancer patients, Am J Cancer Res, 2 (2012) 340-356.

[14] A.T. Collins, P.A. Berry, C. Hyde, M.J. Stower, N.J. Maitland, Prospective identification of tumorigenic prostate cancer stem cells, Cancer Res, 65 (2005) 10946-10951.

[15] P. Dalerba, S.J. Dylla, I.K. Park, R. Liu, X. Wang, R.W. Cho, T. Hoey, A. Gurney, E.H. Huang, D.M. Simeone, A.A. Shelton, G. Parmiani, C. Castelli, M.F. Clarke, Phenotypic characterization of human colorectal cancer stem cells, Proc Natl Acad Sci U S A, 104 (2007) 10158-10163.

[16] C. Li, D.G. Heidt, P. Dalerba, C.F. Burant, L. Zhang, V. Adsay, M. Wicha, M.F. Clarke, D.M. Simeone, Identification of pancreatic cancer stem cells, Cancer Res, 67 (2007) 1030-1037.

[17] M. Zoller, CD44: can a cancer-initiating cell profit from an abundantly expressed molecule?, Nat Rev Cancer, 11 (2011) 254-267.

[18] S.D. Jayasena, Aptamers: an emerging class of molecules that rival antibodies in diagnostics, Clin Chem, 45 (1999) 1628-1650.

[19] C. Tuerk, L. Gold, Systematic evolution of ligands by exponential enrichment: RNA ligands to bacteriophage T4 DNA polymerase, Science, 249 (1990) 505-510.

[20] A.D. Ellington, J.W. Szostak, In vitro selection of RNA molecules that bind specific ligands, Nature, 346 (1990) 818-822.

[21] S.M. Nimjee, C.P. Rusconi, B.A. Sullenger, Aptamers: an emerging class of therapeutics, Annu Rev Med, 56 (2005) 555-583.

[22] A.D. Keefe, S. Pai, A. Ellington, Aptamers as therapeutics, Nat Rev Drug Discov, 9 (2010) 537-550.

[23] J.W. Foy, K. Rittenhouse, M. Modi, M. Patel, Local tolerance and systemic safety of pegaptanib sodium in the dog and rabbit, J Ocul Pharmacol Ther, 23 (2007) 452-466.

[24] G.T. Noble, J.F. Stefanick, J.D. Ashley, T. Kiziltepe, B. Bilgicer, Ligand-targeted liposome design: challenges and fundamental considerations, Trends Biotechnol, 32 (2014) 32-45.

[25] T.M. Allen, P.R. Cullis, Liposomal drug delivery systems: from concept to clinical applications, Adv Drug Deliv Rev, 65 (2013) 36-48.

[26] R.E. Eliaz, F.C. Szoka, Liposome-encapsulated doxorubicin targeted to CD44: A strategy to kill CD44-overexpressing tumor cells, Cancer Research, 61 (2001) 2592-2601.

[27] I. Verel, K.H. Heider, M. Siegmund, E. Ostermann, E. Patzelt, M. Sproll, G.B. Snow, G.R. Adolf, G.A. van Dongen, Tumor targeting properties of monoclonal antibodies with different affinity for target antigen CD44V6 in nude mice bearing head-and-neck cancer xenografts, Int J Cancer, 99 (2002) 396-402.

[28] J.T. Derksen, H.W. Morselt, G.L. Scherphof, Uptake and processing of immunoglobulin-coated liposomes by subpopulations of rat liver macrophages, Biochim Biophys Acta, 971 (1988) 127-136.
[29] J.A. Harding, C.M. Engbers, M.S. Newman, N.I. Goldstein, S. Zalipsky, Immunogenicity and pharmacokinetic attributes of poly(ethylene glycol)-grafted immunoliposomes, Biochim Biophys Acta, 1327 (1997) 181-192.

[30] J.D. Powell, M.R. Horton, Threat matrix - Low-molecular-weight hyaluronan (HA) as a danger signal, Immunol Res, 31 (2005) 207-218.

[31] N. Ababneh, W. Alshaer, O. Allozi, A. Mahafzah, M. El-Khateeb, H. Hillaireau, M. Noiray, E. Fattal, S. Ismail, In vitro selection of modified RNA aptamers against CD44 cancer stem cell marker, Nucleic Acid Ther, 23 (2013) 401-407.

[32] E. Levy-Nissenbaum, A.F. Radovic-Moreno, A.Z. Wang, R. Langer, O.C. Farokhzad, Nanotechnology and aptamers: applications in drug delivery, Trends Biotechnol, 26 (2008) 442-449.

[33] A.D. Bangham, M.M. Standish, J.C. Watkins, G. Weissmann, The diffusion of ions from a phospholipid model membrane system, Protoplasma, 63 (1967) 183-187.

[34] C. Da Pieve, P. Williams, D.M. Haddleton, R.M. Palmer, S. Missailidis, Modification of thiol functionalized aptamers by conjugation of synthetic polymers, Bioconjug Chem, 21 (2010) 169-174.

[35] H. Korkaya, S. Liu, M.S. Wicha, Regulation of cancer stem cells by cytokine networks: attacking cancer's inflammatory roots, Clin Cancer Res, 17 (2011) 6125-6129.

[36] M. Yasuda, Y. Tanaka, K. Fujii, K. Yasumoto, CD44 stimulation down-regulates Fas expression and Fas-mediated apoptosis of lung cancer cells, Int Immunol, 13 (2001) 1309-1319.

[37] S.L. Collins, K.E. Black, Y. Chan-Li, Y.H. Ahn, P.A. Cole, J.D. Powell, M.R. Horton, Hyaluronan fragments promote inflammation by down-regulating the anti-inflammatory A2a receptor, Am J Respir Cell Mol Biol, 45 (2011) 675-683.

5. Supplementary Information

$$N_{Lip} = \frac{M_{lipid} \times N_A}{\frac{4\pi\left(\frac{d}{2}\right)^2 + 4\pi\left(\frac{d}{2} - h\right)^2}{\alpha}}$$

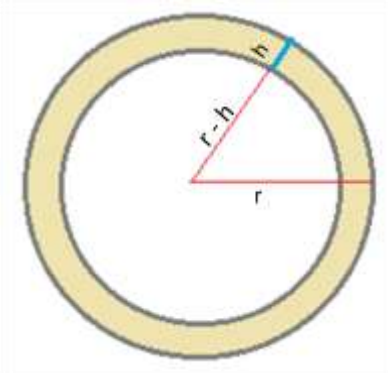

Equation S1: *calculation of the number of liposomes per volume unit N_{Lip}, assuming that liposomes are unilammelar, with r, the average radius of liposome (d, the diameter); α, the area of lipid head group (DPPC: 0.65 nm, Leekumjorn et al., 2006); h, the thickness of lipid bilayer (DPPC liposome: 3.43 nm, Leekumjorn et al., 2006); N_A, the Avogadro number (6.02×10^{23}); M_{lipid}, the molar concentration of lipids.*

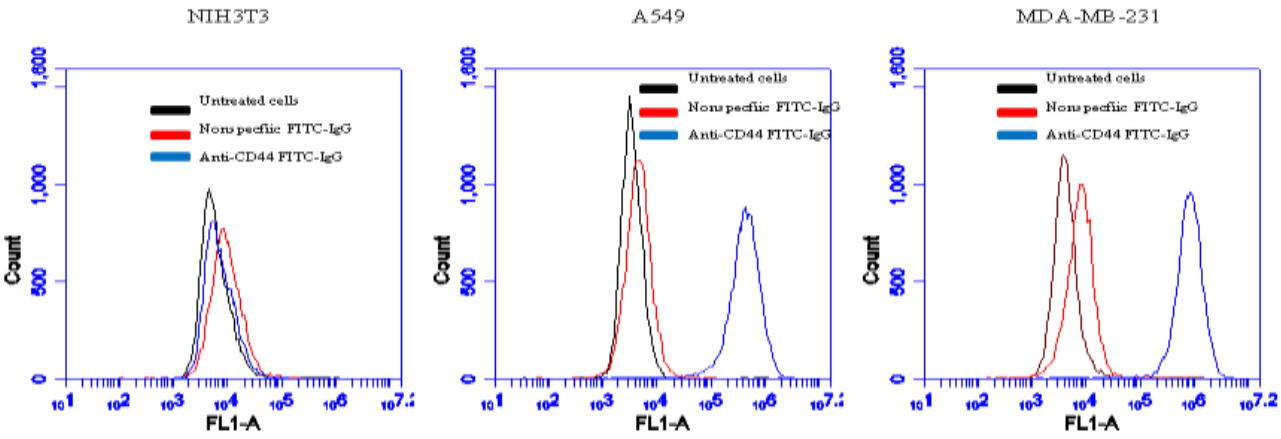

Figure S1: *Flow cytometry analysis for detection of CD44 expression by anti-CD44 FITC-labeled antibodies on the three selected cell lines.*

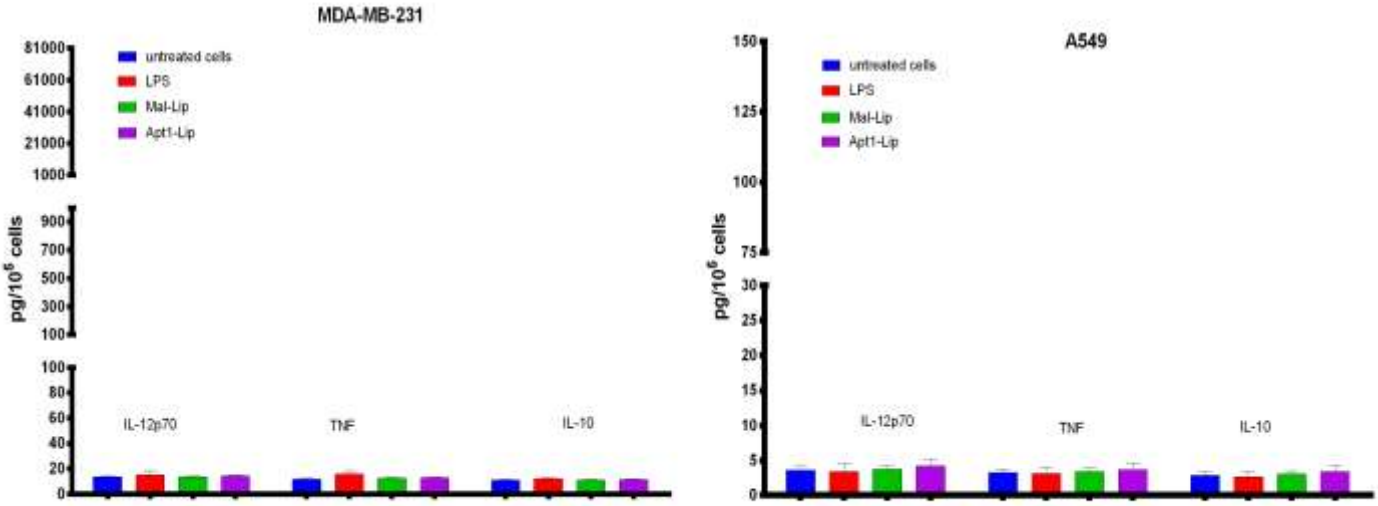

Figure S2: *Inflammatory cytokines secretions IL-12p70, TNF, IL-10. After exposure to Mal-Lip, Apt1-Lip, and 10 μg/mL LPS (mean ± SD, n = 3, *p <0.05 compared to untreated cells).*

Reference of the Supporting Information

(1) Leekumjorn S., and Sum M, Molecular Simulation Study of Structural and Dynamic

Travaux expérimentaux

Chapitre 3

Extinction génique ciblée dans un modèle de cancer du sein exprimant CD44 à l'aide de liposomes chargés en siRNA et fonctionnalisés par un aptamère

Experimental work

Chapter 3

Targeted gene silencing in a CD44-expressing breast cancer model by aptamer-functionalized siRNA-loaded liposomes

Travaux expérimentaux

Chapitre 3

Extinction génique ciblée dans un modèle de cancer du sein exprimant CD44 à l'aide de liposomes chargés en siRNA et fonctionnalisés par un aptamère

Résumé

Dans ce chapitre, nous décrivons un système de délivrance de gènes pour le ciblage actif des cellules exprimant CD44, reposant sur l'utilisation de l'aptamère anti-CD44 Apt1 et de siRNA dirigés contre le gène rapporteur de la luciférase (luc2). Ainsi, un siRNA anti-luc2 a été complexé à la protamine pour former des polyplexes (siRNA/prot) à leur tour encapsulés dans les liposomes PEGylés préformés, aboutissant à des liposomes contenant environ 0,62 nmol de siRNA par mg de lipides (siRNA/prot ⊂ lip). L'aptamère Apt1 a été conjugué à un phospholipide modifié puis introduit sur la surface des liposomes par post-insertion. Les liposomes résultants, fonctionnalisés par Apt1 et chargés en siRNA (siRNA/prot ⊂ lip-Apt1), présentent une taille de 137 ± 3 nm et un potentiel zeta de −26.8 ± 2,3 mV. Ces liposomes ont montré une inhibition spécifique de l'expression de luc2 dans les cellules de cancer du sein MDA-MB-231-luc2-GFP plus élevée comparée aux liposomes non fonctionnalisés siRNA/prot ⊂ lip. Pour évaluer la capacité d'extinction génique in vivo, un modèle murin de xénogreffe orthotopique de cancer du sein humain a été mis au point en implantant les cellules MDA-MB-231-luc2-GFP chez des souris « nude » femelles. Les liposomes siRNA/prot ⊂ lip-Apt1 ont montré une inhibition prolongée de l'expression de luc2 comparés aux liposomes siRNA/prot ⊂ lip après des administrations intraveineuses uniques ou répétées, ce qui a été confirmé par une extinction plus importante de l'ARNm de luc2 dans les cellules des tumeurs réséquées. En conclusion, nous montrons la possibilité de conjuguer un aptamère à des liposomes contenant un siRNA en vue d'une extinction génique efficace dans des cellules tumorales $CD44^+$ in vivo, ceci dans la perspective d'éteindre des gènes spécifiques de pathologies cancéreuses.

Ce chapitre est écrit sous la forme d'un article de recherche en vue d'une publication, avec pour auteurs Walhan ALSHAER, Hervé HILLAIREAU, Ilaria BERTOLINI, Juliette VERGNAUD, Simona MURA, Claudine DELOMENIE, Félix SAUVAGE, Said ISMAIL , Elias FATTAL.

Experimental work

Chapter 3

Targeted gene silencing in a CD44-expressing breast cancer model by aptamer-functionalized siRNA-loaded liposomes

Abstract

CD44 is a glycoprotein receptor known to play a role in cell adhesion, growth, and motility. It is also the most common cancer stem cell surface biomarker and is found overexpressed in many tumors including those affecting colon, breast, pancreas, and head and neck, making this an attractive receptor for therapeutic targeting. In this study, we describe a gene delivery system for the active targeting of CD44-expressing cells using the anti-CD44 aptamer (named Apt1). This system was evaluated for the silencing of the reporter gene of luciferase (luc2) in breast cancer cells *in vitro* and *in vivo*. To do so, an anti-luc2 siRNA was condensed with protamine as polyplexes (siRNA/prot) further trapped into preformed PEGylated liposomes (lip), leading to liposomes containing around 0.62 nmol siRNA per mg lipids (siRNA/prot ⊂ lip). The 2'-F-pyrimidine-modified RNA aptamer (Apt1) was conjugated to a modified phospholipid and then introduced onto the surface of liposomes by post-insertion. The resulting siRNA-loaded, Apt1-functionalized liposomes (siRNA/prot ⊂ lip-Apt1) had a size of 137 ± 3 nm and a zeta potential of −26.8 ± 2.3 mV. These liposomes showed a specific and higher inhibition of luc2 expression in MDA-MB-231-Luc2-GFP breast cancer cells *in vitro*, compared to non-functionalized siRNA/prot ⊂ lip. To evaluate gene silencing *in vivo*, an orthotopic xenograft model of human breast cancer was optimized by implanting the MDA-MB-231-Luc2-GFP cells in female nude mice. The siRNA/prot ⊂ lip-Apt1 showed a prolonged inhibition of luc2 expression compared to siRNA/prot ⊂ lip after both single and multiple intravenous administrations, which was confirmed by a higher knock-down of the luc2 mRNA in resected tumor cells. In conclusion, we show the possibility of conjugating an aptamer to siRNA-containing liposomes for an efficient gene silencing in CD44-expressing tumor cells *in vivo*, in the perspective of silencing disease-related genes in tumors.

This chapter written in the form of research paper to be submeted for publication, with Walhan ALSHAER, Hervé HILLAIREAU, Ilaria BERTOLINI, Juliette VERGNAUD, Simona MURA, Claudine DELOMENIE, Félix SAUVAGE, Said ISMAIL , and Elias FATTAL as Authors.

1. Introduction

The therapeutic innovation has benefited from the development of nanomedicine, which consists in designing nanocarriers that can be loaded with different types of therapeutic and imaging payloads to deliver them into pathological tissues [1, 2]. Nanocarriers offer the possibility to deliver poorly stable therapeutic molecules and improve their pharmacokinetics and pharmacodynamics *in vivo* [3]. The vasculature of solid tumors is often leaky and exhibits characteristic features such as aberrant formation of blood vessels, allowing nanoparticles with a size <150 nm to extravasate into tumors. This so-called enhanced permeation and retention (EPR) effect yielded several clinical achievements in targeting tumors [4]. However, such a passive targeting suffers from low specificity for the on targeting the targeting of tumor cells at the site of distribution [5, 6]. In contrast, active targeting aims at overcoming these limitations by functionalizing nanocarriers with targeting ligands that bind receptors specifically or overexpressed on tumor cells [7-9].

CD44 is a transmembrane glycoprotein, member of the adhesion receptors family, known to play a role in a variety of cellular pathways including adhesion, migration, proliferation, motility, and differentiation [10]. CD44 is also a hyaluronic acid (HA) receptor and is involved in many normal and pathological conditions [11]. In particular, CD44 is present in many types of tumors including breast, prostate, cervical, lung, ovarian, colorectal, and neuroblastoma [10, 12]. Blocking CD44 by antibodies has shown its role in tumorgenesis [13-16]. Moreover, the CD44 receptor has been identified as a marker of cancer stem cells (CSC). CSCs have stem-like properties and are responsible for maintaining tumor propagation, metastasis, and resistance to common tumor chemotherapy [17-19]. Some evidences have shown that the association between CD44 and the JAK2/STAT3 signaling pathway in $CD44^{+}/CD24^{-}$ breast cancer cells induced cancer stem-like properties and resistance to treatment. Inhibition of the IL6/JAK2/STAT3 pathway decreased therapeutic resistance and

increased therapeutic index in breast cancers [20].

Aptamers, from Latin word "*aptus"* which means "fit", are synthetic single stranded oligonucleotides (DNA or RNA) that fold into 3D complex structures and shapes and bind targets with high affinity and selectivity. Aptamers are versatile molecules capable of binding almost any molecules and can be selected from combinatorial library composed up to 10^{15} different sequences using the iterative *in vitro* evolution process termed Systematic Evolution of ligands by EXponential enrichment (SELEX) [21-23]. Because of the versatile binding properties, DNA and RNA aptamers are promising ligands for targeted drug delivery systems using nanocarriers [24, 25]. Targeting ligands such as antibodies and HA have been conjugated to several nanocarriers for targeting CD44-expressing tumors [14, 26]. However, these ligands can induce immune responses and inflammation [27, 28]. In contrast, aptamers are low toxic and immunogenic.

In this study, we investigate the potential of aptamers for guiding nanocarriers to CD44-expressing tumors. To do so, we used a 2′-fluoropyrimidine RNA aptamer named Apt1 that was previously obtained by our group using SELEX and shown to bind the CD44 protein as well as the $CD44^+$ cells with high a affinity [29], especially when conjugated to model liposomes [30]. Apt1 was here conjugated to PEGylated liposomes loaded with siRNA against the luciferase 2 gene. This was achieved by first loading siRNA/protamine polyplexes in PEGylated liposomes and further inserting Apt1 conjugated to PEGylated phospholipids (scheme 1). This delivery system was evaluated *in vitro* on the $CD44^+$ MDA-MB-231-Luc2-GFP breast cancer cells, and *in vivo* on an orthotopic in breast cancer model based on these cancer cells.

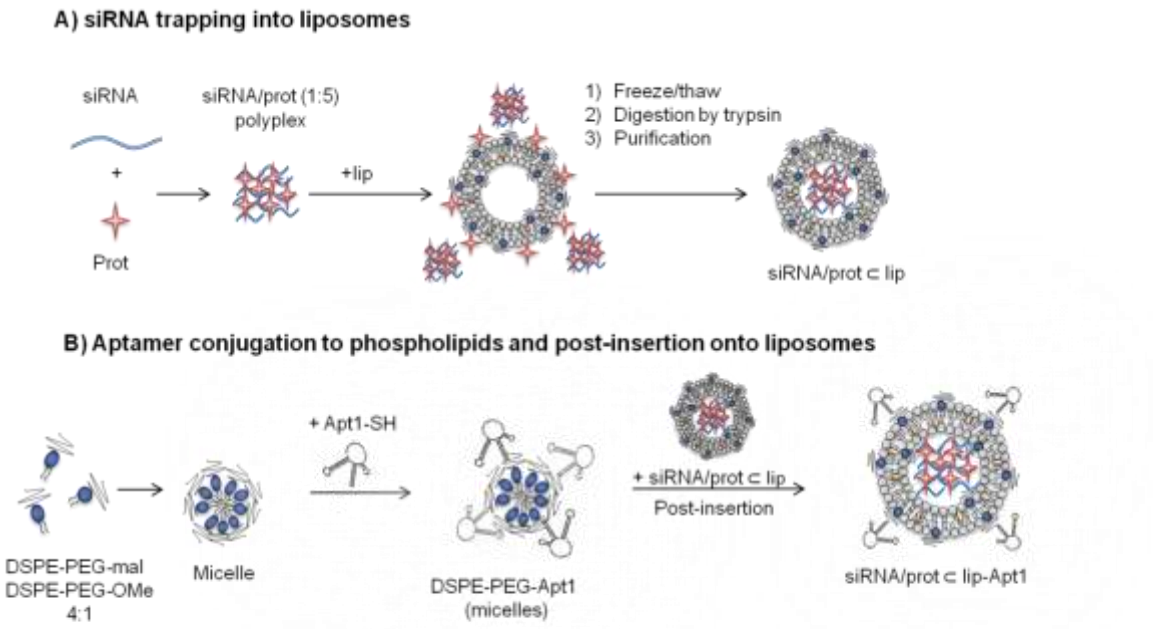

Scheme 1: *Preparation of siRNA-loaded, aptamer-functionalized PEGylated liposomes. (A) siRNA are trapped into PEGylated liposomes by adding siRNA/protamine polyplexes (siRNA/prot) to preformed liposomes (lip), repeating freeze/thaw cycles, and removing surface associated polyplexes by digestion with trypsin. (B) The Apt1 aptamer is conjugated to the DSPE-PEG phospholipids by thiol/maleimide chemistry. The resulting conjugates are mixed with the liposomes prepared in step A, leading to siRNA-loaded, Apt1 functionalized liposomes (siRNA/prot ⊂ lip-Apt1).*

2. Materials and methods

2.1 Materials

Oligonucliotides The Apt1 aptamer with 2'-F-pyrimidines (sequence: 5'-(FITC)GGGA(2'-F-rU)GGA(2'-F-rU)(2'-F-rC)(2'-F-rC)AAG(2'-F-rC)(2'-F-rU)(2'-F-rU)A(2'-F-rC)(2'-F-rU)GG (2'-F-rC)A(2'-F-rU)(2'-F-rC)(2'-F-rU)GGA(2'-F-rU)(2'-F-rU)(2'-F-rU)G(2'-F-rC)G(2'-F-rC) G(2'-F-rU)G(2'-F-rC)(2'-F-rC)AGAA(2'-F-rU)AAAGAG(2'-F-rU)A(2'-F-rU)AA(2'-F-rC)G (2'-F-rU)G(2'-F-rU)GAA(2'-F-rU)GGGAAG(2'-F-rC)(2'-F-rU)(2'-F-rU)(2'-F-rC)GA(2'-F-rU) AGGAA(2'-F-rU)(2'-F-rU)(2'-F-rC)GG-3'(thiol C6 SS) was chemically synthesized using cyanoethyl phosphoramidite chemistry and modified with C6-thiol SS (protected form) at the 3' end (IBA, Germany). The siRNA sense strands luc2 (5′-GCUAUGGGCUGAAUAC AAATT-3) [31] and scrambled siRNA (negative sequence, cat#SR-CL000-005) were obtained from Eurogentech (Angers, France). The Q-PCR primers were obtained from IDT and designed as follows: pGL4.10 [luc2] forward: GAAGGAGATCGTGGACTAT, and reverse: TTGGCCTTAATGAGAATCT; B-Actin reference gene forward: AATGATGAGC CTTCGTG, and reverse: AACTGGTCTCAAGTCA GTGT; POLR2A reference gene forward: GTACATAAATGCCTTGTGG, and reverse: CAGTGAGTTCTAACAGCACA.

Other chemicals. 1,2-dihexadecanoyl-sn-glycero-3-phosphocholine (DPPC) was purchased from Corden Pharma (Germany), while 1,2-distearoyl-*sn*-glycero-3-phosphoethanolamine-N-[methoxy(polyethylene glycol)-2000] (DSPE-PEG) and 1,2-distearoyl-sn-glycero-3-phosphoethanolamine-N-[maleimide (polyethylene glycol)-2000] (DSPE-PEG-mal) were purchased from Avanti Polar Lipids (Alabaster, USA). Cholesterol and protamine sulfate were from Sigma-Aldrich. Tris(2-carboxyethyl)phosphine hydrochloride (TCEP) was from Thermo Fisher Scientific (MA, USA). D-luciferin was obtained from PerkinElmer. QuantiFluor® RNA system for RNA quantification was from Promega (Promega, USA). The anti-CD44 (Human) mAb-APC-Alexa Fluor® 750 was from Beckman Coulter (Fullerton, USA).

2.2 Cell culture

The human breast cancer cell line MDA-MB-231-Luc2-GFP expressing firefly luciferase (luc2) was purchased from Caliper (Almeda, CA). MDA-MB-231-Luc2-GFP cells were cultured in Eagle's Minimum Essential Medium (EMEM) (ATCC® 30-2003™) supplemented with 10% heat-inactivated fetal bovine serum, 2 mM L-glutamine, 100 U/ml penicillin, 100 mg/mL streptomycin and incubated in humidified atmosphere of 5% CO2 at 37°C. Similar culture medium and conditions applied for the wild type MDA-MB-231 cell line.

2.3 siRNA/protamine polyplexes

siRNA sequences were hydrated with free nuclease water at a final concentration of 0.1 mM. Protamine sulfate (MW ~ 5,000 Da) was dissolved in free nuclease water at a final concentration of 0.5 mM. Protamine (prot) was complexed with siRNA in free nuclease water at a molar ratio 1:5 (siRNA:prot), mixed by vortex for few seconds and incubated at room temperature for 10 min.

2.4 Liposome preparation

PEGylated liposomes (lip) were prepared by the thin lipid-film hydration method. Stock solutions of DPPC, cholesterol, and DSPE-PEG in a 62:35:3 molar ratio were mixed and dissolved in 5 mL chloroform. A thin film was obtained by evaporation of chloroform using rotary evaporator for 30 min at 50 °C under decreased atmosphere pressure. The film was then hydrated with 5 mL PBS and vortexed for 30 min, followed by 13 extrusion cycles through 100 nm polycarbonate membrane (Millipore) to obtain liposomes with a size around 100 nm. Liposome suspensions were then concentrated to 200 mM lipids using Amicon® filters (cut-off of 100 kDa).

2.5 siRNA polyplexes trapping into liposomes

Trapping siRNA into liposomes was performed as followed. siRNA/prot polyplexes were incubated with liposomes for 5 min at room temperature. 5 freeze and thaw cycles were then performed. For each cycle freezing was achieved in liquid nitrogen for 1 min and thawing in a water bath at 60 °C for 2 min. The liposome suspension was then treated with trypsin (10 min at 37 °C) to digest protamine and thus remove non-encapsulated protamine or siRNA/prot polyplexes, potentially bound onto liposome surface. Liposomes were finally ultrafiltrated using Amicon® filters (cut-off 100 kDa) to remove residual siRNA, protamine residues and trypsin. This procedure was performed for increasing amounts of siRNA (0.5, 1, 2, and 3 nmol) with fixed amount of lipids (2.5 mg) followed by quantification of siRNA. To investigate the effect of ionic strength on siRNA trapping in liposomes, the procedure was performed in 1 and 10 mM PBS.

Agarose gel electrophoresis was performed to check the integrity of siRNA in the different steps. of the preparation. Samples were loaded into 2% agarose gel (Promega, USA) supplemented with 5 µL of a 2.5 mg/mL ethidium bromide solution followed by electrophoresis in 1X TAE buffer (pH 8.2) at 120 V for 20 to 30 minutes. Images for analysis were obtained using MF-ChemiBIS gel imaging system (DNR Bio-Imaging Systems).

To quantify the encapsulation of siRNA, the amount of untrapped siRNA was measured after the trypsin treatment step using the QuantiFluor® RNA System that contains a fluorescent RNA-binding dye (492 nm excitation / 540 nm emission) by a LS 50B spectrofluorometer (PerkinElmer, USA), after verifying the absence of interference with all formulation constituents. The quantity of trapped siRNA was finally calculated by subtracting the untrapped siRNA quantity to the total siRNA quantity.

2.6 Apt1-conjugation and post insertion

Micelles composed DSPE-PEG and DSPE-PEG-mal in a molar ratio of 1:4 respectively were obtained by mixing them in chloroform, followed by chloroform evaporation using a rotary evaporator and hydration with PBS. Conjugation of Apt1 to DSPE-PEG-mal was performed using a thiol-maleimide cross linking reaction to form thioether bond. The C6-thiol-modified Apt1 (Apt1-(CH2)3-S-S-(CH2)3) was first activated (deprotected) in free nuclease water by treatment with 100 mM TCEP (pH 6.5) for 1 h at room temperature to produce Apt1-SH, which was then conjugated to DSPE-PEG-mal at a 1:40 molar ratio (Apt1:DSPE-PEG-mal) in PBS (pH 7.4) by incubation overnight at room temperature with gentle stirring. Unconjugated DSPE-PEG and DPSE-PEG-mal were removed by treatment with 0.1% SDS for 10 min at room temperature followed by ultrafiltration through 30 kDa Microcon® Centrifugal Filters and washed twice with PBS. The DSPE-PEG-Apt1 conjugate was recovered and post-inserted into siRNA-loaded liposomes by mixing and incubation at 60 °C for 1h, followed by filtration of unbound DSPE-PEG-Apt1 using ultrafiltration through Amicon® filters (cut-off 100 kDa). The quantification of Apt1 and DSPE-PEG-Apt1 was performed using the QuantiFluor® RNA System similarly to siRNA quantification.

2.7 Size and zeta potential:

The size and zeta potential of liposomes were measured at 25ºC by Dynamic Light Scattering (DLS) using a Nano ZS (Malvern instruments, UK). All liposome preparations were diluted in free nuclease water to obtain a final sodium chloride concentration of 8 mM (pH 7.4).

2.8 *In vitro* luciferase knockdown

4×10^3 MDA-MB-231-Luc2-GFP cells was seeded in 96 white solid bottom well plate and incubated for 24 h at 37 ºC. After incubation, cells were treated (in triplicate wells) with siRNA formulations (free siRNA, siRNA/prot polyplexes, siRNA/prot ⊂ lip, and siRNA/prot

⊂ lip-Apt1) at a 250-500 nM siRNA final concentration for 48 h at 37 °C. After incubation, the bioluminescence measurement was performed by addition of 50 µL Brightlight solution containing a lysis buffer and the luciferin substrate, followed by plate vortexing for 1 min and measurement of bioluminescence emission using an Envision Xcite luminometer (PerkinElmer, Life sciences) at a rate of 0.1 sec/well. Scrambled siRNA were used as a negative control for all formulations.

2.9. Optimization of an *in vivo* orthotopic breast cancer model:

Animal experiments were performed according to European rules (86/609/EEC and 2010/63/EU) and the instructions of laboratory animal care and legislation in force in France (Decree No. 2013-118 of Fabruary 1, 2013). 4-6 week-old female Fox1nu (nu/nu) mice (~20 g) were purchased from Harlan (France). MDA-MB-231-Luc2-GFP cells were harvested using trypsin, centrifuged at 1,100 rpm for 5min at 4°C then washed with PBS. The remaining cells were resuspended in PBS on ice at density of 1 x 10^7 cells/mL. For tumor implantation mice were anesthetized with 2.5 % isoflurane, laid on back, their skin cleaned with Betadine, and a 5 to 10 mm incision in the skin was performed so the mammary fat could be seen (figure 1 A). 50 µL of cell suspension was then injected carefully into the mammary fat avoiding any leakage, after which the incision was sutured and the mouse monitored until recovery from anesthesia. Sutures were monitored every day for recovery. Mice weight was monitored and the tumor volume was measured by slide caliper and estimated using the equation $v = ab^2/2$, were a is the higher dimension and b the lower (figure 1 D). Bioluminecence and fluorescence from implanted cells were monitored from day 5 after tumor implantation using an IVIS200 (PerkinElmer) imaging system (figure 1 B). The acquisition procedure was performed as follows. D-luciferin (150 mg/kg of body weight) was first injected intraperitoneally. After 5 min, mice were anesthetized with 2.5 % isoflurane and the total flux (photons/sec) was recorded one minute afterwards, using a 10 s exposure time

(figure 1 F). Fluorescent imaging was measured in parallel using a 465 nm excitation / 520 nm emission filter (figure 1 D) (figure S1). The image signals were analyzed using the Living Image software. All parameters of imaging were fixed for all measurements. The averages of tumors volume were correlated to the average weight of the tumors obtained after sacrificing the mice (table S1).

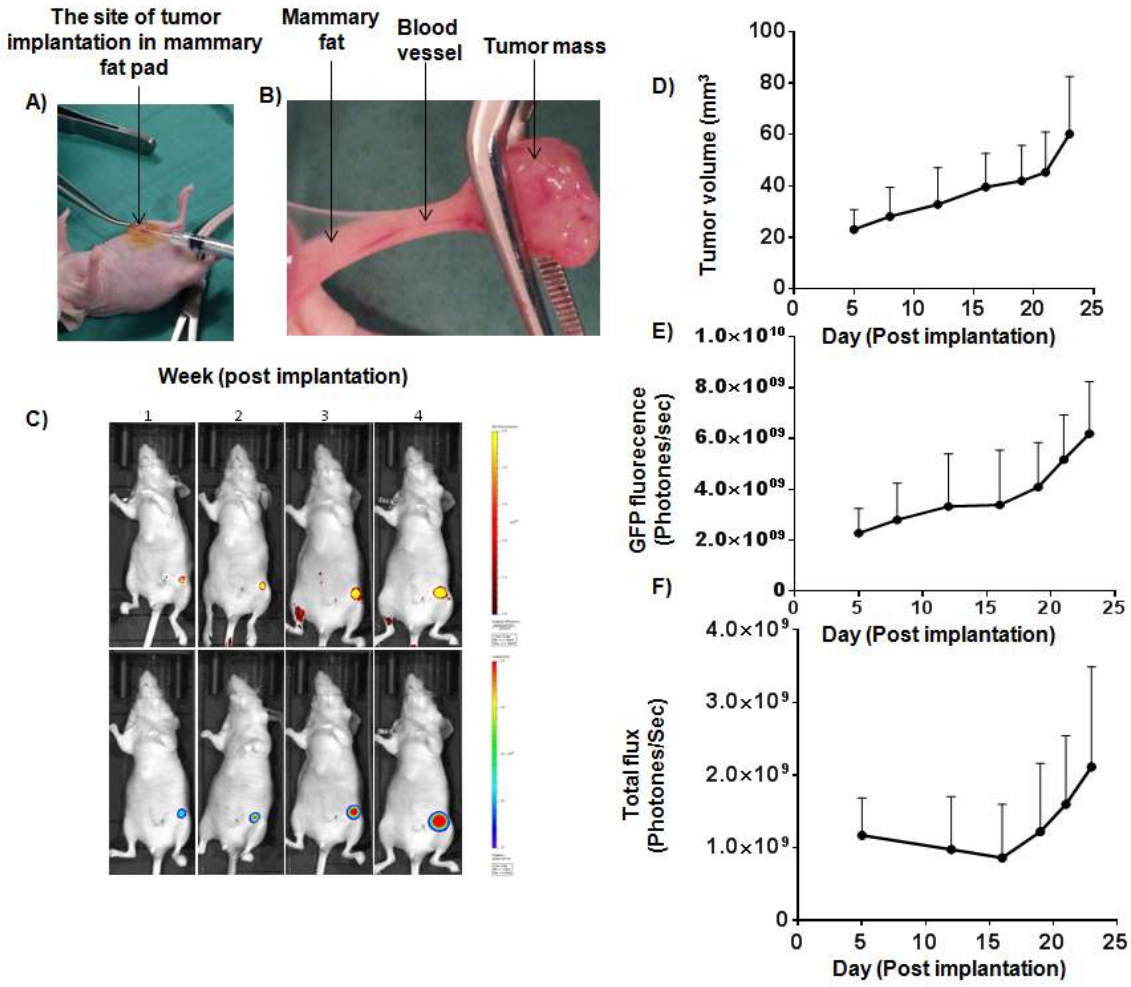

Figure 1: *Establishing in vivo model. (A) Orthotopic implantation of MDA-MB-231-Luc2-GFP cancer cells into the mammary fat pad of mouse. (B) Appearance of tumor mass after scarifying the mice. (C) Representative images for untreated mice show the progression in tumor volume, GFP and Luc2 signal, (D) Tumor volume, (E) GFP fluorescence and (F) luc2 activity after tumor implantation (n=29).*

2.10. *In vivo* silencing of luciferase

In vivo luc2 silencing was first investigated for a single dose, followed by administration of multiple doses. Mice were divided into 5 random groups of 5-7 mice to receive the following compounds: (i) PBS (untreated control), (ii) SC-siRNA/prot ⊂ lip (liposome loaded with scrambled siRNA), (iii) luc2-siRNA/prot ⊂ lip (liposomes loaded with luc2 siRNA), (iv) SC-siRNA/prot ⊂ lip-Apt1 (aptamer-functionalized liposomes loaded with scrambled siRNA), (v) Luc2-siRNA/prot ⊂ lip-Apt1 (aptamer-functionalized liposomes loaded with Luc2 siRNA). The dose of siRNA was set at 2.5 mg of siRNA per kg of mouse body weight. Treatments were initiated at the point of exponential increase in luc2 activity. Multiple doses were administered three times (3×2.5mg/kg) every 24 h. The siRNA preparations were administered intravenously in the tail vein. Tumor volume, luminescence and fluorescence were recorded every day from the day of treatment initiation as described above. One day after the last administration of the multiple dose treatment, mice were sacrificed and the tumors were recovered for further analysis of luc2 mRNA expression using Q-PCR (figure 1B).

2.11 Q-PCR

RNA preparation: The tumors recovered from mice were homogenized in Trizol® RNA isolation reagent (Life Technologies) and stored at –80 °C until used. Total RNA extraction with the Trizol® RNA isolation reagent was performed according to the manufacturer's instructions. RNA purity and quantity was assessed by UV measurement using a BioMate™3S spectrophotometer (Thermo Scientific). RNA integrity was evaluated by capillary electrophoresis using RNA 6000 Nano chips and the Bioanalyzer 2100 (Agilent Technologies).

Q-PCR analysis: For quantification of mRNA expression, a first cDNA strand was reverse-transcribed from 1 µg of total RNA, with random hexamers and oligo-dT priming using the

iSCRIPT enzyme (Bio-Rad), according to the manufacturer's instructions. PCR primer pairs specific to the target and reference genes were designed using the Primer3Plus software (http://primer3plus.com/cgi-bin/dev/primer3plus.cgi). The cDNA synthesized from 4 ng of total RNA was amplified in a CFX96™ real time thermal cycler (Bio-Rad) using the SSoADV Univer SYBR® Green Supermix (Bio-Rad) reagent according to manufacturer's instructions, with 500-nM final concentrations of each primer, in duplicate 10-µl reactions, by 45 two-step cycles (95°C 5s ; 60°C 20 s). RT controls were amplified on all genes to control for genomic DNA contamination, and melting curve analysis was performed to assess the purity of the PCR products. PCR efficiencies calculated for each gene from the slopes of calibration curves generated from the pool of all cDNA samples, were above 90%. GeNorm in qBase Plus tool [32] was used to select Pol2R and ACTB genes as references for normalization of mRNA expression results. The normalized relative expression of target genes in samples was determined using the ΔΔCq method with correction for PCR efficiencies, where NRQ = ETarget ΔCq Target / E Ref ΔCqRef and ΔCq = Cqsample – Cqcalibrator [33]. Final results were expressed as the relative Luc2 gene expression in all mice groups.

2.12 Statistical analysis

All values were expressed as mean ± standard deviation. The statistical significances were determined by performing multiple comparisons using tow-way ANOVA followed by Tukey's post-test. The difference considered significant when the *p* value was less than 0.05.

3. Results and discussion

Although siRNA have received great interest because of their high efficiency in silencing gene expression, especially for disease-related genes in cancer treatment, naked siRNA is relatively unstable in biological fluids and rapidly cleared from the body via degradation by nucleases. Moreover, siRNA are anionic macromolecules and thus exhibit low cellular uptake [34]. Therefore, an appropriate delivery system is required to enhance their stability and to improve the cellular uptake *in vitro* and *in vivo*. While many nanocarriers have been developed for this purpose, few of them have the ability to actively target tumor biomarkers such as CD44 *in vitro* and *in vivo*. In the present work we developed a selective siRNA delivery system for targeting CD44 overexpressed by breast cancer tumors using PEGylated liposomes (lip) functionalized with anti-CD44 RNA aptamer (Apt1).

3.1 Trapping of siRNA

The siRNA was first condensed using the cationic peptide protamine [35] before trapping into pre-formed conventional PEGylated liposomes. The rationale of this approach was to use the advantages of a cationic polymer in terms of siRNA loading and endosomal escape following endocytosis, without the drawbacks of naked cationic polyplexes or lipoplexes as their low stability, their poor safety and difficulties of surface functionalization. Protamine is a 32-amino acid cationic polypeptide rich in arginin (isoelectric point = 11-12). It is a major component of the sperm nucleus as a DNA condensing molecules. It has been used to increase the half-life and action of insulin in diabetic patients and it is approved as a heparin antidote by FDA [36]. Because of its minimal toxicity and immunogenicity as observed by the long history of administration of protamine in patients, this molecule has also been used for the delivery of plasmid DNA and siRNA *in vitro* and *in vivo* and demonstrated its ability to dissociate in the cytoplasm after cellular uptake [35, 37]. Moreover, protamine has been used as nucleic acid condensing agent that enhance transfection efficacy upon mixing with cationic

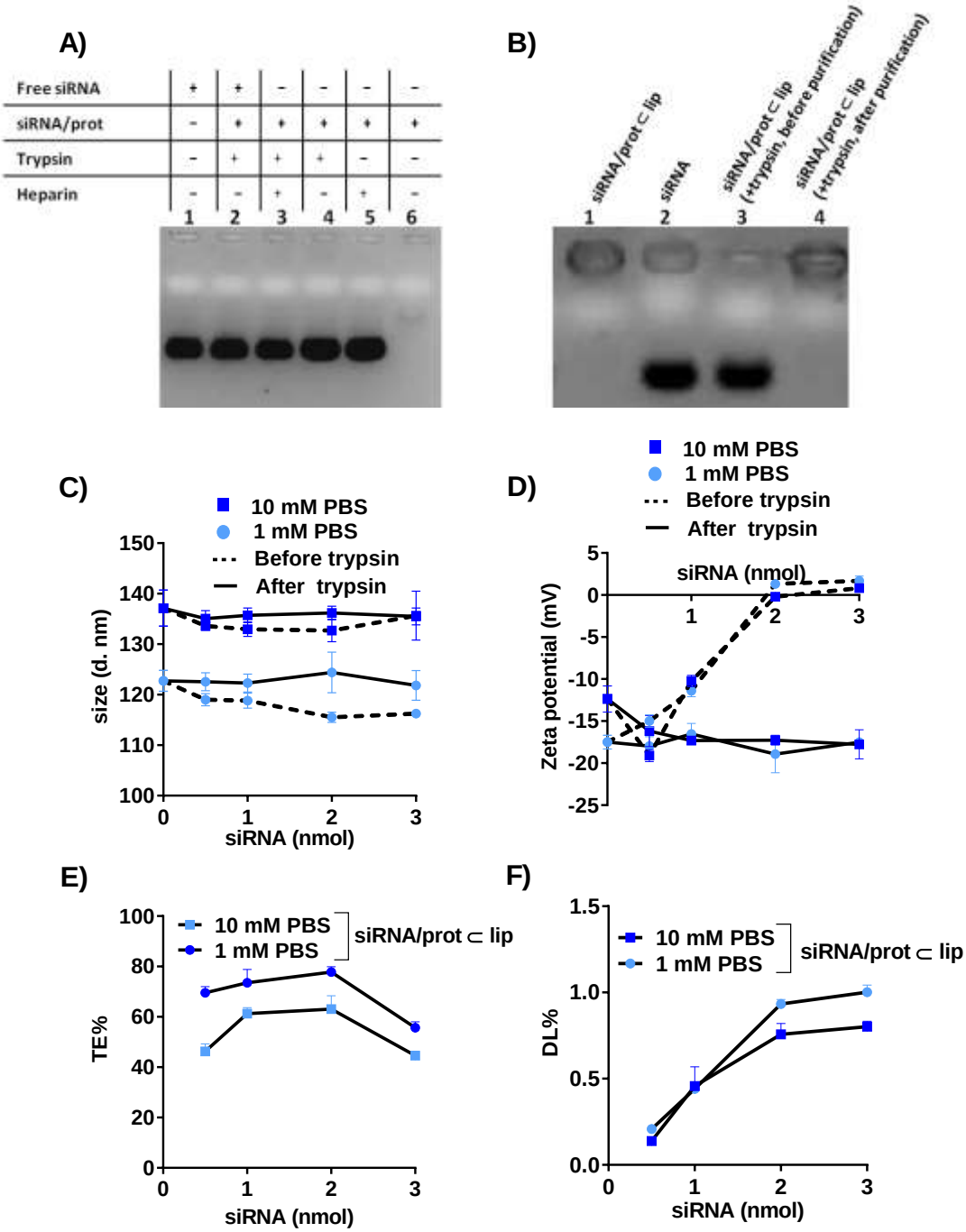

Figure 2: *Characterization of siRNA trapping. (A) Gel electrophoresis analyzing siRNA/prot,polyplexes: lane 1, free siRNA; lane 2,siRNA treated with trypsin; lane 3, siRNA/prot polyplex treated with trypsin and heparin; lane 4, siRNA/prot polyplex treated with trypsin only; lane 5, siRNA/prot polyplex treated with heparin only; lane 6, siRNA/prot polyplex. (B) Gel electrophoresis analyzing siRNA/prot ⊂ lip before and after purification, lane 1, siRNA/prot ⊂ lip before trypsin treatment; lane 2, free siRNA; lane 3, siRNA/prot ⊂*

lip after trypsin treatment; lane 4, siRNA/prot ⊂ lip after purification of untrapped siRNA. (C) size and (D) ζ-potential characterization of siRNA-loaded liposomes before and after trypsin treatment, (E) Trapping Efficacy (TE) and (F) Drug Loading (DL) into preformed liposomes shows the maximum loading capacity and the effect of ionic strength.

liposomes [38]. In this study, we used the cationic polypeptide protamine to condense siRNA at the molar ratio 1:5 (siRNA:prot) which can form polyplexes in nanometric size (192 nm) with positive ζ -potential charge (+32 mV). Gel electrophoresis confirmed the full siRNA complexation. Because trypsin was used in the subsequent steps of liposome preparation, we also verified its impact on siRNA. In our conditions, trypsin induced the disruption of siRNA/prot polyplexes, similarly to the well-established treatment with heparin, without harming siRNA integrity (figure 2 A).

The siRNA/prot polyplexes were mixed with pre-formed PEGylated liposomes and trapped using repeated freeze/thaw cycles. The freeze/thaw method is known for trapping a variety molecules including small and macromolecules into liposomes [39, 40]. The possible mechanism is by disrupting liposome membrane by ice crystals and increasing the trapping volume of liposomes [41]. The size and surface charge of liposomes showed limited changes in the liposome hydrodynamic diameter (figure 2 C) in all cases. However an important increase in the ζ-potential of liposomes was measured immediately after freeze and thaw cycles with increasing amounts of siRNA/prot polyplexes (figure 2 D, dotted lines). Such increase in the ζ-potential can be explained by some association of prot/siRNA at the surface of liposomes, which would interfere with the post-insertion of Apt1 onto liposomes. Therefore, to remove this fraction of prot/siRNA, we used trypsin to clean the surface of liposomes. Trypsin is a serine protease that can hydrolyze peptides at the carboxyl side of lysine and arginin thereby can digest protamine which contains 21 arginin residues. The

treatment with trypsin released a significant fraction of siRNA initially associated to liposomes (figure 2 B, lanes 1 vs. 3). This treatment also decreased the ζ-potential of siRNA-loaded liposomes down to that of empty liposomes, at around –17 mV (figure 1 D, plain lines), confirming the efficacy of trypsin to remove surface-associated siRNA/prot polyplexes. The purification step successfully removed the fraction of released siRNA material (figure 2 B, lane 4).

The quantity of loaded siRNA was found to reach a plateau for an initial ratio of 2 nmol siRNA per 2.5 mg lipids, resulting in a drug loading of around 0.7-1% w/w (0.64-0.71 nmole of siRNA/mg lipids) (figure 2 F), which corresponds to an entrapment efficiency of 60-80% (figure 2 E). No further increase in the loading capacity was observed beyond the initial ratio of 2 nmol siRNA per 2.5mg lipids.

The effect of the medium ionic strength on the siRNA trapping was also investigated. The liposomes were hydrated in 1 or 10 mM of PBS followed by trapping of siRNA/prot polyplexes. We found a significant increase in the trapping efficacy in 1 mM PBS compared to 10 mM PBS (figure 2 E, F), which can be explained by an increased electrostatic shielding of liposomes at higher ionic strength, decreasing the initial adsorption of siRNA/prot complexes and thus their encapsulation. Maintaining a minimal ionic strength was however necessary, as indicated by the observation of liposome aggregation into micrometric particles when freeze and thaw cycles was performed in water (data not shown). Consequently, the best trapping conditions were obtained for 2 nmol siRNA per 2.5 mg lipids in 1 mM PBS resulting in a trapping efficiency of 77.8 ± 5.2% and a drug loading of 0.93 ± 0.03% w/w.

3.2 Apt1 post insertion

After optimizing the siRNA trapping conditions, siRNA-loaded liposomes were functionalized with Apt1 using the post-insertion method [42]. Thiol-maleimide crosslinking chemistry was used for the covalent attachment of Apt1-SH to the DSPE-PEG-mal on

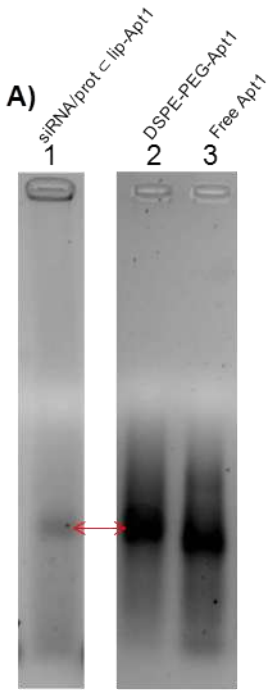

B)

	lip	siRNA/prot ⊂ lip	siRNA/prot ⊂ lip-Apt1
Mean hydrodynamic diameter (nm)	128 ± 4	131 ± 2	137 ± 3
Polydispersity Index (PDI)	0.13 ± 0.02	0.093 ± 0.02	0.085 ± 0.03
ζ-potential (mV)	−15.9 ± 1	−16.6 ± 1.4	−26.8 ± 2.3
siRNA (µg/mg)	-	9.3 ± 0.03	9.3 ±0 .03
Apt1 (µg/mg)	-	-	12.2 ± 0.3

Figure 3: *Apt1 post-insertion onto siRNA-loaded liposomes. (A) Gel electrophoresis analyzing Apt1 conjugation to DSPE-PEG: lane 1, siRNA/prot ⊂ lip-Apt1; lane 2, DSPE-PEG-Apt1; lane 3 free Apt1, the red arrow indicates the DSPE-PEG-Apt1. (B) Table summarizing the hydrodynamic diameter and zeta potential characterization of liposomes before and after siRNA trapping and Apt1 post insertion, and the average amounts of siRNA and Apt1 per 1 mg of lipid.*

micelles, and the resulting DSPE-PEG-Apt1 conjugate was post inserted onto siRNA-loaded liposomes at 60 °C which is above the transition temperature of DPPC (41 °C). Gel electrophoresis showed a slight increase in the molecular weight of the conjugate compared to free Apt1 (figure 3 A, lanes 2 and 3) and its retention with liposomes in the electrophoresis well after the post-insertion step was performed (figure 3 A, lane 1). The amount of Apt1 incorporated onto liposomes was further quantified as 12.2 ± 0.3 µg of Apt1 per mg of lipids. A slight increase in the hydrodynamic diameter of liposomes was measured after DSPE-PEG-Apt1 post insertion, together with a sharp decrease of the zeta potential (from −16.6 ± 1.4 mV

to −26.8 ± 2.3 mV), which is consistent with the liposome functionalization with the negatively charged macromolecule Apt1 (figure 3 B). Moreover, all prepared liposomes have a hydrodynamic diameter around 130 nm which is compatible size for EPR effect.

3.3. *In vitro* luciferase knockdown

The triple negative breast cancer cells (TNBC) lack the expression of the three receptors progesterone (PR), estrogen (ER), and epidermal growth factor receptor (Her2). This type of breast cancer is associated with poor prognosis and lack efficient targeted therapies. TNBC have a high frequency of metastasis especially to distant organs such as brain and viscera. The mortality rates reach 100% in TNBC patients with brain metastasis in the first three months. The MDA-MB-231 cell line used in this study belongs to TNBC [43] and overexpress the CD44 receptor, as verified by cytometry (figure S2). We used MDA-MB-231 cancer cells transfected by a lentivirus vector for the stable expression of the two reporter genes, firefly luciferase (luc2) and eGFP. The high sensitivity and specificity of the chemical reaction between luc2 and its substrate D-luciferin allow a precise quantification of the enzyme activity. Therefore, we used a siRNA specific for luc2 mRNA, and monitored the luc2 activity to evaluate the potential of Apt1-functionalized nanocarriers for cancer gene therapy.

MDA-MB-231-Luc2-eGFP cells were first treated with prot/siRNA-containing Apt1-functionalized liposomes and compared with their non-functionalized counterparts, with protamine/siRNA polyplexes, and with free siRNA. For each of these formulations, anti-luc2 siRNA were evaluated in comparison to scramble siRNA (figure 4 A). After 48 h incubation, only siRNA/protamine-loaded liposomes lead to a specific luminescence decrease, unlike free siRNA and protamine/siRNA polyplexes alone (figure 4 A), showing the ability of this delivery system to deliver intracellularly active siRNA. Among liposomes, the luminescent signal was reduced to 25.7 ± 15.1% for luc2-siRNA/prot ⊂ lip-Apt1 compared to 47.2 ± 10.6% by luc2-siRNA/prot ⊂ lip. This effect was siRNA dose-dependent as shown in figure 4

B. Such a higher inhibition by luc2-siRNA/prot ⊂ lip-Apt1 may be explained by a higher uptake of aptamer-functionalized liposomes, as evidenced in our previous report using model liposomes [30].

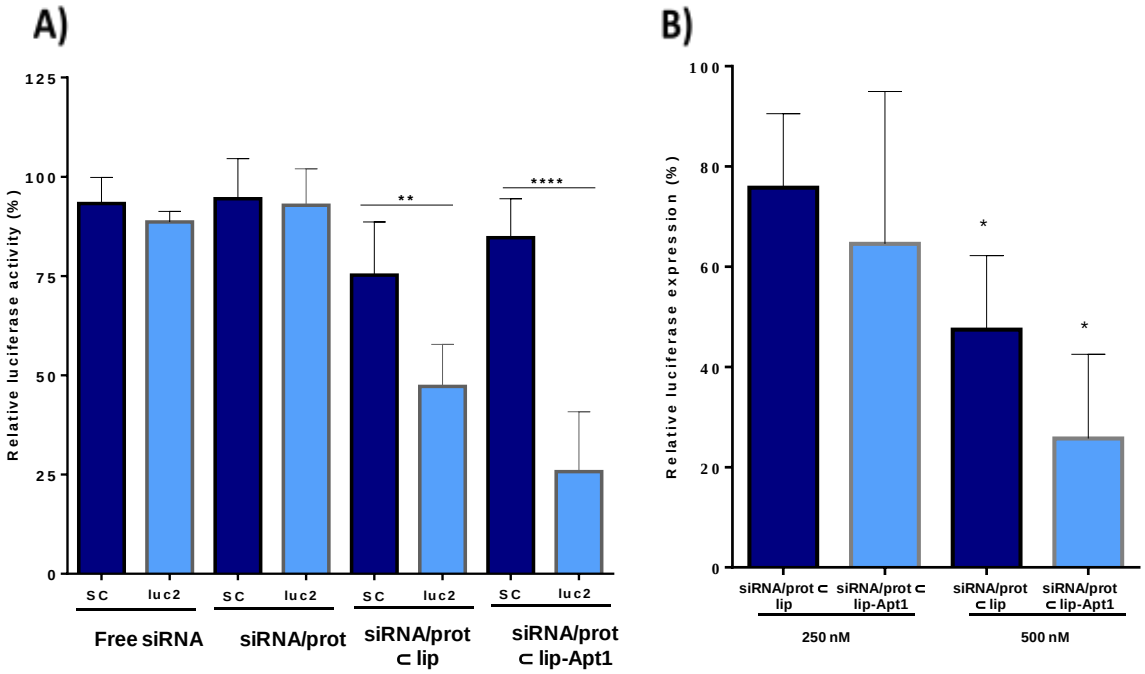

Figure 4: *In vitro Luc2 gene silencing by siRNA/prot ⊂ lip-Apt1 on MDA-MB-231-Luc2-GFP. (A) 4 x 10^3 MDA-MB-231-Luc2-GFP cells were treated for 48 h with 500 nM of one of the siRNA preparations including free siRNA, siRNA/prot, siRNA/prot ⊂ lip, siRNA/prot ⊂ lip-Apt1. Results of inhibition are related to untreated control cells. (B) Dose dependent effect of luc2 silencing by siRNA/prot ⊂ lip and siRNA/prot ⊂ lip-Apt1compared to untreated control cells. All data points were repeated three times in triplicate wells for each repeat (*p<0.05, **p<0.01, ****p<0.0001).*

3.4 *In vivo* orthotopic breast cancer model

Breast cancer is influenced by tissues surrounding the tumor and by various inflammatory mediators. Therefore, the injection of breast cancer cells orthotopically into mammary fat pad is a useful and more realistic model which display a proper stromal compartment that mimic the human cancer disease. In this study we first optimized and characterized an MDA-MB-231-Luc2-eGFP based breast cancer model by orthotopic implantation in the fourth left inguinal mammary fat pad of athymic female nude mouse. The monitoring of tumor size, luciferase activity by luminesence and eGFP fluorescence *in vivo* showed a good correlation between tumor size and eGFP fluorescence, whereas the luminescence signal followed tumor size only after a lag phase (figure 1 D, E, and F). This delay could be due to the time needed for tumor vascularization allowing proper luciferin supply to luciferase-expressing cancer cells.

3.5 *In vivo* luciferase knockdown

Despite the efficient silencing of genes expression by siRNA *in vitro*, silencing genes *in vivo* is challenging issue for many reasons related to rapid clearance, unspecific biodistribution, and cellular barriers. Lipid-based siRNA delivery systems showed enhanced cellular uptake and intracellular release of siRNA. An obvious progress was accomplished in siRNA delivery *in vivo* using neutral lipids to address the toxicity of cationic lipids [35]. Therefore, we did investigate the efficacy of our siRNA delivery system to reach the tumor site and to silence luc2 target gene *in vivo*. To do so, first we have been evaluated the effect of single dose administration of 2.5mg/kg (~270 mg/kg of lipids) of siRNA on luc2 silencing. There were no signs of acute toxicity (weight, behavior of treated mice) (figure S3 A). Moreover, no significant impact was visible on tumor growth as indicated by the increase of tumor volume and GFP expression compared to untreated mice (figure S3 B and C). These results showed the absence of visible cytotoxicity or antitumoral effect of liposomes preparations, thus

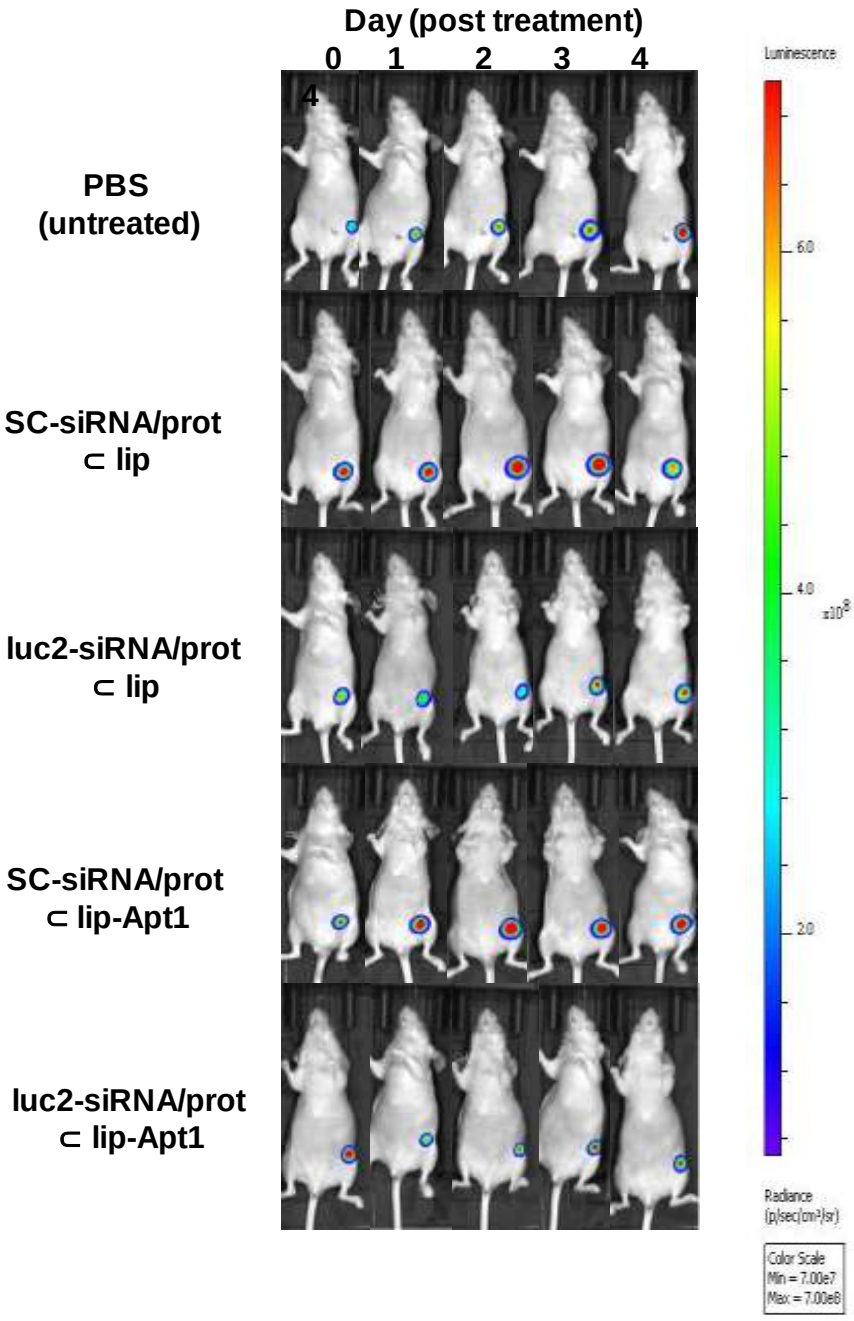

Figure 5: *Representative images of one mouse from each group showing the bioluminescence related to the luc2 relative expression from day 0 to 4 of treatment.*

allowing proper evaluation of gene silencing. Furthermore, both luc2-siRNA/prot ⊂ lip and luc2-siRNA/prot ⊂ lip-Apt1 liposomes decreased bioluminescence compared to their

scramble siRNA counterparts or PBS treatment. The luc2 silencing by luc2-siRNA/prot ⊂ lip (non-targeted liposomes) was slight and transient, and only visible at 24 h. On the other hand, the effect of luc2-siRNA/prot ⊂ lip-Apt1 (targeted liposomes) was more pronounced and significantly different after 24 h of administration compared to PBS-treated mice, with a visible inhibition lasting 3 days before reaching the signal of untreated mice (figure 6 A, figure 7A). Based on these data, a multiple administration schedule has been performed to maintain luc2 inhibition. Likewise, no observed significant toxicity or impact on tumor growth was noticed after multiple administrations (figure S3 A, B and C). Here again, only luc2-siRNA/prot ⊂ lip and luc2-siRNA/prot ⊂ lip-Apt1 liposomes induced decrease of bio luminescence (figure 5). Furthermore, a significant reduction of luc2 expression was maintained until the end of the experiment (4 days) in mice treated with luc2-siRNA/prot ⊂ lip-Apt1 liposomes while no more visible luc2 silencing was observed after 3 days in mice treated with only luc2-siRNA/prot ⊂ lip (figure 6 B, figure 7B). Moreover, inhibition of luc2 showed no effect on GFP expression as indicated by the decrease in the luc2/GFP ratio in luc2-siRNA loaded liposomes compared to control mice (figure S4). At the end of treatment, the mice were sacrificed to obtain tumors for further analysis of luc2 expression at level of mRNA using Q-PCR. The results of Q-PCR confirmed the effect luc2 silencing at mRNA level and showed significant reduction in luc2 expression in tumors treated with luc2-siRNA/prot ⊂ lip-Apt1 liposomes compared to untreated control group as shown in figure 8.

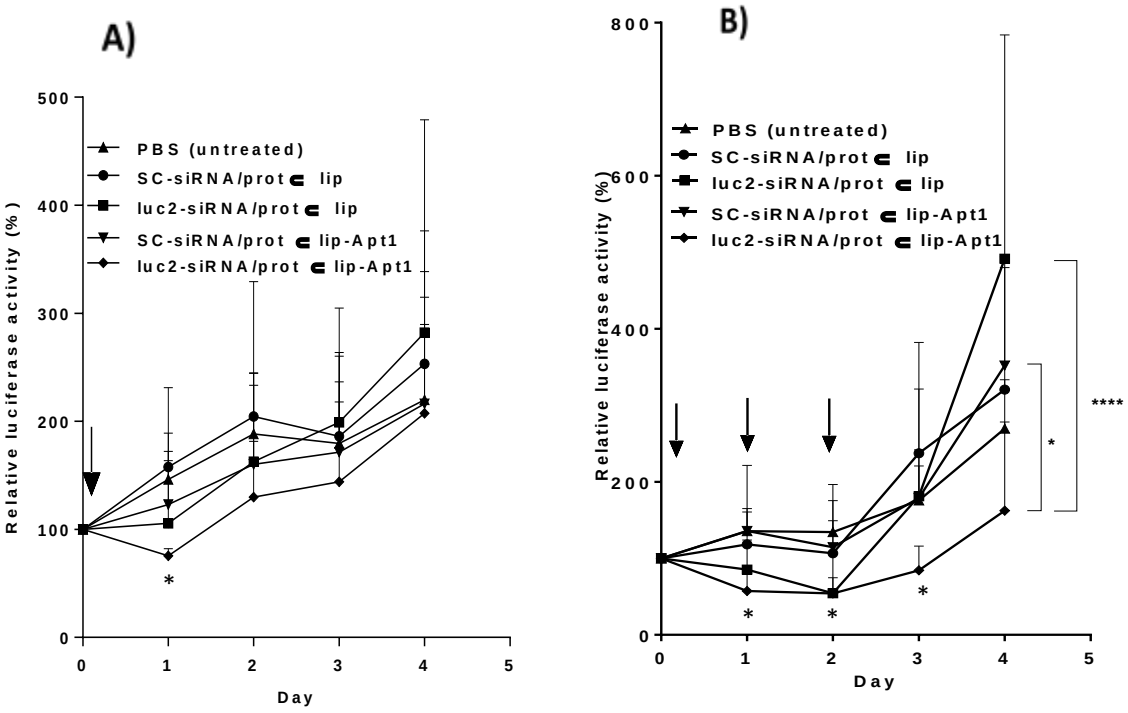

Figure 6: *Relative luc2 gene inhibition in orthotopically injected MDA-MB-231-Luc2-GFP cells in the mammary fat pad of female nu/nu mice. Liposomes preparations of Luc2-siRNA (luc2-siRNA/prot ⊂ lip, luc2-siRNA/prot ⊂ lip-Apt1) or SC-siRNA (SC-siRNA/prot ⊂ lip-, SC-siRNA/prot ⊂ lip-Apt1) were intravenously administered (2.5 mg/kg). (A) at day 0 (single dose) or (B) 0, 1, and 2 (multiple doses) (black arrows). The bioluminescence (total flux) was detected once every 24h in the area of interest (ROI) after administration of D-luciferin (150 mg/kg). Bioluminescence results were normalized using day 0 as a reference.(*p<0.05, **p<0.01, ****p<0.0001).*

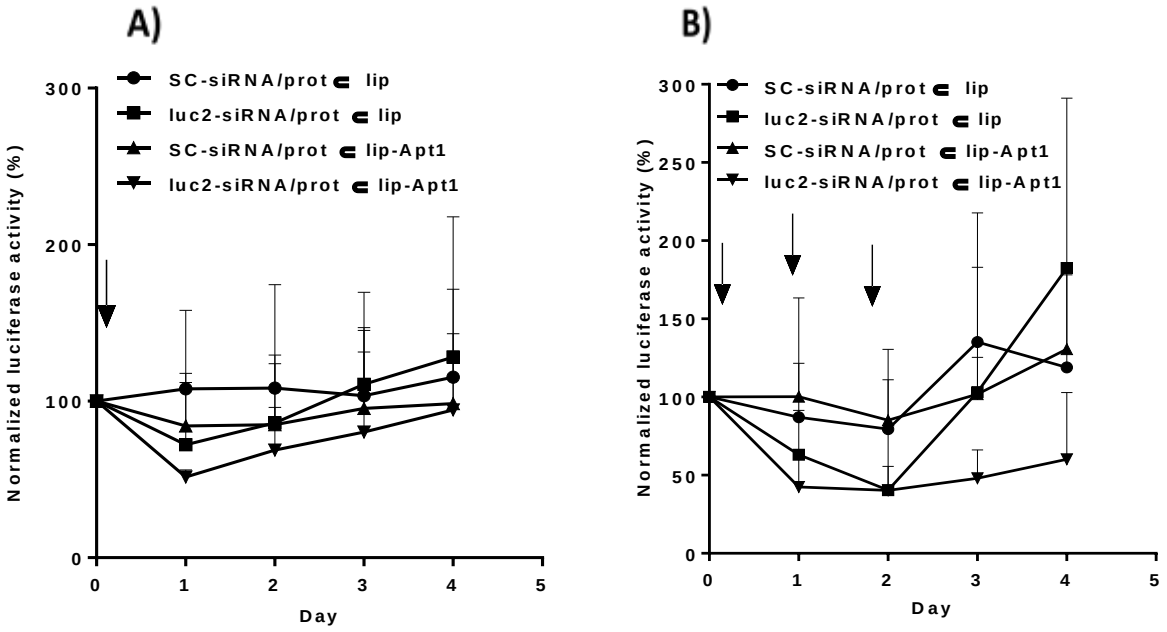

Figure 7: *Normalized in vivo Luc2 gene silencing results for data in figure 6. Luc2 silencing is here expressed as relative Luc2 expression compared untreated group for each day.*

Taken together, these results showed an efficient inhibition of luc2 by luc2-siRNA loaded liposomes, consistent with a passive targeting through EPR effect. Moreover, no significant effect was results from controls containing SC-siRNA-loaded liposomes, thus confirming the specificity of this gene silencing strategy. Most important, the prolonged inhibition of luc2 expression obtained by luc2-siRNA/prot ⊂ lip-Apt1 liposomes functionalized with Apt1. Such prolong effect could be explained by additional active targeting and/or be due to the accumulation of luc2-siRNA/prot ⊂ lip-Apt1 liposomes in tumors.

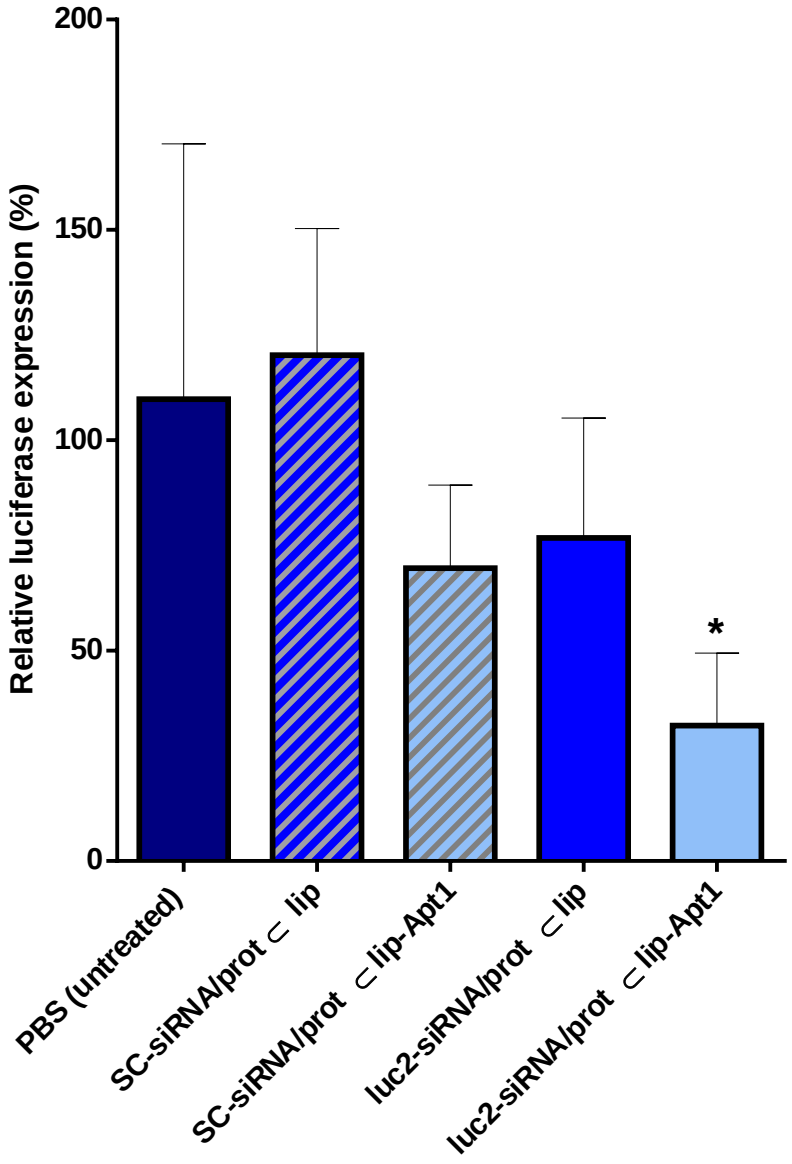

Figure 8: *Luc2 expression in tumors. The mRNA extracted from tumors at day 4 post treatments and the expression of Luc2 mRNA analyzed by Q-PCR. (*P<0.05 , n=5).*

4. Conclusions

We describe a siRNA delivery system *in vitro* and *in vivo* in which protamine is used to condense siRNA for trapping into PEGylated liposomes. The siRNA loaded liposomes can be successfully functionalized with an anti-CD44 aptamer that previously selected to bind CD44 receptor in high affinity. The data of this study showed that higher luc2 inhibition aptamer functionalized liposomes-loaded with siRNA *in vitro*, and prolong inhibition *in vivo*. Our siRNA delivery and active targeting system may be useful for targeting CD44-expressing tumors and suppressing tumor growth *in vivo*. The next step is to load this delivery system with siRNA that induce silencing of disease genes.

5. References

[1] K.Y. Kim, Nanotechnology platforms and physiological challenges for cancer therapeutics, Nanomedicine, 3 (2007) 103-110.

[2] D. Peer, J.M. Karp, S. Hong, O.C. Farokhzad, R. Margalit, R. Langer, Nanocarriers as an emerging platform for cancer therapy, Nat Nanotechnol, 2 (2007) 751-760.

[3] N. Bertrand, J. Wu, X. Xu, N. Kamaly, O.C. Farokhzad, Cancer nanotechnology: the impact of passive and active targeting in the era of modern cancer biology, Advanced drug delivery reviews, 66 (2014) 2-25.

[4] V. Sanna, N. Pala, M. Sechi, Targeted therapy using nanotechnology: focus on cancer, International Journal of Nanomedicine, 9 (2014) 467-483.

[5] T. Lammers, F. Kiessling, W.E. Hennink, G. Storm, Drug targeting to tumors: principles, pitfalls and (pre-) clinical progress, Journal of controlled release : official journal of the Controlled Release Society, 161 (2012) 175-187.

[6] U. Prabhakar, H. Maeda, R.K. Jain, E.M. Sevick-Muraca, W. Zamboni, O.C. Farokhzad, S.T. Barry, A. Gabizon, P. Grodzinski, D.C. Blakey, Challenges and key considerations of the enhanced permeability and retention effect for nanomedicine drug delivery in oncology, Cancer research, 73 (2013) 2412-2417.

[7] J.D. Byrne, T. Betancourt, L. Brannon-Peppas, Active targeting schemes for nanoparticle systems in cancer therapeutics, Advanced drug delivery reviews, 60 (2008) 1615-1626.

[8] T. Sun, Y.S. Zhang, B. Pang, D.C. Hyun, M. Yang, Y. Xia, Engineered nanoparticles for drug delivery in cancer therapy, Angewandte Chemie, 53 (2014) 12320-12364.

[9] D. Hanahan, R.A. Weinberg, Hallmarks of cancer: the next generation, Cell, 144 (2011) 646-674.

[10] H. Ponta, L. Sherman, P.A. Herrlich, CD44: from adhesion molecules to signalling regulators, Nature reviews. Molecular cell biology, 4 (2003) 33-45.

[11] J.M. Louderbough, J.A. Schroeder, Understanding the dual nature of CD44 in breast cancer progression, Molecular cancer research : MCR, 9 (2011) 1573-1586.

[12] D. Naor, S.B. Wallach-Dayan, M.A. Zahalka, R.V. Sionov, Involvement of CD44, a molecule with a thousand faces, in cancer dissemination, Seminars in cancer biology, 18 (2008) 260-267.

[13] L. Li, X. Hao, J. Qin, W. Tang, F. He, A. Smith, M. Zhang, D.M. Simeone, X.T. Qiao, Z.N. Chen, T.S. Lawrence, L. Xu, Antibody against CD44s inhibits pancreatic tumor initiation and postradiation recurrence in mice, Gastroenterology, 146 (2014) 1108-1118.

[14] K. Sandstrom, M. Nestor, T. Ekberg, M. Engstrom, M. Anniko, H. Lundqvist, Targeting CD44v6 expressed in head and neck squamous cell carcinoma: preclinical characterization of an 111In-labeled monoclonal antibody, Tumour biology : the journal of the International Society for Oncodevelopmental Biology and Medicine, 29 (2008) 137-144.

[15] S. Zhang, C.C. Wu, J.F. Fecteau, B. Cui, L. Chen, L. Zhang, R. Wu, L. Rassenti, F. Lao, S. Weigand, T.J. Kipps, Targeting chronic lymphocytic leukemia cells with a humanized monoclonal antibody specific for CD44, Proceedings of the National Academy of Sciences of the United States of America, 110 (2013) 6127-6132.

[16] A. Dufay Wojcicki, H. Hillaireau, T.L. Nascimento, S. Arpicco, M. Taverna, S. Ribes, M. Bourge, V. Nicolas, A. Bochot, C. Vauthier, N. Tsapis, E. Fattal, Hyaluronic acid-bearing lipoplexes: physico-chemical characterization and in vitro targeting of the CD44 receptor, J Control Release, 162 (2012) 545-552.

[17] M. Zoller, CD44: can a cancer-initiating cell profit from an abundantly expressed molecule?, Nature reviews. Cancer, 11 (2011) 254-267.

[18] A. Jaggupilli, E. Elkord, Significance of CD44 and CD24 as cancer stem cell markers: an enduring ambiguity, Clinical & developmental immunology, 2012 (2012) 708036.

[19] T. Klonisch, E. Wiechec, S. Hombach-Klonisch, S.R. Ande, S. Wesselborg, K. Schulze-Osthoff, M. Los, Cancer stem cell markers in common cancers - therapeutic implications, Trends in molecular medicine, 14 (2008) 450-460.

[20] L.L. Marotta, V. Almendro, A. Marusyk, M. Shipitsin, J. Schemme, S.R. Walker, N. Bloushtain-Qimron, J.J. Kim, S.A. Choudhury, R. Maruyama, Z. Wu, M. Gonen, L.A. Mulvey, M.O. Bessarabova, S.J. Huh, S.J. Silver, S.Y. Kim, S.Y. Park, H.E. Lee, K.S. Anderson, A.L. Richardson, T. Nikolskaya, Y. Nikolsky, X.S. Liu, D.E. Root, W.C. Hahn, D.A. Frank, K. Polyak, The JAK2/STAT3 signaling pathway is required for growth of CD44(+)CD24(-) stem cell-like breast cancer cells in human tumors, The Journal of clinical investigation, 121 (2011) 2723-2735.

[21] A.D. Ellington, J.W. Szostak, In vitro selection of RNA molecules that bind specific ligands, Nature, 346 (1990) 818-822.

[22] C. Tuerk, L. Gold, Systematic evolution of ligands by exponential enrichment: RNA ligands to bacteriophage T4 DNA polymerase, Science, 249 (1990) 505-510.

[23] S.M. Nimjee, C.P. Rusconi, B.A. Sullenger, Aptamers: an emerging class of therapeutics, Annual review of medicine, 56 (2005) 555-583.

[24] G. Zhu, G. Niu, X. Chen, Aptamer-Drug Conjugates, Bioconjugate chemistry, 26 (2015) 2186-2197.

[25] B. Liu, J. Zhang, J. Liao, J. Liu, K. Chen, G. Tong, P. Yuan, Z. Liu, Y. Pu, H. Liu, Aptamer-functionalized nanoparticles for drug delivery, Journal of biomedical nanotechnology, 10 (2014) 3189-3203.

[26] R.E. Eliaz, F.C. Szoka, Jr., Liposome-encapsulated doxorubicin targeted to CD44: a strategy to kill CD44-overexpressing tumor cells, Cancer research, 61 (2001) 2592-2601.

[27] J.T. Derksen, H.W. Morselt, G.L. Scherphof, Uptake and processing of immunoglobulin-coated liposomes by subpopulations of rat liver macrophages, Biochimica et biophysica acta, 971 (1988) 127-136.

[28] J.D. Powell, M.R. Horton, Threat matrix: low-molecular-weight hyaluronan (HA) as a danger signal, Immunologic research, 31 (2005) 207-218.

[29] N. Ababneh, W. Alshaer, O. Allozi, A. Mahafzah, M. El-Khateeb, H. Hillaireau, M. Noiray, E. Fattal, S. Ismail, In vitro selection of modified RNA aptamers against CD44 cancer stem cell marker, Nucleic acid therapeutics, 23 (2013) 401-407.

[30] W. Alshaer, H. Hillaireau, J. Vergnaud, S. Ismail, E. Fattal, Functionalizing Liposomes with anti-CD44 Aptamer for Selective Targeting of Cancer Cells, Bioconjugate chemistry, 26 (2015) 1307-1313.

[31] N. Yonenaga, E. Kenjo, T. Asai, A. Tsuruta, K. Shimizu, T. Dewa, M. Nango, N. Oku, RGD-based active targeting of novel polycation liposomes bearing siRNA for cancer treatment, J Control Release, 160 (2012) 177-181.

[32] J. Vandesompele, K. De Preter, F. Pattyn, B. Poppe, N. Van Roy, A. De Paepe, F. Speleman, Accurate normalization of real-time quantitative RT-PCR data by geometric averaging of multiple internal control genes, Genome Biol, 3 (2002) RESEARCH0034.

[33] J. Hellemans, G. Mortier, A. De Paepe, F. Speleman, J. Vandesompele, qBase relative quantification framework and software for management and automated analysis of real-time quantitative PCR data, Genome Biol, 8 (2007) R19.

[34] K.A. Whitehead, R. Langer, D.G. Anderson, Knocking down barriers: advances in siRNA delivery, Nat Rev Drug Discov, 8 (2009) 129-138.

[35] D. Peer, E.J. Park, Y. Morishita, C.V. Carman, M. Shimaoka, Systemic leukocyte-directed siRNA delivery revealing cyclin D1 as an anti-inflammatory target, Science, 319

(2008) 627-630.

[36] K. Biegeleisen, The probable structure of the protamine-DNA complex, J Theor Biol, 241 (2006) 533-540.

[37] S. Motta, P. Brocca, E. Del Favero, V. Rondelli, L. Cantu, A. Amici, D. Pozzi, G. Caracciolo, Nanoscale structure of protamine/DNA complexes for gene delivery, Appl Phys Lett, 102 (2013).

[38] F.L. Sorgi, S. Bhattacharya, L. Huang, Protamine sulfate enhances lipid-mediated gene transfer, Gene Ther, 4 (1997) 961-968.

[39] L. Boulmedarat, G. Piel, A. Bochot, S. Lesieur, L. Delattre, E. Fattal, Cyclodextrin-mediated drug release from liposomes dispersed within a bioadhesive gel, Pharm Res, 22 (2005) 962-971.

[40] U. Pick, Liposomes with a large trapping capacity prepared by freezing and thawing of sonicated phospholipid mixtures, Arch Biochem Biophys, 212 (1981) 186-194.

[41] A.P. Costa, X. Xu, D.J. Burgess, Freeze-anneal-thaw cycling of unilamellar liposomes: effect on encapsulation efficiency, Pharm Res, 31 (2014) 97-103.

[42] S.E. Baek, K.H. Lee, Y.S. Park, D.K. Oh, S. Oh, K.S. Kim, D.E. Kim, RNA aptamer-conjugated liposome as an efficient anticancer drug delivery vehicle targeting cancer cells in vivo, J Control Release, 196 (2014) 234-242.

[43] K.J. Chavez, S.V. Garimella, S. Lipkowitz, Triple negative breast cancer cell lines: one tool in the search for better treatment of triple negative breast cancer, Breast Dis, 32 (2010) 35-48.

6. Supplementary information

Table S1: Average of tumor volume and weight in the last day of experiment.

Tumor volume (mm^3)	Tumor weight (mg)
149.7 ± 54.8	155.8 ± 61.2

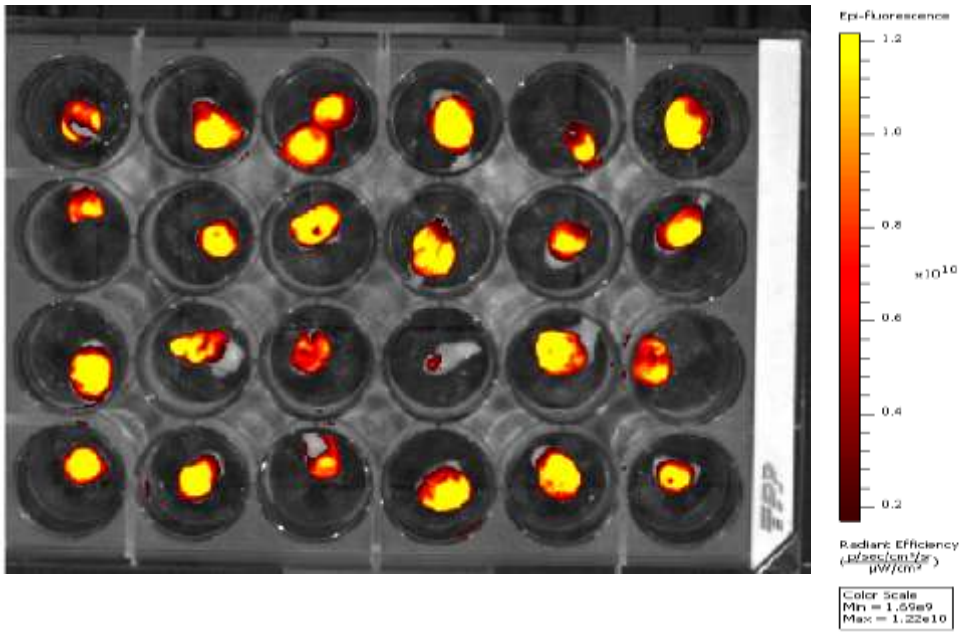

Figure S1: *Ex vivo imaging of GFP in tumors performed in the last day of the experiments*

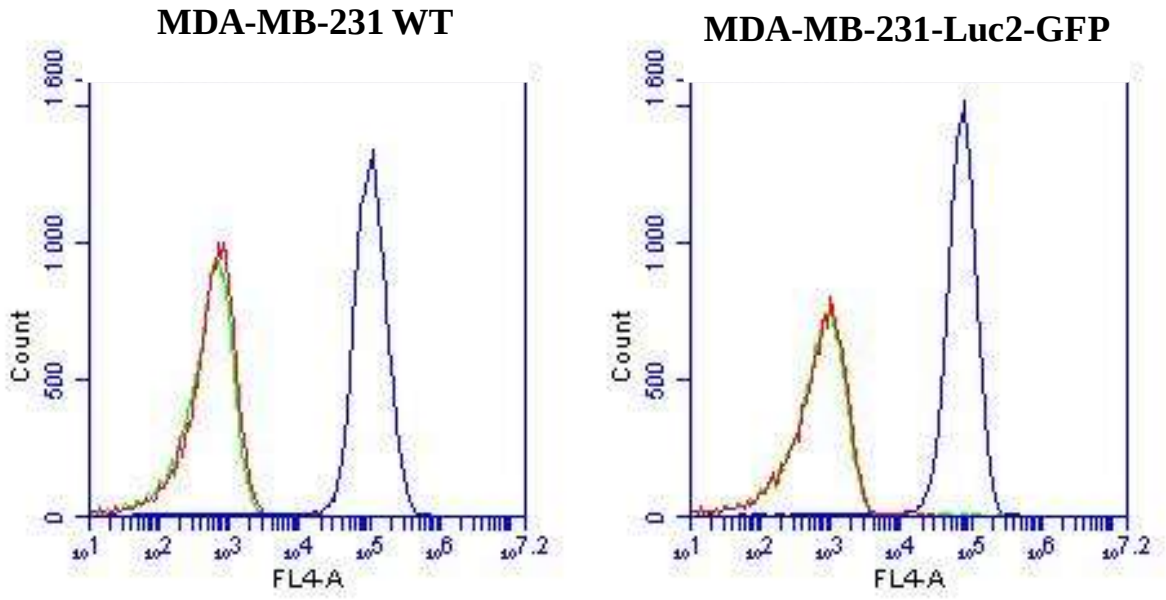

Figure S2: *CD44 expression in wild type MDA-MB-231 and MDA-MB-231-Luc2-GFP cells tested by flow cytometry. Around 100% of both MDA cells express CD44 receptor.*

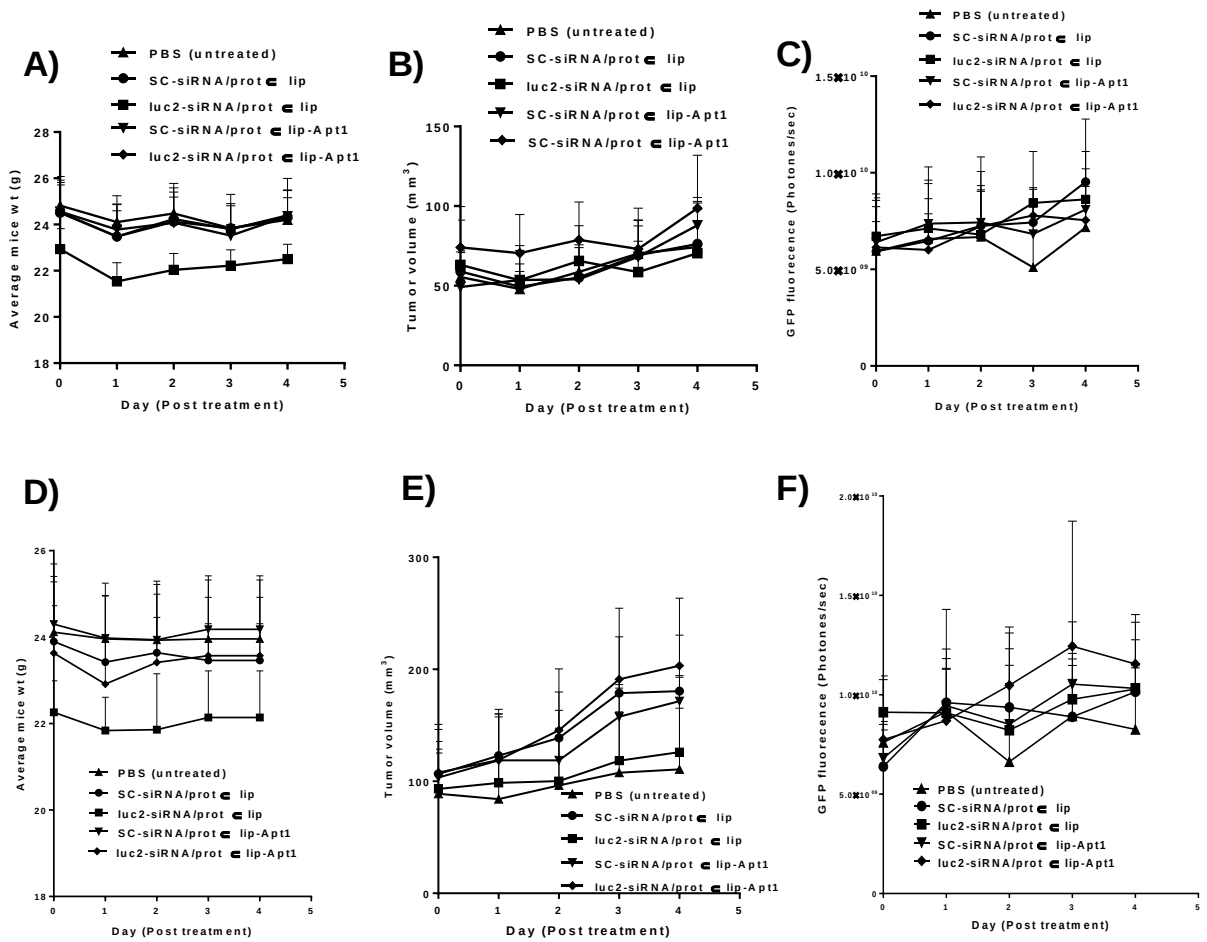

Figure S3: *Progression of mice weight, tumor growth, and GFP expression among during treatments. by a single dose ((A) weight, (B) tumor volume, and (C) GFP expression) and by multiple doses ((D) weight, (E) tumor volume, and (F) GFP expression).*

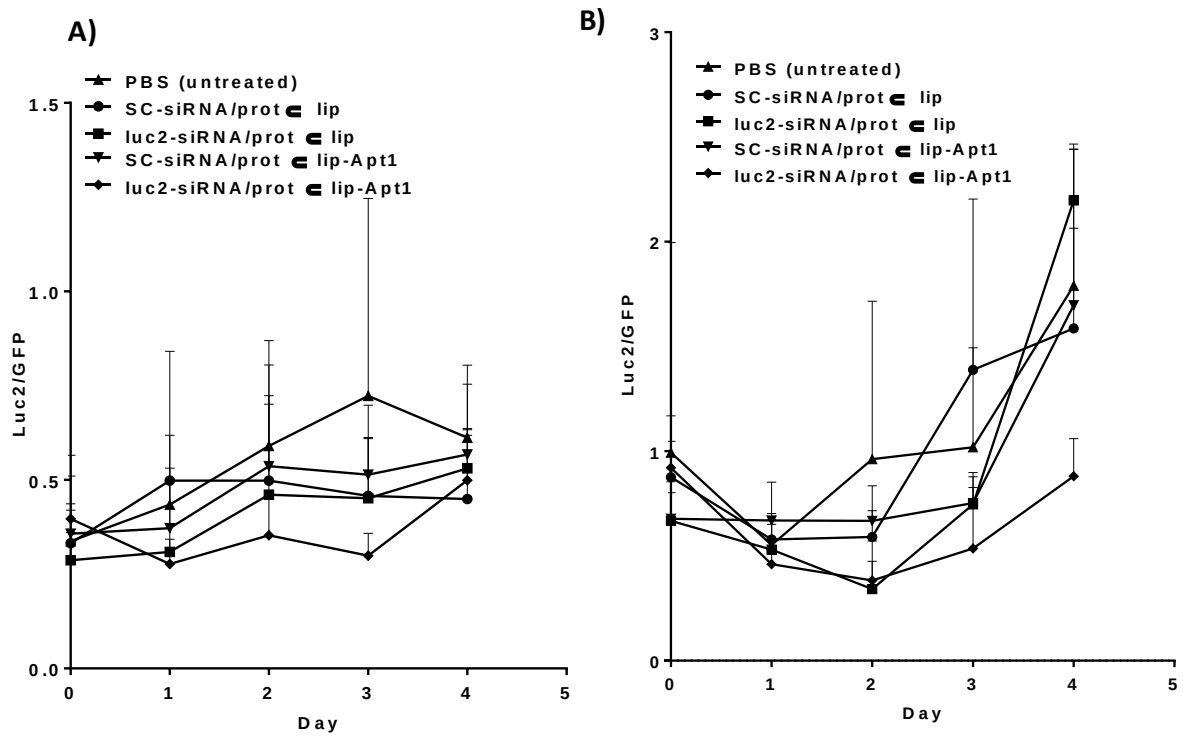

Figure S4: *Luc2/GFP expression ratio, when the Luc2 expression silenced, the GFP/Luc2 ratio increased, (A) Single dose and (B) multiple doses.*

General Discussion

General Discussion

Context and hypothesis

Cancer remains one of the leading causes of morbidity and mortality worldwide with approximately 14 millions new cases and 8.2 millions deaths in 2012 [1]. The term cancer gathers a heterogeneous group of diseases characterized by the uncontrolled growth of cells which can affect almost any part of the body. The better understanding of tumor biology has supported the development of effective therapeutic and diagnostic strategies. Tumors are composed of heterogeneous groups of cells, including a small population of cells named cancer stem cells (CSCs) [2, 3]. CSCs are characterized by the ability to renew, proliferate, and differentiate into other tumor cells. They can initiate tumors and are highly resistant to chemotherapy. Although conventional therapeutics including chemotherapy and radiotherapy are still the main therapeutic choice for treating tumors, they lack specificity and suffer important side effects. Therefore, developing therapeutic systems that aim to decrease the unwanted side effects with higher therapeutic outcomes is of central interest in tumor therapeutic innovations. To achieve this goal, "targeted" therapies have emerged. However this terms may refer to two different strategies: (i) targeting a specific molecular pharmacological target or pathway involved in tumor progression, or (ii) targeting specific biomarkers of cancer cells, which can be used to design specific ligands able to guide drug-loaded nanocarriers to these cells. The latter strategy will be further developed in this work, with the CD44 biomarker.

The CD44 receptor is a tumor biomarker overexpressed and involved in the progression of a variety of tumors such as breast, lung, colorectal, pancreatic and head and neck cancers [4]. In addition, CD44 is the main receptor for hyaluronic acid (HA) and is among the best known and characterized CSC markers. Therefore, our group and others have considered HA as a promising ligand for the active targeting of therapeutics and imaging molecules to CD44-

expressing tumor cells [5-7]. Despite some success of this strategy, HA can also bind to several proteins other than the CD44 receptor which may induce tumor proliferation and immune responses [8]. Antibodies are another type of targeting ligands with a promising potency. However, antibodies may be immunogenic and sometimes limited by a decreased activity due to the conjugation process [9]. In contrast, aptamers are a class of nucleic acid-based ligands that can bind their targets with a high affinity and specificity, with virtually no toxicity and immunogenicity [10]. Aptamer-functionalized nanocarriers have thus been increasingly investigated as targeted drug delivery systems to various tumors and have showed some success in improving therapeutic outcomes [11]

In this thesis, we have explored the hypothesis that selecting an RNA aptamer against the CD44 receptor and conjugating this aptamer to the surface of drug-loaded liposomes would improve drug delivery to CD44-expressing tumor cells *in vitro* and *in vivo*.

Selection of an anti-CD44 aptamer

Our group has managed to successfully select high affinity RNA aptamers against standard CD44 (CD44s) by the SELEX process using a 2′-F-pyrimidine RNA library [12]. The use of 2′-F-pyrimidine-modified RNAs addressed an important limitation of nucleic acids-based therapeutics in general and aptamers in particular, which is their susceptibility to degradation by nucleases [13]. Because RNA degradation by serum nucleases is directed by the pyrimidine nucleotides, modifications to cytosine and uridine are beneficial to increase stability in serum. Indeed the ribonuclease A (RNase A) attacks the 2′-hydroxyl group of the ribopyrimidines and cleaves the phosphodiester bond in the sugar-phosphate backbone of the RNA molecule (figure 1B) [14]. The substitution of the 2′-hydroxyl group of ribopyrimidines by 2′-amino or 2′-fluoro groups (figure 1A) has been found to significantly improve the RNA stability against nucleases [15].

Although introducing such modifications to aptamers after selection is possible, it is better to

incorporate them before aptamer selection to overcome the risk of losing proper folding of the aptamer structure, which could affect the binding affinity. The 2'-amino modification of aptamers dramatically increases their half-life in serum, from around 10 s (estimated) for natural RNA aptamers to 170 h. However, this 2′-amino substitution decreases the base pairing thermodynamic stability, which may affect the binding affinity of aptamers to their targets [16]. Moreover, difficulties in synthesis and PEGylation with NHS-esters disfavor the use of 2′-amino modifications [17], limiting their use in aptamer selection. In contrast, 2′-fluoro modifications increase the stability of base pairing, and generate aptamers with higher affinities compared to the 2′-amino aptamers. Such modified RNA transcripts display a half-life of 90 h in serum [18, 19]. While studies have shown that these nucleotides can be used as substrate for the mitochondrial DNA polymerases, there are no specific toxicities associated with the 2′-fluoropyrimidines aptamers, [20]. In particular, Macugen®, the first RNA aptamer-based therapeutic passing the clinical trials and approved for the treatment of age-related macular degeneration disease, is modified with 2′-fluoropyrimidines. Finally, these modifications did not entail interferences with the amplification by reverse transcriptase enzyme [12, 15]. For these reasons, we chose to transcribe our RNA library using the modified pyrimidines 2´-Fluorine-CTP (2´-F-dCTP) and 2´-Fluorine-UTP (2´-F-dUTP), besides the natural purines ATP and GTP.

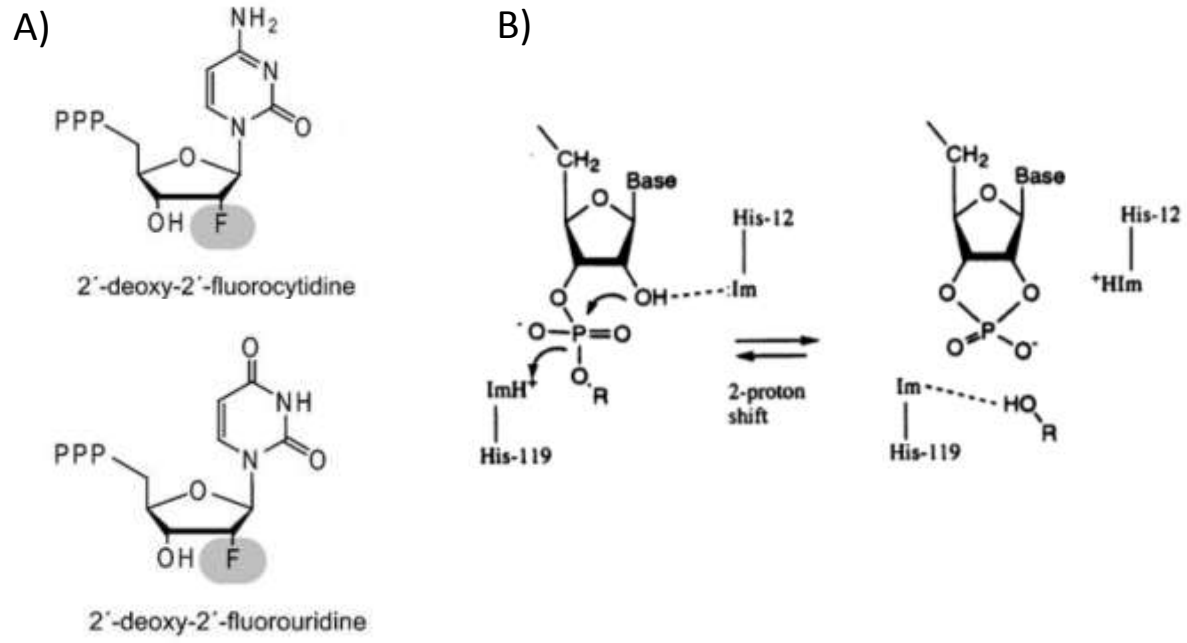

Figure 1: *(A) The 2'-fluoro substituted pyrimidines 2´-Fluorine-CTP (2´-F-dCTP) and 2´-Fluorine-UTP (2´-F-dUTP) [21]. (B) Classical mechanism of RNA cleavage by ribonuclease A [14].*

The *in vitro* selection of RNA aptamers against the CD44 protein has been performed in physiological conditions using 11 rounds of SELEX to ensure the enrichment of aptamers with highest affinity. After the last round, the PCR product has been cloned and sequenced to identify the aptamer "winner" sequences. Three aptamers have been identified among 25 representative colonies and named Apt1, Apt2, and Apt3. Apt1 was the dominant aptamer as it was present in 19 colonies out of the 25 sequenced ones, while Apt2 and Apt3 sequences were less dominant with only 3 colonies for each of them. The domination of Apt1 is an indication for the higher binding preferences over the other aptamers. This is the reason why all further experiments were performed with Apt1.

Binding affinities of Apt1 to the CD44 pure protein

We have measured the binding affinity of Apt1 toward the CD44 pure protein using two different labeling techniques: fluorescence (FITC-labeled Apt1) and radioactity (phosphate

transfer from [γ-^{33}P]-ATP). The use of radioactivity allowed to lower the limit of detection and thus to explore lower aptamer/CD44 ratios. Our results have clearly shown a high binding affinity with a K_d in the nanomolar range (21 to 81 nM). Such affinity was higher compared to the micromolar affinity of HA to CD44, and even compared to the reported affinity of an anti-CD44 DNA aptamer (180-295 nM) [22].

Binding specificity of Apt1 to CD44-expressing tumor cells

The binding specificities for Apt1 were assessed using representative breast cancer cell lines expressing the CD44 receptor, namely MDA-MB-231, MCF7 and T47D. The selected Apt1 was found to interact selectively with such cancer cells when analyzed by flow cytometry and fluorescent microscopy with different intensities of fluorescence, reflecting the level of CD44 expression on the surface of these cells. The MCF7 and T47D cells are luminal molecular subtype of breast cancer cell lines and contribute to express high levels of CD24 and low levels of CD44 ($CD44^{-/low}CD24^{+}$). In contrast, the MDA-MB-231 is a basal/mesenchymal molecular subtype and contributes to express low level of CD24 and high level of CD44 ($CD44^{+}CD24^{-/low}$). Moreover, more than 90% of the basal breast cancer cells (MDA-MB-231) were found to express the molecular subtype $CD44^{+}CD24^{-/low}$ and to harbor 1 % tumor cells with the CSC phenotype $CD44^{+}CD24^{-/low}$ and $ALDH1^{+}$, while only 20 to 34 % of the luminal breast cancer cells MCF7 and T47D expressed CD44, respectively [23].

PEGylated liposomes

Liposomes with the size of 100 nm have been prepared using thin-film hydration and extrusion through 100 nm polycarbonate membrane. Limited variations in the hydrodynamic diameters and the ζ-potential of liposomes were noticed among different preparations. The liposomes prepared in this thesis were composed of DPPC as neutral phospholipid,

cholesterol which aids in the stability of liposomes, and DSPE-PEG to confer "stealth" properties to the liposomes. This composition has been used throughout the study, avoiding the use of cationic lipids even for siRNA encapsulation, in order to minimize toxicity issues, and to maintain a liposome surface suited to functionalization with aptamers.

Conjugation of Apt1 to the surface of PEGylated liposomes

Several scenarios were explored to functionalize Apt1 to the surface of liposomes, including:

i) Conjugation of Apt1 to DSPE-PEG or cholesterol and then mixing with lipid film before extrusion. However, such a method may harm the Apt1 and induce degradation during the liposomes preparation procedure. Moreover, some aptamers may occupy the core of the liposomes, thereby losing some targeting functionality of the aptamers.

ii) Conjugation of Apt1 to DSPE-PEG and post-insertion into pre-formed PEGylated liposomes. To do so the Apt1-SH conjugated to micelles composed of DSPE-PEG-Maleimide by establishing a covalent interaction between the –SH and –maleimide active groups. Then the resulting DSPE-PEG-Apt1 conjugate can be post-inserted into the liposomes.

iii) Conjugation of a complementary strand to the sequence-linker extended to the aptamer on the surface of the PEGylated liposomes and then annealing the aptamer to the complementary strand. However, this method requires two steps of functionalization and may not be compatible with further experiments requiring temperatures above the melting temperature of the complementary strands.

iv) Conjugation of the aptamer onto preformed PEGylated liposomes by forming an amide bound from activated –NH2 and –COOH functional groups using carbodiimide chermistry, or a thioether bond from –SH and maleimide groups. To

compare both possibilities, liposomes prepared with 3% of DSPE-PEG-COOH or 3% of DSPE-PEG-maleimide were incubated with Atp1 derivatives, respectively Apt1-NH2 and Apt1-SH. A high conjugation efficacy was achieved for the thiol-maleimide crosslinking, while no or low conjugation of Apt1 obtained by carbodiimide chemistry, which may require further optimization steps. Therefore, the covalent conjugation of Apt1 was performed on the surface of performed PEGylated liposomes containing DSPE-PEG-maleimide and Apt1-SH derivatives.

We chosed the method iv) in a first approach and then method ii) in presence of siRNA.

Inflammatory potential of Apt1-liposomes

In addition to the role of CD44 receptor in tumor metastasis and growth, CD44 was found to be involved in inflammation processes [24]. Blocking CD44 by monoclonal antibodies in mouse models of chronic inflammatory disease was showed to reduce the disease severity as assessed by the recruitment of leukocytes at the inflammatory site [25, 26]. Moreover, some studies have shown the potential of inflammatory cytokines to induce the proliferation of tumor cells [27]. Therefore, we did investigate if our Apt1-liposomes induced inflammatory cytokines production by the tumor cells (MDA-MB-231 and A549). Our findings showed no change in the inflammatory cytokines secretion after treating the tumor cells by Apt1 liposomes, compared to plain liposomes and untreated cells, indicating that Apt1 liposomes may not affect the tumor cells proliferation which may results from inflammatory cytokines.

Binding specificity of Apt1-liposomes to CD44

We addressed the question of whether the conjugation of Apt1 to the surface of liposomes may affect its binding affinity for the pure CD44 protein, compared to the free form. We found a 3-fold increase in the binding affinity of Apt1 when conjugated to liposomes

compared to free Apt1, which shows that the conjugation chemistry did not alter the binding capacity of the aptamer. On the contrary, the higher affinity obtained is consistent with multivalent interactions involving several Apt1 units conjugated on the liposomes.

siRNA trapping into liposomes

The mechanism of action of small interfering RNA (siRNA) is based on post-transcriptional gene silencing. siRNA are usually specific and efficient in knocking down disease-related genes such as oncogenes. However, siRNA suffer low stability in biological media, susceptibility to degradation by nucleases, and low uptake by cells. Therefore, siRNAs require a carrier for their protection and efficient delivery into the target cells.

Lipid-based siRNA delivery systems are attractive due to their biocompatibility and versatility. Cationic lipids are the most common lipid carriers for the delivery of siRNA with several functions. First, they induce the ionic interactions with and the negatively charged siRNA molecules allowing high encapsulation efficiencies (above 95% in some cases). Another function is to increase binding to the negatively charged cell membrane, thereby increasing internalization and also to promote endosomal escape following endocytosis. Despite their efficacy as siRNA delivery system, cationic lipids suffer significant toxicity and low stability in biological media [30]. Cationic lipids have been found to interact with negatively charged serum proteins and activate the classical complement pathway, which leads to rapid clearance from the blood circulation [31].

In contrast to cationic lipids, neutral lipids are usually non toxic do not induce immune responses. The delivery of siRNA by liposomes composed of neutral lipids has been addressed, using for example 1,2-dioleoyl-sn-glycero-3-phosphatidylcholine (DOPC) for the delivery of siRNA targeting the oncoprotein EphA2 in a mouse orthotopic model of ovarian cancer. The trapping efficacy of siRNA was 65% [32]. Currently, the DOPC liposomes

encapsulating EphA2 siRNA are in a phase I clinical trial [33]. Despite some success, such liposomes are often limited by the siRNA loading amounts achievable, and by their ability to release siRNA intracellularly.

The challenges in designing siRNA-loaded and aptamer-functionalized liposomes lies in combining the high entrapment efficiency usually allowed by cationic systems such as lipoplexes, and the control of liposome surface for its proper functionalization, for which neutral liposomes are more suited that lipoplexes. In this thesis we chose to first condense siRNA with the cationic protamine, to encapsulate the resulting polyplexes in neutral liposomes, to "clean" the surface of the resulting liposomes from residual polyplexes or protamine, and to finally post-insert the aptamer previously conjugated to a phospholipid.

The siRNA was first condensed with the cationic protamine for its protection and efficient trapping into PEGylated liposomes. Protamine is small polycationic peptide (MW ~5 kDa), which is highly basic due to its high arginin content. Protamine is expressed naturally in sperms of all mammals and is often purified from salmon fish [34]. In sperm, the protamine binds, compacts, and delivers DNA into the egg after fertilization. Protamine is considered as biocompatible and exhibits a low toxicity. It is approved by FDA as an antidote to heparin used as anti-coagulation agent. Protamine has also been used for the delivery of nucleic acids such as siRNA and plasmid DNA into cells [35-37]. Therefore, we postulate to use it for its versatile properties in condensing, protection, and delivery of nucleic acids.

The siRNA/protamine polyplexes were loaded in preformed PEGylated liposomes by mixing and subsequent freeze/thaw cycles, which has been demonstrated as an efficient entrapment technique for peptides and nucleic acids [38, 39]. However, our zeta potential measurements have shown that reaching the maximum loading capacity resulted in the adsorption of some protamine or protamine/siRNA polyplexes at the surface of liposomes, which could hamper the surface functionalization with aptamers. We therefore took advantage of the peptide

nature of protamine to remove it from the surface of liposomes by treatment with trypsin, followed by purification of liposomes by centrifugal filtration. The final trapping efficiency of siRNA reached 77.8 ± 5.2% which is comparable to the data obtained for similar delivery systems by Peer et al. [37] with around 80% and higher than the 65% of reported by Landen et al. [32].

Cellular delivery and *in vitro* gene silencing

The uptake of the Apt1-liposomes by cells *in vitro* was investigated on two cancer cell lines that are highly expressing CD44 receptor, the breast cancer cell line MDA-MB-231 and the lung cancer cell line A549, representative of the major types of cancers. A 2- to 3-fold improvement was measured in the liposome uptake by these two cancer cell lines compared to the unconjugated liposomes, while no difference was observed between in the cellular uptake of conjugated and unconjugated liposomes in case of the $CD44^-$ 3T3 cell line. The uptake mechanism of Apt1-liposomes by cells may be explained by the high-binding affinity of Apt1 to CD44 receptor on the cell surface which could increase the persistence of liposomes on the surface of the tumor cells and then increase the rate of internalization into the cells by receptor-mediated endocytosis [28, 29].

The gene silencing efficacy of siRNA/prot ⊂ lip-Apt1 *in vitro* was higher compared to the of siRNA/prot ⊂ lip. Such observation can be explained by the higher cellular uptake of the aptamer-conjugated liposomes due to the binding affinity of Apt1 to CD44 receptor, thereby higher accumulation of siRNA, while the unconjugated liposomes lake the affinity offered by Apt1. This explanation is consistence with the cellular uptake study.

Ligand-functionalized nanocarriers usually enter cells via receptor-mediated endocytosis, followed by entry into endosomal compartments of the cells, which begins with early

endosome at slightly acidic pH~6 due to the ATP dependent proton pump [30]. The early endosome then matures and becomes more acidic (pH 5-6), after fusion with lysosome and pH decrease (pH 4-5), and the release of hydrolytic enzymes active at acidic pH. Therefore, the cargos of the liposomes should escape the endosomal barrier and reach the cytosol before the degradation by the hydrolytic enzymes.

In this thesis, the mechanism of cellular uptake and release was not investigated. However, the observation of an efficient and specific silencing of luc2 activity demonstrates a successful endosomal escape and the release of some intact siRNA into the cytosol. In the literature, it is not clear whether and how protamine may induce endosomal escape. Therefore, we suggest two hypotheses that may explain this endosomal escape. The first hypothesis is based on the proton sponge effect. During the maturation of the endosomes, the membrane-bound ATP-dependent proton pump transfers the protons from the cytoplasm into the endosome to activate the hydrolytic enzymes. Some polymers with high buffering capacity can resist this acidification. This increases the protons pumping from the cytosol, associated with the chloride ion passive diffusion, which in turn increases the ionic strength in the endosome and the water influx into the endosomes. The resulting swelling triggers the rupture of the endosomes and the release of the siRNA into the cytoplasm. The second hypothesis is based on the endosomal fusion (also known as destabilizing mechanism). In the late endosome, the pH decrease would increase the net charge of the protamine, resulting in conformational changes of the protamine structure, fusion with and rupture of the endosomal membrane, therefore releasing the siRNA cargo into the cytosol.

In vivo gene silencing

The PEGylated liposomes can work as a lipid carrier of the siRNA/protamine polyplex and and protect siRNA/protamine association with serum proteins. Moreover, they offer stealth

stability and functional groups for conjugation with targeting ligands (figure 2). In this thesis, to confirm the delivery efficiency of Apt1-functionalized, siRNA-loaded liposomes (siRNA/prot ⊂ lip-Apt1), the luc2 gene silencing was evaluated after intravenous administrations of single and multiple doses to mice bearing orthotopic breast cancer tumors (MDA-MB-231 cells). The results demonstrated that luc2-siRNA/prot ⊂ lip-Apt1 lead to significant gene silencing compared with luc2-siRNA/prot ⊂ lip, while no significant increased gene silencing effect occurred with liposomes loaded with control-scrambled siRNA.

To our knowledge there is no study describing the targeted delivery of siRNA-loaded liposomes mediated by an anti-CD44 aptamer. However, some studies addressed the targeted delivery of siRNA into tumors using aptamers functionalized liposomes. For instance, Li et al, (2014) [40] described the complexation of siRNA (specific for BRAF oncoprotein) with cationic PEGylated liposomes followed by covalent conjugation of the anti-nucleolin aptamer to the surface of siRNA-loaded liposomes. In this study the BRAF gene silencing was evaluated on a mouse xenograft model of human melanoma cancer and a significant inhibition was obtained by the aptamer functionalized liposomes compared to control liposomes [40]. Despite this success in knocking down BRAF gene, the anti-nucleolin aptamer is a DNA aptamer and may suffer degradation by nucleases.

To target CD44-expressing tumor cells, the hyaluronic acid was used in several studies to increase the transfection efficiency of siRNA-loaded cationic liposomes [5, 7, 41]. However, the hyaluronic acid targeting efficacy is strongly size-dependent, the binding affinity to CD44 increasing with increasing hyaluronan molecular weight [42]. Moreover, the low molecular weight hyaluronan (MW < 10^6 Da) was found to increase cell tumor cell invasion, CD44

cleavage, and angiogenesis. On the other hand, the high molecular weight hyalouronan (MW > 10^6 Da) was found to reduce tumorgenesis [43]. Although high molecular weight hyalouronan was shown to increase the transfection efficacy of siRNA-loaded into liposomes, the high molecular weight may limit the application as a targeting ligand for drug-conjugate, while the aptamers are small in size with better properties of tumor penetration. Moreover, an in vitro and *in vivo* comparative study by mean of targeting efficacy between hyalouronic acid and anti-CD44 aptamers could reveal more information about the potency of the two targeting modality.

However, while *in vivo* there was no significant difference noticed for the first three days of siRNA administration, a prolong silencing effect was noticed for the siRNA/prot ⊂ lip-Apt1 (active targeting) compared to the siRNA/prot ⊂ lip (passive targeting). Such a result can be explained by the differences in the biodistribution between the siRNA/prot ⊂ lip-Apt1 (active targeting) and the siRNA/prot ⊂ lip (passive targeting), which may result from the higher uptake of siRNA/prot ⊂ lip of siRNA/prot ⊂ lip-Apt1 by the tumor cells compared to siRNA/prot ⊂ lip (passive targeting). Therefore, a biodistribution study could help explaining this result.

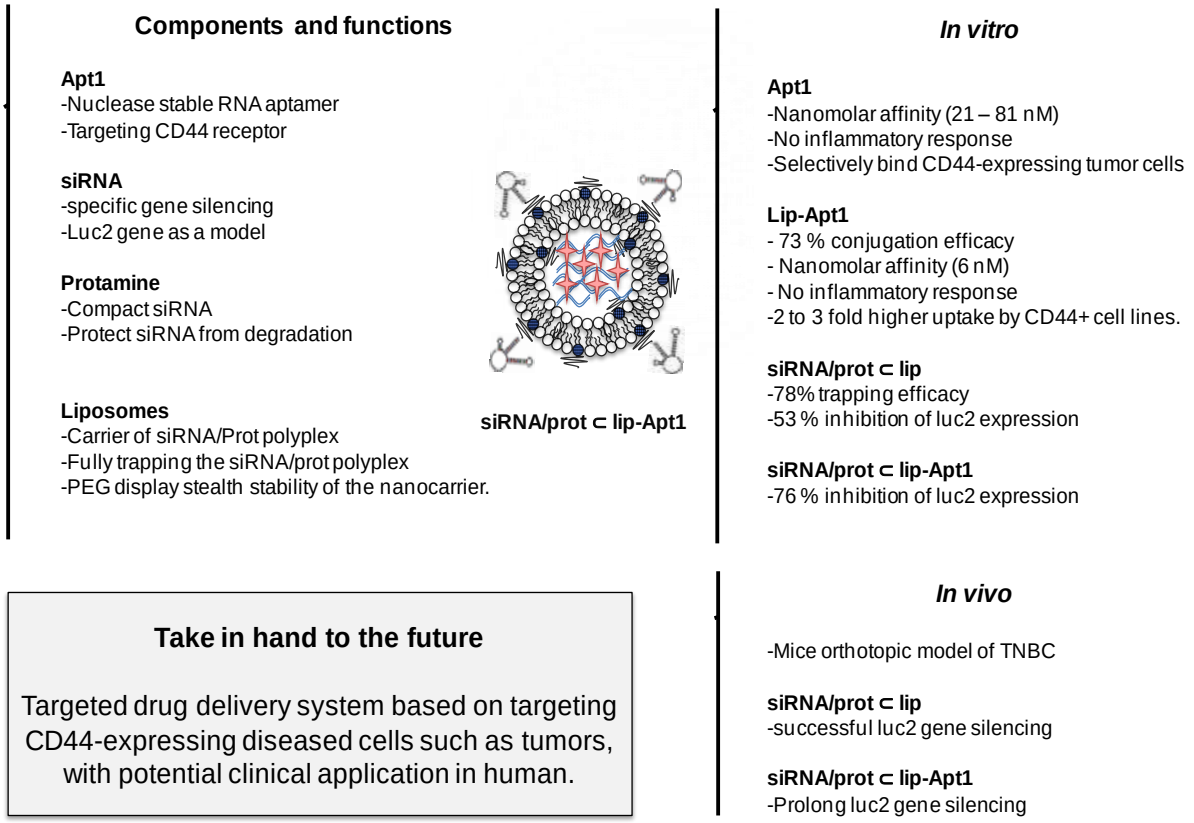

Figure 2: *Summary of the main characteristics and results obtained with the aptamer-functionalized, siRNA-loaded liposomes described in this thesis.*

General conclusions and perspectives

In conclusion, our work is the first to describe the successful selection of 2′-F-pyrimidine-modified RNA aptamers against the CD44 receptor protein, and its use as a targeting ligand attached to the surface of liposomes, able to deliver siRNA and knock down genes in triple-negative orthotopic breast cancer model in mice.

The initial hypothesis was that Apt1 covalently linked to PEGylated liposomes would increase the drug delivery to CD44-expressing tumor cells. Moreover, we had postulated that neutral liposomes containing siRNA complexed to protamine would be able to deliver the nucleic acids to the cytoplasm which would silence the target gene. We believe we have obtained enough data to prove that the initial concept was right.

Future investigations should be performed to demonstrate that the improved gene inhibition observed *in vivo* is due to an active targeting of CD44 at the molecular level. To do so, biodistribution studies could be performed, as well as competition studies with anti-CD44 antibodies or anti-dots of Apt1. The use of breast cancer cell line with low amount of CD44 could provide interesting comparisons.

In addition to the gene silencing efficacy, our results have shown no signs of toxicity or immunogenicity in the mouse orthotopic experimental model of human breast cancer. Liposomal based drug delivery systems are well established and safe, and their use for siRNA delivery may make this therapeutic modality clinically attractive. With further studies and caution approaches, this is a potential model that can be taken in hand into the clinical use for cancer therapy as well as for other related conditions amenable to selective CD44 targeting and specific gene knockdown. Along this way, several questions or perspectives should be addressed, including: i) with a length of 90 bases, Apt1 is a relatively large aptamer compared to those usually described in the literature; a truncation of Apt1 into smaller sequences with

preserved affinity could decrease its cost and facilitate its use for larger studies; ii) the density of Apt1 on the surface of liposomes could be optimized to achieve the highest targeting efficacy with minimal effect on the stealth properties of the PEGylated liposomes, iii) the siRNA/protamine molar ratio could also be optimized to achieve highest encapsulation efficacy and release inside the cells; vi) *in vitro* and *in vivo* kinetic uptake, trafficking and release studies would improve the understanding of such gene silencing effect; v) loading the liposomes with relevant oncogene-specific siRNA sequences, and/or with small anti tumor chemotherapy, should be performed to investigate the efficacy in tumor growth inhibition *in vivo*.

References

[1] B.W. Stewart, C.P. Wild, World cancer report 2014, IARC Press, Lyon, 2014.

[2] A. Kreso, J.E. Dick, Evolution of the cancer stem cell model, Cell Stem Cell, 14 (2014) 275-291.

[3] S.I. Ismail, A. Walhan, A. Nidaa, F. Elias, Aptamers: Promising Molecules for Cancer Stem Cell Targeting. J Mol Genet Med 7 (2013): 90.

[4] C. Tang, B.T. Ang, S. Pervaiz, Cancer stem cell: target for anti-cancer therapy, FASEB journal : official publication of the Federation of American Societies for Experimental Biology, 21 (2007) 3777-3785.

[5] A. Dufay Wojcicki, H. Hillaireau, T.L. Nascimento, S. Arpicco, M. Taverna, S. Ribes, M. Bourge, V. Nicolas, A. Bochot, C. Vauthier, N. Tsapis, E. Fattal, Hyaluronic acid-bearing lipoplexes: physico-chemical characterization and in vitro targeting of the CD44 receptor, Journal of controlled release : official journal of the Controlled Release Society, 162 (2012) 545-552.

[6] F. Dosio, S. Arpicco, B. Stella, E. Fattal, Hyaluronic acid for anticancer drug and nucleic acid delivery, Adv Drug Deliv Rev, (2015).

[7] T.L. Nascimento, H. Hillaireau, M. Noiray, C. Bourgaux, S. Arpicco, G. Pehau-Arnaudet, M. Taverna, D. Cosco, N. Tsapis, E. Fattal, Supramolecular Organization and siRNA Binding of Hyaluronic Acid-Coated Lipoplexes for Targeted Delivery to the CD44 Receptor, Langmuir : the ACS journal of surfaces and colloids, 31 (2015) 11186-11194.

[8] H. Zhang, S. Huang, X. Yang, G. Zhai, Current research on hyaluronic acid-drug bioconjugates, Eur J Med Chem, 86 (2014) 310-317.

[9] K.Y. Choi, G. Saravanakumar, J.H. Park, K. Park, Hyaluronic acid-based nanocarriers for intracellular targeting: interfacial interactions with proteins in cancer, Colloids Surf B Biointerfaces, 99 (2012) 82-94.

[10] A.D. Keefe, S. Pai, A. Ellington, Aptamers as therapeutics, Nat Rev Drug Discov, 9 (2010) 537-550.

[11] A.C. Yan, M. Levy, Aptamers and aptamer targeted delivery, RNA Biol, 6 (2009) 316-320.

[12] N. Ababneh, W. Alshaer, O. Allozi, A. Mahafzah, M. El-Khateeb, H. Hillaireau, M. Noiray, E. Fattal, S. Ismail, In vitro selection of modified RNA aptamers against CD44 cancer stem cell marker, Nucleic acid therapeutics, 23 (2013) 401-407.

[13] E. Fattal, A. Bochot, Ocular delivery of nucleic acids: antisense oligonucleotides, aptamers and siRNA, Advanced drug delivery reviews, 58 (2006) 1203-1223.

[14] R. Breslow, W.H. Chapman, Jr., On the mechanism of action of ribonuclease A: relevance of enzymatic studies with a p-nitrophenylphosphate ester and a thiophosphate ester, Proc Natl Acad Sci U S A, 93 (1996) 10018-10021.

[15] H. Aurup, D.M. Williams, F. Eckstein, 2'-Fluoro- and 2'-amino-2'-deoxynucleoside 5'-triphosphates as substrates for T7 RNA polymerase, Biochemistry, 31 (1992) 9636-9641.

[16] H. Aurup, T. Tuschl, F. Benseler, J. Ludwig, F. Eckstein, Oligonucleotide duplexes containing 2'-amino-2'-deoxycytidines: thermal stability and chemical reactivity, Nucleic Acids Res, 22 (1994) 20-24.

[17] J. Ruckman, L.S. Green, J. Beeson, S. Waugh, W.L. Gillette, D.D. Henninger, L. Claesson-Welsh, N. Janjic, 2'-Fluoropyrimidine RNA-based aptamers to the 165-amino acid form of vascular endothelial growth factor (VEGF165). Inhibition of receptor binding and VEGF-induced vascular permeability through interactions requiring the exon 7-encoded domain, J Biol Chem, 273 (1998) 20556-20567.

[18] R. Padilla, R. Sousa, Efficient synthesis of nucleic acids heavily modified with non-canonical ribose 2'-groups using a mutantT7 RNA polymerase (RNAP), Nucleic Acids Res, 27 (1999) 1561-1563.

[19] A. Sabahi, J. Guidry, G.B. Inamati, M. Manoharan, P. Wittung-Stafshede, Hybridization of 2'-ribose modified mixed-sequence oligonucleotides: thermodynamic and kinetic studies, Nucleic Acids Res, 29 (2001) 2163-2170.

[20] F.C. Richardson, C. Zhang, S.R. Lehrman, H. Koc, J.A. Swenberg, K.A. Richardson, R.A. Bendele, Quantification of 2'-fluoro-2'-deoxyuridine and 2'-fluoro-2'-deoxycytidine in DNA and RNA isolated from rats and woodchucks using LC/MS/MS, Chem Res Toxicol, 15 (2002) 922-926.

[21] G. Mayer, The chemical biology of aptamers, Angew Chem Int Ed Engl, 48 (2009) 2672-2689.

[22] A. Somasunderam, V. Thiviyanathan, T. Tanaka, X. Li, M. Neerathilingam, G.L. Lokesh, A. Mann, Y. Peng, M. Ferrari, J. Klostergaard, D.G. Gorenstein, Combinatorial selection of DNA thioaptamers targeted to the HA binding domain of human CD44, Biochemistry, 49 (2010) 9106-9112.

[23] S. Ricardo, A.F. Vieira, R. Gerhard, D. Leitao, R. Pinto, J.F. Cameselle-Teijeiro, F. Milanezi, F. Schmitt, J. Paredes, Breast cancer stem cell markers CD44, CD24 and ALDH1: expression distribution within intrinsic molecular subtype, Journal of clinical pathology, 64 (2011) 937-946.

[24] D. Naor, S. Nedvetzki, M. Walmsley, A. Yayon, E.A. Turley, I. Golan, D. Caspi, L.E. Sebban, Y. Zick, T. Garin, D. Karussis, N. Assayag-Asherie, I. Raz, L. Weiss, S. Slavin, I. Golan, CD44 involvement in autoimmune inflammations: the lesson to be learned from CD44-targeting by antibody or from knockout mice, Annals of the New York Academy of Sciences, 1110 (2007) 233-247.

[25] G. Hutas, E. Bajnok, I. Gal, A. Finnegan, T.T. Glant, K. Mikecz, CD44-specific antibody treatment and CD44 deficiency exert distinct effects on leukocyte recruitment in experimental arthritis, Blood, 112 (2008) 4999-5006.

[26] H.C. DeGrendele, P. Estess, M.H. Siegelman, Requirement for CD44 in activated T cell extravasation into an inflammatory site, Science, 278 (1997) 672-675.

[27] F. Colotta, P. Allavena, A. Sica, C. Garlanda, A. Mantovani, Cancer-related inflammation, the seventh hallmark of cancer: links to genetic instability, Carcinogenesis, 30 (2009) 1073-1081.

[28] H.K. Park, S.J. Lee, J.S. Oh, S.G. Lee, Y.I. Jeong, H.C. Lee, Smart Nanoparticles Based on Hyaluronic Acid for Redox-Responsive and CD44 Receptor-Mediated Targeting of Tumor, Nanoscale research letters, 10 (2015) 981.

[29] W. Alshaer, H. Hillaireau, J. Vergnaud, S. Ismail, E. Fattal, Functionalizing Liposomes with anti-CD44 Aptamer for Selective Targeting of Cancer Cells, Bioconjugate chemistry, 26 (2015) 1307-1313.

[30] S.T. Guo, L. Huang, Nanoparticles Escaping RES and Endosome: Challenges for siRNA Delivery for Cancer Therapy, Journal of Nanomaterials, (2011).

[31] J.C. Kraft, J.P. Freeling, Z. Wang, R.J. Ho, Emerging research and clinical development trends of liposome and lipid nanoparticle drug delivery systems, Journal of pharmaceutical sciences, 103 (2014) 29-52.

[32] C.N. Landen, A. Chavez-Reyes, C. Bucana, R. Schmandt, M.T. Deavers, G. Lopez-Berestein, A.K. Sood, Therapeutic EphA2 gene targeting in vivo using neutral liposomal small interfering RNA delivery, Cancer Research, 65 (2005) 6910-6918.

[33] C.-f. Xu, J. Wang, Delivery systems for siRNA drug development in cancer therapy, Asian Journal of Pharmaceutical Sciences, 10 (2015) 1-12.
[34] R. Balhorn, The protamine family of sperm nuclear proteins, Genome Biol, 8 (2007) 227.

[35] Y.-S. Choi, J.Y. Lee, J.S. Suh, Y.-M. Kwon, S.-J. Lee, J.-K. Chung, D.-S. Lee, V.C. Yang, C.-P. Chung, Y.-J. Park, The systemic delivery of siRNAs by a cell penetrating peptide, low molecular weight protamine, Biomaterials, 31 (2010) 1429-1443.

[36] F.L. Sorgi, S. Bhattacharya, L. Huang, Protamine sulfate enhances lipid-mediated gene transfer, Gene Ther, 4 (1997) 961-968.

[37] D. Peer, E.J. Park, Y. Morishita, C.V. Carman, M. Shimaoka, Systemic leukocyte-directed siRNA delivery revealing cyclin D1 as an anti-inflammatory target, Science, 319 (2008) 627-630.

[38] L. Boulmedarat, G. Piel, A. Bochot, S. Lesieur, L. Delattre, E. Fattal, Cyclodextrin-mediated drug release from liposomes dispersed within a bioadhesive gel, Pharmaceutical research, 22 (2005) 962-971.

[39] U. Pick, Liposomes with a large trapping capacity prepared by freezing and thawing of sonicated phospholipid mixtures, Archives of biochemistry and biophysics, 212 (1981) 186-194.

[40] L. Li, J. Hou, X. Liu, Y. Guo, Y. Wu, L. Zhang, Z. Yang, Nucleolin-targeting liposomes guided by aptamer AS1411 for the delivery of siRNA for the treatment of malignant melanomas, Biomaterials, 35 (2014) 3840-3850.

[41] S. Taetz, A. Bochot, C. Surace, S. Arpicco, J.M. Renoir, U.F. Schaefer, V. Marsaud, S. Kerdine-Roemer, C.M. Lehr, E. Fattal, Hyaluronic acid-modified DOTAP/DOPE liposomes for the targeted delivery of anti-telomerase siRNA to CD44-expressing lung cancer cells, Oligonucleotides, 19 (2009) 103-116.

[42] S. Arpicco, G. De Rosa, E. Fattal, Lipid-Based Nanovectors for Targeting of CD44-Overexpressing Tumor Cells, Journal of drug delivery, 2013 (2013) 860780.

[43] J.M. Louderbough, J.A. Schroeder, Understanding the dual nature of CD44 in breast cancer progression, Molecular cancer research : MCR, 9 (2011) 1573-1586.

Fonctionnalisation de liposomes par des aptamères pour le ciblage actif des cellules cancéreuses

Mots clés : Aptamères, CD44, Liposomes, siARN, Délivrance ciblée

Dans ce travail, nous avons réussi à sélectionner par la méthode SELEX un aptamère ARN modifié nommé Apt1, celui ci se lie avec une haute affinité à la protéine du récepteur CD44. L'aptamère sélectionné a été modifié avec de la 2'-F-pyrimidine pour augmenter sa stabilité contre les nucléases et améliorer son action biologique. Cet apatamer a été ensuite fonctionnalisé sur des liposomes et des séquences de SiRNA ont été encapsulé à l'intérieur. Ce système permet un ciblage actif des cellules tumorales exprimant le récepteur CD-44 pour une délivrance ciblée des SiRNA *in vitro* et *in vivo*. Une telle fonctionnalisation a été réalisée par une conjugaison chimique de type thiol-maléimide entre le 3'-thiol modifié de Apt1 et le maléimide fonctionnalisé à la surface des liposomes. Les liposomes formulés présentent une forte affinité pour les cellules exprimant le CD44 sans déclencher de réponse inflammatoire indésirable au sein de ces cellules. En outre, les données de cette étude montrent que l'inhibition du gène ciblé par le siARN est augmentée *in vitro* et *in vivo* grâce à notre liposome couplé à l'aptamer. Le ciblage des siRNA par ce système de ciblage actif peut être utilisé pour le traitement de tumeurs exprimant le récepteur CD44 et inhiber la croissance tumorale *in vivo*. L'étape suivante consiste à charger ce système de délivrance de siRNA par d'autres séquences qui permettent de réprimer des gènes de la maladie.

Functionalizing liposomes with aptamers for active targeting of tumor cells

Keywords : Aptamers, CD44, Liposomes, Active targeting

In this work we succeeded to select a modified RNA aptamer, named Apt1, to bind the human CD44 receptor protein with high affinity using the SELEX method. The selected aptamer was modified with 2'-F-pyrimidine to increase stability against nucleases for biological applications. Furthermore, we developed an aptamer-functionalized-liposome loaded with siRNA molecules as a model of drug delivery system that selectively target CD44-expressing tumor cells *in vitro* and *in vivo*. Such functionalization was performed by thiol-maleimide conjugation chemistry between 3'-thiol modified Apt1 and the maleimide functionalized to the surface of the liposomes. The targeted liposomes were shown to express high affinity for CD44 positive cells without triggering any inflammatory response within these cells. Moreover, the data of this study showed that higher inhibition of targeted gene by the aptamer functionalized liposomes-loaded with siRNA *in vitro*, and prolong inhibition *in vivo*. Our siRNA delivery and active targeting system may be useful for targeting CD44-expressing tumors and suppressing tumor growth *in vivo*.